DUAL PLANETARY BASED CONTINUOUSLY VARIABLE TRANSMISSION FOR ELECTRIC VEHICLES

Abdeslam Medouar

Department of Electrical & Computer Engineering

McGill University

Montreal, Quebec

August 2019

A thesis submitted to McGill University in partial fulfillment of the requirements of the degree of Master of Engineering

Abstract

In an effort to reduce the energy consumption and increase the range of electric vehicles, while driving down their cost and environmental impact, the addition of transmission systems has been suggested. Multiple possible configurations are emerging, specifically designed to take advantage of the high controllability and wide range of operation of electric motors.

A novel Continuously Variable Transmission (CVT) design is proposed, which suggests the addition of a motor to the common sun of the existing Dual-Brake Transmission, extending the range of achievable gear ratios. This flexibility allows the CVT to operate the traction motor of the vehicle closer to the optimal regions of its torque speed curve.

To test for the viability of the novel design, a full electric vehicle simulation was implemented. The simulated vehicle was equipped with the CVT, and compared to two existing benchmark designs, a single speed transmission (SST) and Dual-Brake transmission.

In all configurations, the vehicle was successful in accurately tracking four tested drive cycles, selected to depict the wide range of driving styles of an electric vehicle. Significant improvements in average input motor efficiency were observed in testing drive cycles when the vehicle was equipped with the CVT over the other two benchmarks. The addition of the sun motor however resulted in some of the power being absorbed away from the drivetrain by the sun motor. Overall vehicle efficiency was nevertheless improved, given the ability of the sun motor to recharge the battery of the vehicle.

Simulations were conducted with varying degrees of battery recharge efficiency, to establish the breakpoint where the addition of the CVT no longer improved overall vehicle efficiency. Results show an improvement in high speed driving cycles given a battery recharge efficiency greater than 95%.

Abrégé

Afin de réduire la consommation d'énergie et d'augmenter l'autonomie des véhicules électriques, tout en réduisant leur coût et leur impact sur l'environnement, l'ajout de systèmes de transmission a été suggéré. De multiples configurations sont présentées, spécialement conçues pour tirer parti de la haute contrôlabilité et large plage d'opération des moteurs électriques. Un nouveau concept de transmission à variation continue (CVT) est proposé, qui suggère l'ajout d'un moteur au pignon solaire commun de la transmission à deux vitesses sans interruption de couple (DBT), élargissant ainsi la gamme de rapports de transmission réalisables. Cette flexibilité permet à la CVT de faire fonctionner le moteur du véhicule près des régions optimales de sa courbe de vitesse et de couple. Afin de tester la viabilité de la nouvelle conception, une simulation de véhicule entièrement électrique a été mise en œuvre. Le véhicule est simulé, équipé de la CVT et comparé à deux modèles de référence existants, une transmission à une vitesse (SST) et la DBT.

Dans toutes les configurations, le véhicule a réussi à suivre avec précision quatre cycles de conduite testés, sélectionnés pour illustrer le large éventail de styles de conduite d'un véhicule électrique. Des améliorations significatives de l'efficacité moyenne du moteur ont été observées lors des tests de cycle de conduite affichant des vitesses élevées, lorsque le véhicule était équipé de la CVT par rapport aux deux autres points de référence. L'ajout du moteur au pignon solaire a toutefois entraîné une partie de la puissance absorbée de la transmission par ce moteur solaire. L'efficacité globale du véhicule a été améliorée, compte tenu de la capacité du moteur solaire à recharger la batterie du véhicule.

Des simulations ont été effectuées avec différents degrés d'efficacité de recharge de la batterie, afin d'établir le point de rupture où l'ajout de la CVT n'améliorait plus l'efficacité globale du véhicule. Les résultats montrent une amélioration ; lors des cycles de conduite à grande vitesse ; avec une efficacité de recharge de la batterie supérieure à 95%.

Acknowledgments

I would like to thank my supervisor, professor Benoit Boulet, for his guidance, insight and commitment to this research. His deep knowledge of the subject matter, his problem-solving skills and his patience were precious assets to this project.

Additionally, I extend my thanks to the Natural Sciences and Engineering Research Council of Canada (NSERC) for its financial support.

I would like to thank Dr. Saman Rahimi Mousavi for his help introducing me to the DBT project, and his facilitating my understanding of his work.

I would also like to thank Dr. Hosssein Vahid Alizadeh for his invaluable advice throughout this project.

I would also like to thank Mr. Marc-Antoine Beaudoin for his very constructive remarks.

I would like to express my appreciations to my colleagues Dr. Yingxuan Duan, Mr. Mostapha Darabi, Mrs. Zeinab Sobhani and Dr. Di Wu.

I would like to thank my parents for their love and unwavering support throughout my life.

Finally, I thank my family and friends for their encouragements during my master's degree.

Contributions

The novel transmission design presented in this thesis is based on the Dual-Brake Transmission developed by Mousavi [10].

Design, analysis, simulation of the Continuously Variable Transmission, as well as the full vehicle simulations were conducted by the author.

This study was conducted under the supervision of Professor Benoit Boulet.

List of Tables

List of Figures

List of Acronyms

CVT: Continuously Variable Transmission

SST: Single Speed Transmission

DBT: Dual-Brake Transmission

NSERC: Natural Sciences and Engineering Research Council of Canada

GHG: Greenhouse Gases

PPM: Parts Per Million

PCA: Paris Climate Accords

WTT: Well-to-Tank

TTW: Tank-to-Wheel

EF MIX: Emission Factor Mix

ICEV: Internal Combustion Engine Vehicles

HEV: Hybrid Electric Vehicles

BEV: Battery Electric Vehicles

EV: Electric Vehicles

IEA: International Energy Agency

SoC: State of Charge

RPM: Rotations per Minute

DC: Direct Current

AC: Alternating Current

PMSM: Permanent Magnet Synchronous Motor

IM: Induction Motor

SRM: Switched Reluctance Motors

MT: Manual Transmission

AT: Automatic Transmission

AMT: Automated Manual Transmission

DCT: Dual Clutch Transmissions

RWD: Rear Wheel Drive

FWD: Front Wheel Drive

TCU: Transmission Control Unit

IVT: Infinitely Variable Transmission

GM: General Motors

FCEV: Fuel Cell Electric Vehicles

FC-HEV: Fuel Cell Hybrid Electric Vehicles

FC-PHEV: Fuel Cell Plug-in Hybrid Electric Vehicles

PG: Planetary Gear

FR: Fixed Ratio

HIL: Hardware in the Loop

PI: Proportional Integral (Controller)

IME: Input Motor Efficiency

EUDC: Extra Urban Drive Cycle

HWFET: Highway Fuel Economy

WLTP: Worldwide Harmonized Light Vehicles Test Procedure

UDDS: Urban Dynamometer Driving Schedule

Table of Contents

1 Introduction

1.1 Environmental necessity

The Earth's atmosphere has been undergoing major changes throughout the past centuries, in large part due to the contribution of human activities. Since the industrial revolution in the 18th century, enormous amounts of greenhouse gases (GHG) have been discharged in the atmosphere in the process of burning fossil fuels. The transportation sector, which includes all methods for the transport of humans, animals and goods, accounts in the United States for 28% of GHG emission in 2016, while the production of electricity produces another 28%. An example of such an augmentation is the average level of carbon dioxide increasing from 280 parts per million (ppm) in 1750 to 410 ppm today. If this general trend continues, experts predict it could harm ecosystems, biodiversity and human livelihood worldwide. The Paris Climate Agreements (PCA) saw 184 countries consent to mitigate the effects of global warming by limiting the global average temperature increase below 2 degrees celsius. Part of the plan is to reduce GHG emissions of the transportation sector worldwide, through a vast electrification of the transportation fleets, as well as more research into the exploitation of renewable resources to power such fleets.

Such a plan must take into consideration the full lifecycle emissions of the vehicles used, which combines the GHG footprint of the construction, usage and maintenance of the vehicle, but also that of the different power plants used to generate the necessary power to fuel the vehicle. Studies must be conducted to both account for Well-to-Tank (WTT); the generation and distribution of electricity to the vehicle; and Tank-to-Wheel (TTW) emissions; those emitted from the conversion of electric power to mechanical traction [1].

On one hand, the WTT emissions for EVs are largely dependent on the environment-friendliness of an electric grid. This, in turn, is determined by the Emission Factor Mix (EF MIX), representing the different energy sources used to produce electricity. The proportions of each of nuclear, fossil fuel, hydroelectric, geothermal, wind and

solar power generators determines the level of CO2 emitted per kilowatt hour (kWh) of energy generated [3]. Economic, environmental and political factors play a key role in deciding the EF MIX of any given country. Renewable sources such as solar and wind power plants have long suffered from necessarily high initial investments and relatively low returns on such investments, especially compared to their fossil fuel counterpart. More research has tightened that gap over the last few decades, and agreements such as those of Paris may encourage more investment on such research. On the other hand, while recent governmental directives have pushed car manufacturers to improve ICE vehicle efficiencies, the consensus is that ICE vehicles have reached their technological limits, and that the dire global situation requires a marked transition towards more efficient types of locomotion [1]. An electrification thus implies a conversion of the world transportation fleet from internal combustion engine vehicles (ICEV) to hybrid (HEV) or battery electric vehicles (BEV). Electric vehicles (EVs) have been shown to reduce upwards of 75% of TTW emissions as compared to their ICEV counterparts [2]. They also provide the added benefit of removing tailpipe emissions, which is a key attribute in densely populated areas for human health.

Electric vehicles present an interesting alternative to the current internal combustion engines but exhibit their own limitations. An important such limitation is the high initial cost, rare-material hungry process of battery production. This presents a high initial investment from the consumer, and large initial release of GHG into the atmosphere, which is later offset by the energy savings discussed above. The current battery technology is trailing compared to energy dense fossil fuels, which is restraining mass adoption of EVs. Customers may be reluctant to adopt EVs because of their relatively low range, longer charging time, and the uncertainty relative to the battery lifetime [1].

These limitations must be investigated and mitigated in order to facilitate the adoption of the PCA initiatives. The study of lifecycle emissions of EVs is highly subject to parameters such as the type of driving (stop frequency, average speeds,

commute duration, etc.), the region electric grid EF MIX, time and place of charge… As [3] explains, different drive cycles result in different performance, consumption and emission for the different types of vehicles studied.

1.2 Electric Vehicles Powertrain Background

The International Energy Agency (IEA) reports [4] that EV sales have seen a dramatic rise over the past decade, surpassing 1 million units in 2017 alone, taking the global EV fleet to over 3 million. This steep increase is mostly concentrated in the People's Republic of China (or China), where half of the global sales have been registered. A significant trend is also observable in Scandinavian countries where EVs represent 54, 12 and 6% of new sales in Norway, Iceland and Sweden respectively. This trend can be attributed to heavy governmental investments in China and the United States, but is also due to significant advances in battery and vehicle technology from the private industry, most notoriously Elon Musk's Tesla.

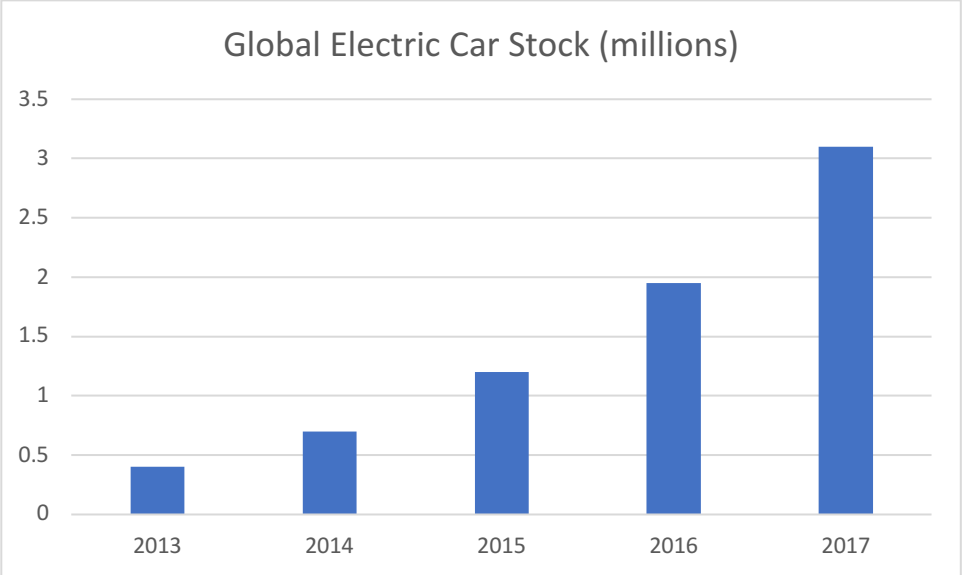

Figure 1-1 Global Electric Car Stock (See [4])

Initial designs of EVs saw manufacturers simply replace internal combustion engines and fuel tank for electric motors and batteries. However, the many limitations of designs tailored for ICEVs, such as heavy weight, lower flexibility and little efficiency,

forced a transition to different designs. In fact, modern EVs differ greatly from their ICE counterparts. As described in [5], the powertrain of an EV is comprised of at least one electric motor, a transmission, a differential and a final drive connected to the wheels. The electric motor uses the energy stored in either a battery, fuel cells, ultracapacitors or flywheels to provide the necessary traction for vehicle movement after going through an electronic power converter. A vehicle controller acts as the outer layer of control, interpreting the accelerator and brake pedal activation as torque demands for the motor, while the energy management unit coordinates with the vehicle controller for phases of regenerative braking.

While alternative architectures for EVs exists, such as the omission of a mechanical transmission for in a Single-Speed Transmission, or the use of dual motors such as in the Tesla Model S, the subsequent sections will detail the aforementioned powertrain components.

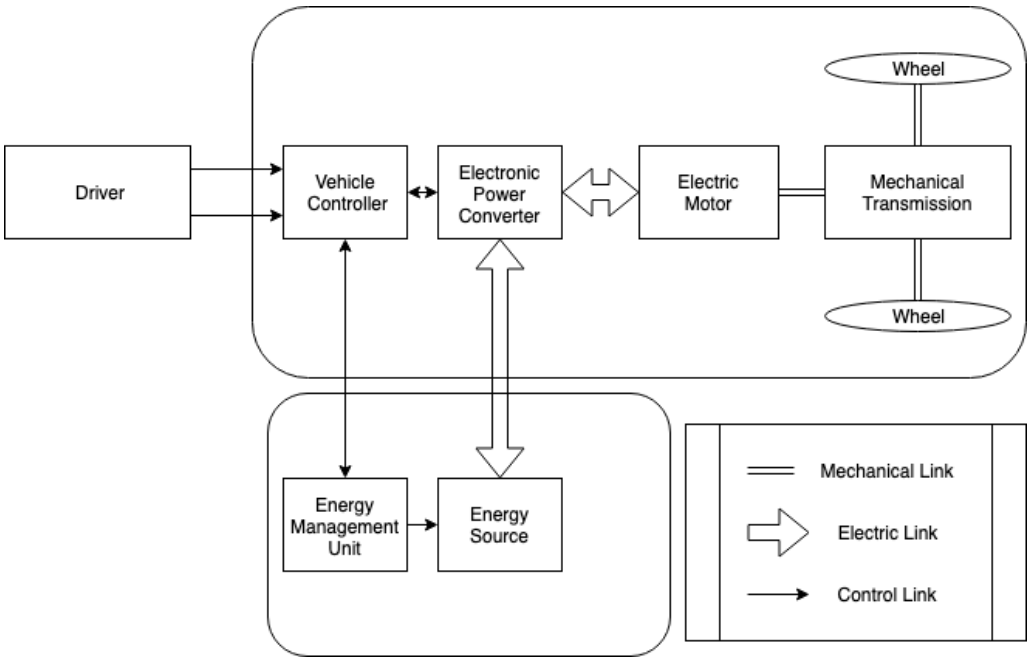

Figure 1-2 Typical EV Powertrain Architecture (See [5])

Energy Storages

The energy storage of an EV is defined as the device that stores energy, which is either used to deliver energy to other elements (discharge) or accepts energy through

an energy refueling unit or regenerative braking (charge). An ideal energy storage should be designed to maximize specific power, specific energy, efficiency, safety and eco-friendliness while minimizing cost and maintenance requirements [5].
On one hand, specific energy and energy density are the amounts of electrical energy stored per kilogram of mass and per cubic meter of volume, respectively. On the other hand, specific power is the amount of power obtained per kilogram. Because removing the energy out of an energy storage quickly, which equates to high power, rapidly decreases the energy available, there is a clear trade-off between high specific power and energy [6]. This trade-off is a major factor affecting the mass adoption of EVs, because of its clear impact on the vehicle range and performance.
Different types of energy storages exist with different architectures to mitigate this trade-off.

In nearly all EVs, the battery is the component with the highest weight, volume and cost. Because of this, it is the element that is subject to most of the current research. It consists of at least two cells stacked together, called positive and negative electrodes, that convert chemical energy to electrical energy. Batteries have the benefit of being able to reverse this process and be returned to a charged stage by turning electrical energy to chemical energy. Other important parameters of a battery are the state-of-charge (SoC); the ratio of present charge capacity to fully charged capacity, life cycle; the number of cycles of charge and discharge it can go through and cost. Different technologies address these issues with different advantages and disadvantages:

- Lead-Acid battery;
- Nickel-metal hydride (Ni-MH) battery;
- Nickel-Zing (Ni-Zn) battery;
- Nickel-Cadmium (Ni-Cd) battery;
- Lithium-Ion (Li-ion) battery.

The latter being the most promising technology today, for its high energy density (140-200 Wh/l), high-temperature performance, high specific power (250-450 W/kg)

and long lifecycle (800-1200 cycles), as well as being recyclable. Its limitations, however, reside in its high cost and high self-discharge rates; which is the rate of discharge when unused [7].

Khajepour et al. [7] explains that in a typical drive cycle of an EV, the frequent stopping and starting of the vehicle is detrimental to the life cycle of the batteries. The design of batteries for EVs confer them with large energy density, for increased driving range at moderate speeds. However, rapid acceleration over short durations necessitate an energy storage with higher power density to be used at such moments where the power demand is up to 10 times higher than the rated power of the battery. Ultracapacitors are such an energy storage mechanism. They are large capacitors with high specific power and low specific energy. This high specific power can be used to provide additional power during accelerations and hill climbing, but also for capturing more energy during regenerative braking. If combined with batteries in a hybrid power storage system, each can boast their strengths while palliating for the others weakness. While it increases vehicle performance, extends battery life and shrinks it size, such a hybridization comes at a higher cost and structural complexity. Flywheels are an alternative, purely mechanical energy source. Original designs were bulky and heavy rotors operating at low speeds, that needed frequent recharge, but could operate a passenger bus. Current flywheels are made of lightweight materials and operate at very high speeds, in the order of ten thousand rotations per minute (rpm). They present a mechanical alternative to ultracapacitors, to be used in conjuncture with chemical batteries to provide high specific power in a hybrid energy storage system [7].

Electric Propulsion

The main components of the electric propulsion in an EV are the electric motor, the power converters and electronic controller. The electric motor is the key constituent in this system, as it provides the traction for the vehicle by turning the electrical energy provided by the energy storage to mechanical energy. In the event of deceleration or braking, it can also reverse that action and recharge the battery,

ultracapacitor or flywheel. The power converter provides the proper voltage and current to the electric motor, following the commands of the electronic controller. The latter also interprets accelerator and brake commands from the driver and appropriately produces a torque demand to the electric motor [5].

The design process of an electric propulsion system considers performance capabilities such as acceleration, maximum speed, hill climbing; vehicle constraints of volume and weight; the available energy source compatibility, and cost [5]. As depicted in the figure 1-3 below, modern electric motors include two modes of operation, namely constant torque and constant power. The latter is the ideal characteristic for automotive powertrains, offering high traction at low speeds until base speed for acceleration and hill climbing, and low traction at high speeds [7].

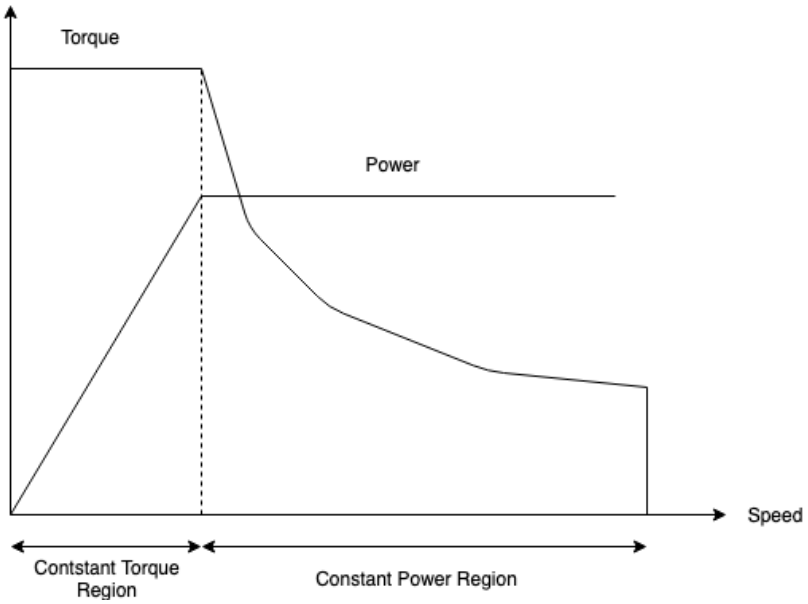

Figure 1-3 Electric Motor Typical Torque Speed Curve (See [5])

An important consideration for electric motors is their regions of high efficiency. It is defined as the ratio of output power to input power [7]. These regions are typically depicted in efficiency maps and are highly dependent on the type of motor at hand. The sources of losses affecting different designs are numerous, such as friction, copper, stray and mechanical losses [7].

Early electric motors were designed to use direct current (DC) motors with a commutator switch. These motors were simple to control and provided the sufficient traction requirements because of their torque-speed characteristics [5, 7]. Traditional DC motors include series excited, shunt excited, compound excited and permanent magnet (PM) excited motors [5]. These designs were ultimately phased out because of their high maintenance cost and heavy weight, low speed and low specific power [5].

Recent developments saw the rise of commutator-less, alternating current (AC) motors, who, though they come with a higher complexity, offer higher efficiency, power density, lighter weight and maintenance needs. The higher complexity is mostly due to the need to convert the DC from the energy storage to AC [7]. The three main types of AC motors currently used in the automotive industry are:

- Induction Motors (IM);
- Synchronous Motors;
- Switched Reluctance Motors (SRM).

Because of their different attributes, these AC motors are used in different applications. IMs are prevalent for larger vehicles such as trucks and buses, while synchronous motors are being adopted for passenger cars [7]. SRM are also considered for EVs but at the moment have too many disadvantages for mass adoption, such as acoustic noise and torque ripple [7].

Transmission

A transmission is the mechanism in any type of vehicle that manages the output torque and power of the engine or electric motor to the drive wheels. It consists of several gear ratios designed to achieve some pre-established performance, efficiency, drivability and cost specifications. The chosen strategy depends mostly on the speed-torque characteristics of the motor, with the most prevalent designs being [7]:

- Manual Transmissions (MT);
- Automatic Transmissions (AT);
- Automated Manual Transmission (AMT);
- Dual Clutch Transmissions (DCT);

- Continuous Variable Transmissions (CVT);

First, MTs are the oldest and most common type of transmission, with its history tracing back to the earliest automobiles. It transmits engine power by gear pairs on fixed axes from input to output, and is shifted between the different ratios by the driver. Because of their simplicity and long history of improvements, they remain the cheapest and among the most fuel-efficient forms of transmissions. The main components of such a transmission are the clutch, the gears, the shafts and the synchronized collars [7]. The driver, using the clutch pedal, disengages the engine from the transmission system. In that process, he/she can shift into gears of different size and number of teeth in order to change the engine torque and speed from the input to the output shaft of the transmission. The advent of the synchronizer, which matches the rotational speed of the gear and shaft during the shifting process, has greatly improved drivability and performance in cars equipped with MTs [8]. An important distinction is to be made between manual transmissions; typically used for powertrains where the engine and the drive wheels are at opposite ends, in a rear wheel drive (RWD) configuration; and manual transaxle, used when the engine and the drive-wheels are on the same end of the vehicle, in a front wheel drive (FWD) arrangement [7].

Second, ATs remove the burden of gear shifting from the driver. Instead, a control system makes gear selection and shift decisions as a function of engine load prediction, current vehicle speed and throttle position [7]. To achieve this, new components are introduced, such as a torque converter and planetary gear sets. The torque converter removes the need for a clutch, and is used to transfer the motor power to the gear unit in ICEVs [9]. Moreover, it greatly improves drivability by allowing to decouple the traction unit from the transmission; making the shifting smoother; providing torque multiplication at low speeds and preventing engine stalls [10, 7, 9]. The other main point of divergence with traditional MTs is the use of multiple planetary gear sets to achieve multiple gear ratios [7]. In short, a planetary gear set is composed of a sun, planet and ring gears of different sizes. The planet

gears, connected to the planet carrier, rotate around the sun gear at the center of the unit. The ring gear has internal teeth encircling the sun and planets. A series of clutches and band brakes allows specific rotation of gears, which in turn allows different gear ratios to be selected [9].

An intermediate solution between these two technologies, AMTs reproduce similar mechanical layouts as MTs, which allows them to keep their simplicity and high efficiency, and add an automatic shifting layer like ATs to improve drivability, efficiency and system lifecycle. This is done through the addition of sensors, clutch and gear actuators and a transmission control unit (TCU) [9].

Similarly, DCTs aim to combine the best of MTs and ATs, by allowing dynamic driving without manual shifting, and yet maintaining the fuel economy standards found in MTs [9]. They are designed such as two clutches; for two separate sub-gearbox configurations; forming two separate power paths; with the even and odd gear ratios, connect the traction motor to the driveline [9]. Torque is always transferred from the input to the output, and thus no torque interruption is observed.

Finally, CVTs offer continuous and step-less gear ratios, as opposed to all of the aforementioned technologies. This configuration allows the selection of the gear ratio that would place the traction motor in its optimum operating point [5]. This operation at the most efficient region thus enhances fuel economy, environmental friendliness and performance, while the absence of step gear ratios allows for higher acceleration and passenger comfort [7]. A specific type of CVT is the infinitely variable transmission (IVT) that allows a null gear ratio, effectively decoupling the traction motor from the driveshaft, allowing idling of the motor [7]. While market penetration is still fairly small, many CVT designs are currently researched. Currently available CVTs are spherical, hydrostatic, magnetic, ratcheting, cone, radial roller and toroidal CVTs [7].

Because of the wide speed range in most electric motors used in the automotive industry, typical EVs do not need the multitude of speed-ratios in their transmissions systems. Most commercial EVs today use a speed-reduction gearbox or a two-speed transmission to increase performance and efficiency or downsize the traction motor [8].

Drivetrain

The drivetrain is the last element to connect the electric motor traction to the road, and depends on the vehicle configuration. A typical scenario would see a driveshaft connecting the transmission detailed in the last section with a differential. The latter would then join the driven wheels through drive axel [5]. The differential is a gear box that directs the engine power to the pair of driving wheels, and allows the pair to rotate at different speeds during cornering [7]. Finally, the difference in gear size in the differential allows for a final step down of the overall gear ratios from the engine to the driven wheels.

1.3 Literature Review: EV Powertrain Efficiency

As described in previous sections, the biggest factors preventing mass market penetration of EVs are related to performance and range anxiety from potential buyers. To circumvent such limitations, private and public sector research is aiming at developing batteries with high specific energy, specific power and lifetime while maintaining an acceptably low cost [8,11,12]. Li-Ion have shown better performance compared to other types of batteries in terms of specific energy and specific power [8,12,13], which explains their larger market share for EVs. Current research and expert analysis predict that Li-Ion batteries will remain the most competitive technology for automotive applications in the short and medium term [12], with optimistic projections predicting their cost to go down to between $200 and $400/kWh [8]. Researchers are also exploring alternative, greener energy storage technologies, removing the need for rare metals in their composition [11] or using cleaner materials such as in Lithium-air or Zinc-air batteries [12, 14].

Battery lifetime is a fundamental facet to consider when analyzing for economic and environmental impact of EV utilization. Aspects limiting the lifetime are the aging of Li-Ion cells, electrolyte system and the thermal and energy management systems [11]. For range and performance reasons, batteries are considered for replacement when they fall to 80% of performance. This is an opportunity for repurposing the batteries for other applications, such as stationary energy storage systems [15,17,18]. While such a process is undoubtedly costly, it paves the way to a more sustainable lifecycle of batteries, from mining fewer primary materials to better waste disposals. Repurposing batteries could also offer economic incentives, such as storing off-peak energy and helping balance the energy grid [21].
In addition to repurposing batteries for post-vehicular usage, research shows that battery recycling can play a significant role in expanding the EV market. Government regulation for battery recycling would force manufacturers to produce larger quantities of EVs, to offset the research and development cost of battery recycling [20]. While vehicle (without battery) recycling is a simple and cost-effective endeavor, battery recycling is more complex due to its multipart physical and chemical composition [16,19].

With such an emphasis put on research to improve battery technology, and its economic, environmental and performance aspects, it is obvious that efficient use of the provided energy in the vehicle, from battery to wheel and road traction, is of paramount importance. Several electrification plans exist to transition from conventional combustion engine vehicle to fully electric vehicles, including hybrid, fuel cell and battery electric vehicles [5,22,23].

First, Hybrid Electric Vehicles (HEVs) are characterized by the use of two power sources, typically a combination of combustion engine and electric motor. The main issue remains the efficient delivery of energy from the sources to the loads, which means a more complex apparatus, electrical and mechanical, than in conventional ICEVs [22]. Different HEV configurations have been proposed, allowing for multiple

ways to connect the different components, defining specific energy flow routes and are classified as Series Hybrid, Parallel Hybrid, Series Parallel Hybrid and Complex Hybrid architectures [5,22,23]. The current dominating architecture for HEVs is the input-split configuration from Toyota and Ford, but other manufacturers such as General Motors (GM) are introducing other designs, such as the GM Volt's series-split powertrain [24]. The Toyota Prius couples an ICE, an alternator and an electric motor via a planetary gear set [22]. Studies also examine the effect of dual motor configurations, allowing improvements in tank to wheel efficiency, reducing battery size and maintenance costs [25]. Hybrid powertrains have the capabilities to dominate the world fleet in the near future, as they substantially reduce ownership costs, natural resources consumption and GHGs emissions [23]. Consumers appear more likely to adopt HEVs over full EVs at present, valuing maintenance and refueling cost savings primarily, while high initial cost and lack of government subsidies prevent adoption of plug-in EVs [26]. This trend is rapidly shifting however towards EV adoption.

Secondly, a fuel cell electric vehicle (FCEV) differentiates itself by generating energy from a fuel source, typically hydrogen, which provides longer range without shorter charging times compared to battery EVs [5]. The absence of combustion, as in ICEVs, by turning free energy into electrical energy, also improves overall energy efficiency while maintaining low tailpipe emissions. The previously stated advantages make FCEVs an ideal candidate for quick electrification of certain applications, such as public transportation and ride sharing [27]. Studies show that in their current state, FCEV emit less Well-to-Wheel GHGs than ICEVs, HEVs and EVs in certain countries, depending on the means of hydrogen and electricity production [28]. Fuel cells can also be used in hybrid (FC-HEV) and plug-in hybrid (FC-PHEV) electric vehicles, where the former presents lower costs and life cycle impact, while the latter could potentially achieve higher operation efficiencies [29]. From an economic perspective, [30] suggests that by the 2030 horizon, FCEV could achieve cost parity with ICEVs, but hints that BEVs and FC-HEV could realize even lower costs.

After investigating the different types of configurations currently suggested as a replacement for conventional ICEVs, the transmission component, or lack thereof, warrants a deeper investigation. Due to the outstanding flexibility and performance of electric motors, most BEVs today are equipped with a fixed ratio single reduction transmission, including the popular Nissan Leaf and Tesla Model S [31,32,33,34]. This is explained by the wide range of torques and speeds that the different types of electric motors can achieve, as is explained in section 1.2. While such configuration might have been deemed satisfactory for the first generations of EVs, it inevitably requires a trade-off between longer drive range and dynamic performance, depending on the single gear reduction ratio [33,34]. In addition, while an electric motor may achieve a wide range of torques and speeds, experimental testing shows that it does not achieve high efficiency over the entire range. This is due in large part to heat, hysteresis and eddy current losses, and can drop the overall efficiency of the motor by 30% in certain points, from 95 to 65% [33,35,36,37]. Operating the electric motor at its most efficient regions is desirable, and research [33,34,38,39,41] suggests that can be achieved using a transmission component. Limitations, however, reside in the added cost, longevity, weight, complexity of such an ideal transmission, and its own added mechanical inefficiencies. Adding a transmission system, depending on the selected type, has the additional benefit of downsizing the motor needed to achieve vehicle performance specifications [34].

Multiple designs for transmission systems exist in the literature, with the most prevalent being two speed transmissions [10,40,41,42] and continuously variable transmissions (CVTs) [42,43,44]. For both of the cited types of transmissions, one of the main areas of research in this regard is the development of mechanical designs to achieve the stated goals. Two-speed transmission designs based on planetary gear sets [10,40] or dual clutches [42] have been proposed. Research also delves on the selection of the best gear ratios, with a first gear selected for acceleration and gradeability performance, and a second gear for top speed [44]. CVTs on the other hand, allow the achievement of an infinite number of gear ratios within a specific range. This flexibility comes at a cost of complexity, with multiple architectures

attempting to achieve the best results, including belt and chain [43], half and full toroidal [45,46], hydrostatic [47], electronic [35,36] and electro-mechanical [37] continuously variable transmissions. The abundance of CVT designs in the literature demonstrate the interest for such a system in EV deployment, but also the lack of consensus for a valid design. This, in turn, explains the current lack of CVT market penetration. The presented works often fail to convey sufficient transmission efficiency, negating the gains achieved in operating the electric motor at its optimum point. Experts thus postulate that in order to maximize dynamic performance and energy efficiency, better controllers are needed for the CVT, as well as identification of loss mechanisms, and characterizing operating regimes for better transmission efficiency [43]. Both of these issues can be addressed by developing efficiency maps for the proposed designs, as a complement for electric motor efficiency maps [44]. Infinitely Variable Transmissions (IVT) are obtained by attaching a CVT to a set of planetary gears (PG) and a fixed ratio (FR) mechanism. A large set of gear ratios can be obtained, as well as achieving a null speed ratio where the output speed is null [44]. Different arrangements of CVT, PG and FR mechanisms have been suggested to maximize overall efficiency [52], including series and parallel configurations [48,49].

In order to test the potential of a given transmission system for performance, energy efficiency, and to a certain extent drivability, it is necessary to rely on modelling and simulation tools in the early stages. This model-based development phase is extensively used in research, both academic and in the industry, and is necessary to reduce costs and implementation times [50]. For powertrain simulation, a multi-physics approach is required to account for the mechanical power flow, as well as the electric energy expenditure. [51, 52] postulate that for an ideal design, optimization should focus on three levels, namely system layout, component selection and parametrization and optimal control. This can be done by simulating an entire powertrain, modeling the plant, synthesizing a controller and simulating the entire process [50]. Numerous studies have been conducted to validate simulation results

against experimental set-ups, either in Hardware-in-the-Loop (HIL) configurations [53,50] or using test vehicles [54,55].

1.4 Thesis Outline

This thesis first lays the foundation of the novel transmission design, as well as the electric vehicle simulation used to replicate operating a vehicle equipped with the CVT in chapter 2. In the subsequent chapter 3, each element of the simulation is analyzed. The results of the simulation are detailed in chapter 4. A discussion of the implications of these results is presented in chapter 5. Finally, a summary of this is provided in chapter 6, which then attempts to expose the limitations and opportunities for improvement of this work.

2 Design & Simulation of Continuously Variable Transmission

This chapter presents the background, design and kinematic analysis of a novel Continuously Variable Transmission (CVT) for electric vehicles, as well as the set-up of an electric vehicle fitted with the designed transmission. Because this CVT proposal is based on the Dual-Brake Transmission (DBT) presented in [10], it is beneficial to first describe this foundation. Next, section 2.2 presents the novel CVT design and the desired goals of such a device, before delving into the kinematic analysis of the transmission in section 2.3. The final section explains the range of gear ratios chosen for the CVT.

2.1 Dual-Brake Transmission Background

Mousavi [10,56,57] presents a novel, seamless, clutch-less and compact transmission comprising two planetary gear sets with common sun and common ring gears. The two gear ratios are achieved when a braking mechanism is activated to block either the sun or ring gears, allowing the different pitch diameter of the ring and sun gear in the first and second planetary to provide two distinct gear ratios. The input and output shafts are respectively connected to the carriers of the first and second stages; which allows gear shifting without a clutch, and thus a perpetual mechanical connection of the powertrain.

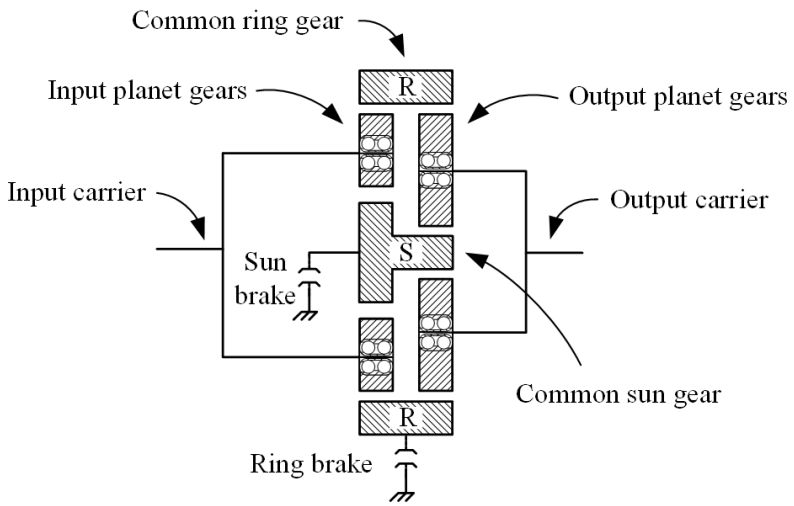

Figure 2-1 DBT Schematic Diagram (See [10])

The paths of power flow are highlighted in figure 2-2, with three existing paths. A first gear ratio where the ring is grounded, where the power transfer is done through the sun. A second gear ratio where the sun brake is active, and the power is transferred through the ring. Finally, a transition phase; here seen during the gear shift, where neither brake is active and both the ring and sun transmit power to the wheels. The braking mechanisms applied on the ring and sun are chosen to be of the dry, mechanical type, namely band and multi-plate respectively, in order to maximize energy efficiency [10].

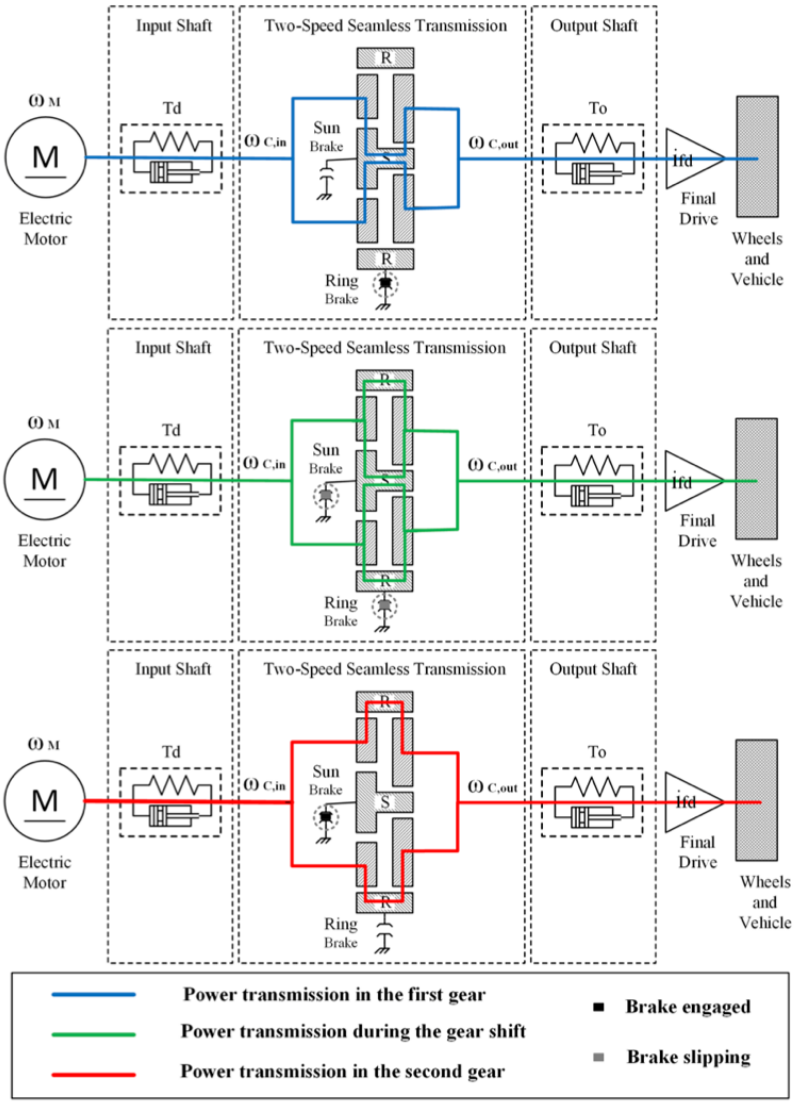

Figure 2-2 Schematic View DBT Transmission Paths (See [10])

The kinematic analysis between the carrier (C), sun (S), planets (P) and ring (R) of such a transmission mechanism is elaborated in [10]. The overall gear ratio (*GR)*, that is, the ratio of input to output speed, is largely dependent on the rotation speed of the ring (ω_r) and sun gear (ω_s), as well as the selected gear radii ratios of the ring and sun gear, $R_1$and R_2, in the first and second planetary gear set respectively. It is given by:

$$GR = \frac{\omega_{C,in}}{\omega_{C,out}} = \frac{(R_2+1)(\omega_s+R_1\omega_r)}{(R_1+1)(\omega_s+R_2\omega_r)} \qquad (2\text{-}1)$$

On the one hand, applying the ring brake ($\omega_r = 0$), gives a first gear ratio of:

$$GR_1 = \frac{\omega_{C,in}}{\omega_{C,out}} = \frac{(R_2+1)}{(R_1+1)} \qquad (2\text{-}2)$$

On the other hand, braking the sun gear ($\omega_s = 0$) gives a second gear ratio of:

$$GR_2 = \frac{\omega_{C,in}}{\omega_{C,out}} = \frac{(R_2+1)R_1}{(R_1+1)R_2} \qquad (2\text{-}3)$$

In [10], optimization design led to the selection of ring and sun radii ratios of R1 = 2 and R2 =4, in the first and second planetary set respectively, leading to a first and second gear ratio of GR1 = 1.667 and GR2 = 0.833. These values were then used for simulation and implemented on the test bed, available in the Intelligent Automation laboratory at McGill University, depicted in figure 2-3.

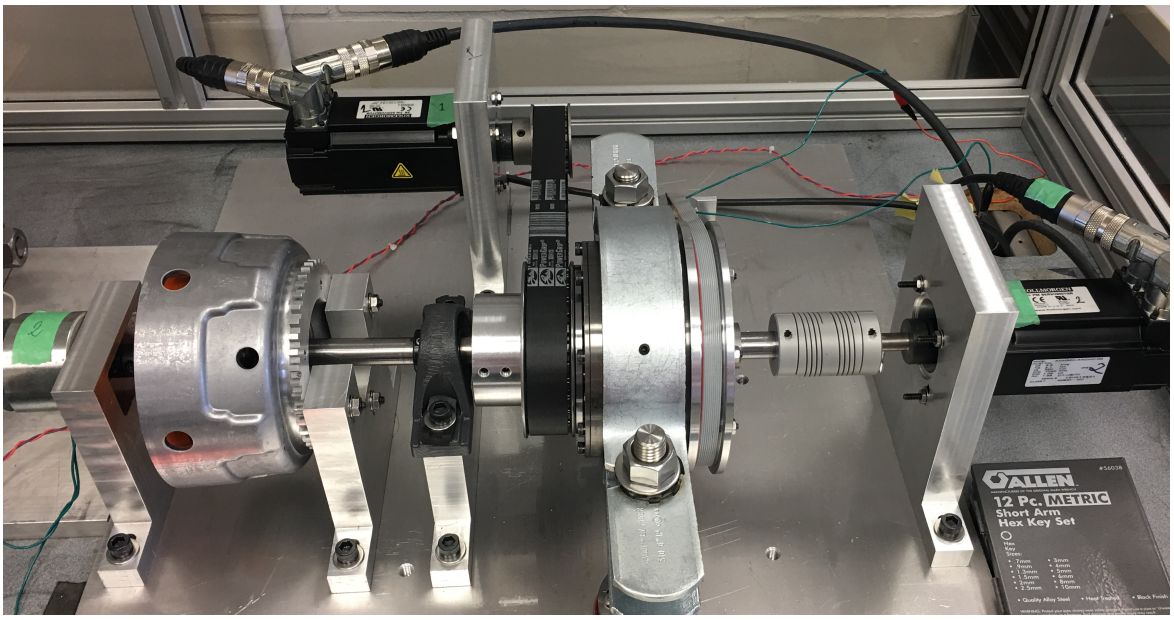

Figure 2-3 DBT Test bed, Intelligent Automation Laboratory, McGill

2.2 Design of the novel CVT

The presented design aims to make the most of the seamless, clutch-less nature of the DBT, as well as its high efficiency [10], while exploring the benefit of adding a range of achievable gear ratios, thus turning the mechanism into a continuously variable transmission. As explained in the literature review, CVTs allow the electric motor to operate in its highest efficiency regions more frequently, thus achieving lower energy consumption and overall GHG emissions.

This is achieved by placing an additional, smaller, torque-controlled electric motor connected to the common sun gears of the DBT, while disengaging the two braking mechanisms. This enables the operation of the transmission, in the transient gear ratio expressed in equation (2-4). By controlling the angular velocity of the common sun gears, given the current velocity of the input and ring gears, we demonstrated the ability of such a system to achieve a wide range of gear ratios.

This design proves worthwhile based on the observation that very low torque was required at the ring and sun brakes during the gear shifting process of the DBT. Mousavi notes that during gear shifting operations, the engagement and disengagement of the ring or sun gear, depending on the direction of the shift, facilitate the shift action by accelerating the on-coming gear and decelerating the off going gear. For example, during upshift, engaging the sun brake exerts a positive torque on the ring and negative torque on the sun gear, while gradually disengaging the ring brake has the inverse effect [10].

In addition to this new transient mode, the proposed system maintains the use of the braking mechanisms at the sun and ring gears, permitting the same underdrive and overdrive speed ratios. Certain modes of operations, such as rapid acceleration or high cruising speed, require the use of these extremum cases. The key difference is the population of the large step between the first and second gears with an infinite number of gears ratios.

The specified design is further explored in a kinematic analysis in the following section, and then simulated in MATLAB/Simulink to provide a proof of concept, proving the potential for energy consumption reduction and developing an optimal controller.

2.3 Kinematic Analysis

As explained in the previous section, we are interested in operating the DBT mechanism with neither sun nor ring brake activated, effectively using the transient gear ratio described by the equation:

$$GR_T = \frac{\omega_{C,in}}{\omega_{C,out}} = \frac{(R_2+1)(\omega_s+R_1\omega_r)}{(R_1+1)(\omega_s+R_2\omega_r)} \qquad (2\text{-}4)$$

Which can be rewritten to find the value of ω_s that will achieve a desired gear ratio GR_D:

$$\omega_s = \omega_r \times \frac{R_2(R_1+1)-GR_D R_1(R_2+1)}{GR_D(R_2+1)-(R_1+1)} \qquad (2\text{-}5)$$

This means that, at any point in time during operations, the transmission can be controlled to achieve a speed ratio that would place the electric motor at a more efficient operating point, by setting the corresponding sun gear velocity.

For acceleration purposes, when underdrive is needed to maximize torque, the transmission brakes the ring gear to achieve an underdrive gear ratio of GR1 = 1.667, as found in the DBT. Once the electric motor is operating in a more strategic region, we start controlling ω_s to decrease the gear ratio, optimizing the input motor along the power lines in its torque speed curve. A maximum speed is forced on the sun gear, which is the speed bringing ω_r to zero, where the sun brake is now activated. This later condition corresponds to the second gear ratio of the DBT, namely GR2 = 0.833, or overdrive operation.

2.4 Electric Vehicle Simulation

In order to gain insight on the potential of this new CVT configuration, we implement a full electric vehicle simulation, and fit it with the CVT. This simulation aims to measure the effect of using this CVT and compares the energy efficiency achieved

over multiple drive cycles when compared to using the DBT or single speed configuration.

2.4.1 Testing Blocks

A simplified electric vehicle is used to implement this test. It includes a torque controlled electric motor, with defined torque speed characteristics and efficiency map. A longitudinal driver is used to track different drive cycles and sends out acceleration or deceleration commands to the motor. The torque generated is transmitted into the tested transmission, before going into a final drive consisting of the differential and the wheels. These three later stages define the overall speed ratio observed between the electric motor output speed and the vehicle speed.

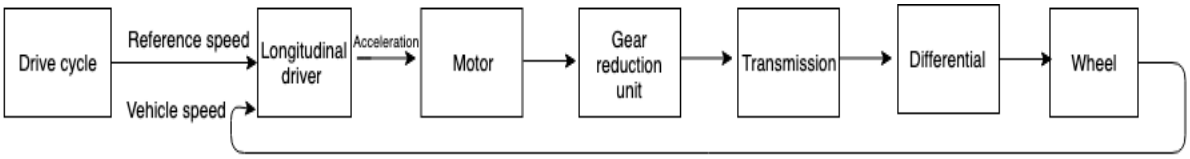

Figure 2-4 Configuration of Electric Vehicle Simulation

Vehicle acceleration, deceleration and cruising at a constant speed all require overcoming resistances: aerodynamic resistance, tire rolling resistance, powertrain friction, gravity and inertia [9]. The SimDriveLine vehicle body block is used to measure the vehicle speed given normal forces applied on the wheels. This block considers the aforementioned resistive forces.

2.4.2 Efficiency Metrics

The main objective of this simulation is to measure efficiency improvements achieved with the novel CVT design. Overall electrical efficiency, as well as vehicle range, are two metrics to measure this improvement. Overall electrical efficiency measures the ratio of mechanical energy outputted by the vehicle to the electrical energy consumed. It encompasses the efficiency of all the components, including electric motor, transmission system and battery. Range, on the other hand, measures the distance a

vehicle equipped with a powertrain can travel given an initial battery capacity and charge.

As discussed in the literature review, these two metrics are heavily influenced by the driving style of the vehicle. Aggressive driving with rapid and frequent changes of velocity, either by acceleration or deceleration, would output extremely different figures than a cruising at constant speed. The former would be typically found in city driving patterns, whereas the latter is usually found when driving on a highway. For this reason, it is of interest to compare the different efficiency metrics described over multiple driving cycles, mimicking a multitude of EV driving scenarios.

3 System Analysis Optimization & Control

This chapter is dedicated to the implementation of a simulation of an electric vehicle, equipped with the designed continuously variable transmission. This simulation is conducted using MATLAB/Simulink modeling, and with the mechanical components of the powertrain modeled using the SimDriveLine library. Figure 3-1 outlines the structure of the simulation.

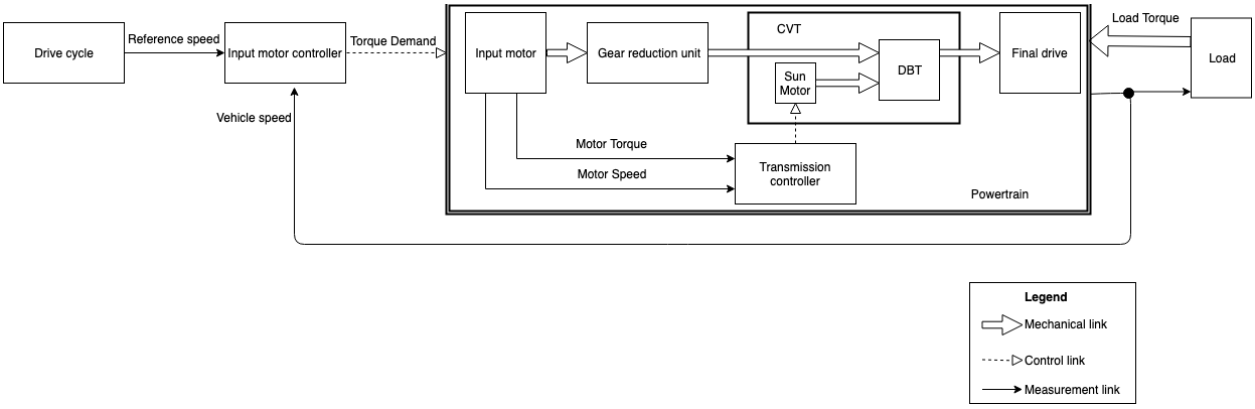

Figure 3-1 EV simulation equipped with CVT

The simulation set up consists of an EV powertrain implementation, containing an input motor, a gear reduction unit, the designed CVT and a final drive. For the sake of testing, the tested CVT can be replaced with any other transmission system, or by a simple gear reduction unit to test for single speed transmission configurations. In addition to the powertrain, a driver following a desired drive cycle delivers a torque demand to the input motor, and a load is simulated as a function of the vehicle speed. The last section details the design of an optimal transmission controller, that sets the gear ratio of the CVT as a function of both the input motor torque and speed. This implementation is pictured in the figure 3-2.

3.1 Powertrain Simulation

The figure 3-3 details the entirety of the EV powertrain simulation. Green elements and connection represent SimDriveLine components and mechanical connections. Black elements and connections are regular Simulink connections

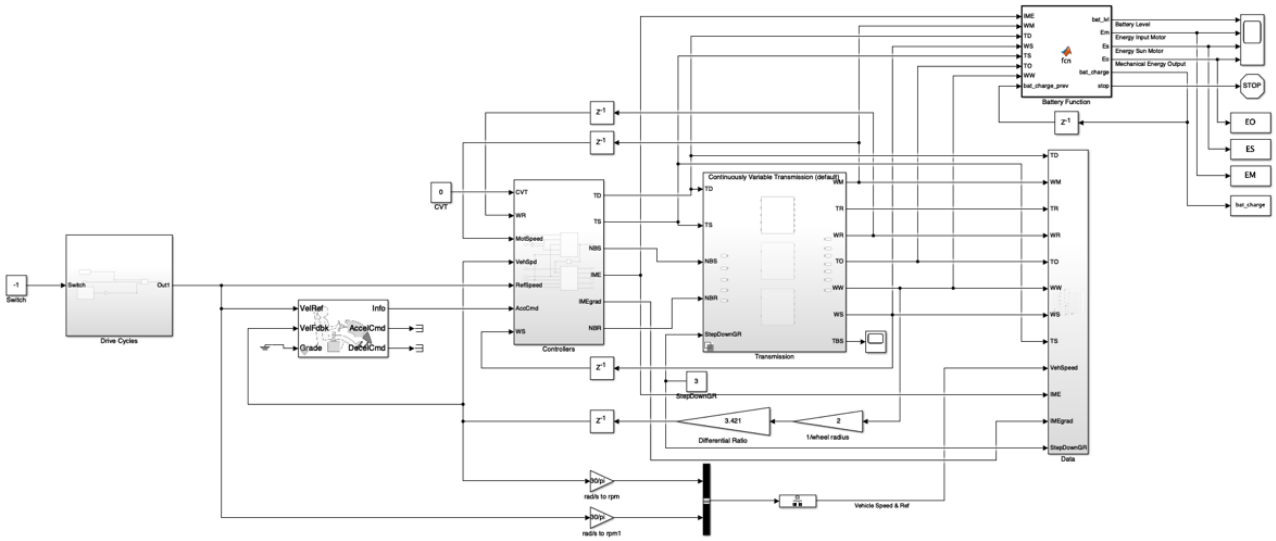

Figure 3-2 EV Simulink block diagram

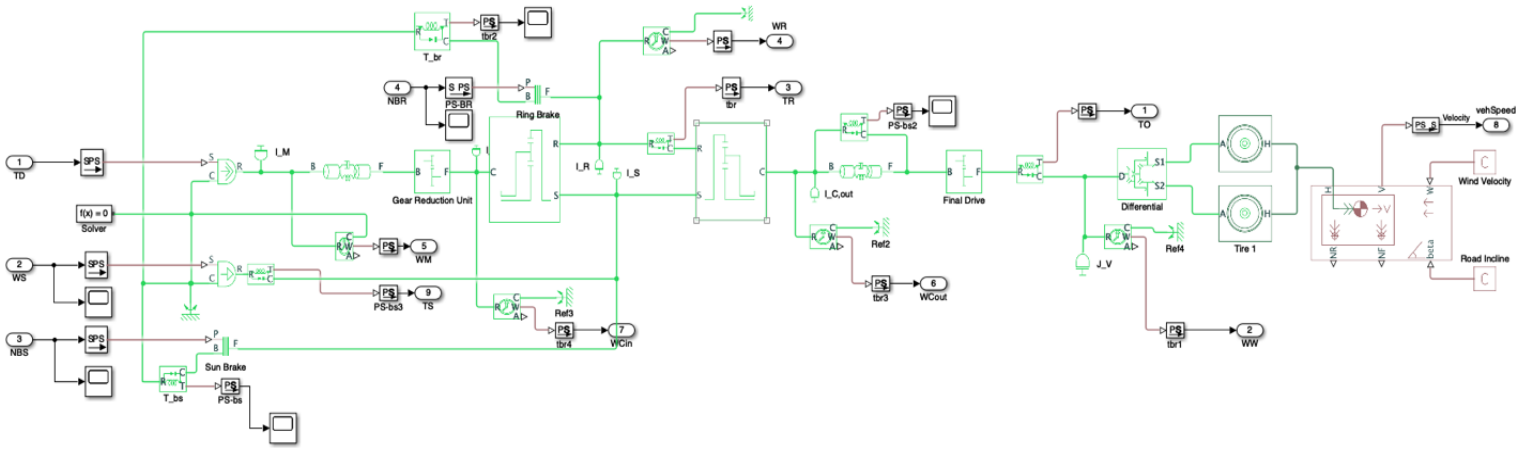

Figure 3-3 Powertrain with CVT Simulink block diagram

3.1.1 Powertrain Parameters

The simulation parameters are based on the MY 2013 S trim Nissan Leaf [32]. The vehicle body characteristics of mass, dimensions and drag coefficient are all used to accurately represent said vehicle, which is then equipped with the DBT and CVT. The synchronous motor of the vehicle is also simulated, in addition to the vehicle battery. The masses, moments of inertia of each component, as well as the viscous and friction coefficient of the braking mechanisms of the DBT testbed were derived in [10] and used in the following simulation. The values obtained were identified using the MATLAB System Identification Toolbox. The selected figures are detailed in the following table.

Category	**Parameter**	**Value**	**Unit**
Vehicle	Curb Weight	1580	kg
	Frontal Area	2.8	m^2
	Drag Coefficient	0.28	unitless
Environment	Air Density	1.2041	$kg.m^{-3}$
Input Motor	Maximum torque	280	N.m
	Maximum Speed	10000	rpm
	Rated Power	80	kW
	Base Speed	3000	rpm
Transmission	Input Carrier Moment of Inertia	1.8×10^{-3}	$kg.m^2$
	Common Ring Moment of Inertia	3×10^{-3}	$kg.m^2$
	Common Sun Moment of Inertia	8×10^{-4}	$kg.m^2$
	Output Carrier Moment of Inertia	6×10^{-3}	$kg.m^2$
	Planetary Set 1 Ring/Sun Radii Ratio	2	unitless
	Planetary Set 2 Ring/Sun Radii Ratio	4	unitless
Differential	Differential Ratio	7.94:1	unitless
Wheel	Wheel Radius	0.31623	m
	Tire Rolling Resistance Coefficient	0.015	unitless
Battery	Capacity	24	kWh

Table 3-1 Simulation Parameters

3.1.2 Input Motor

The 2013 Nissan Leaf is equipped with an 80kW synchronous motor [32], of which the characteristics are presented in table 3-1. [58] presents the torque-speed efficiency map of the latter motor combined with the Leaf inverter. This map was obtained by measuring at a DC-link voltage of 375V, a frequency of 5kHz and a Water-Ethylene Glycol temperature of 65°C [58]. It is presented below in figure 3-4, and presents a wide operation range at above 90% efficiency, with up to 96% achieved between 6500 and 9000 rpm. However, as is typically seen in synchronous motors, the efficiency drops at low speeds to under 70%.

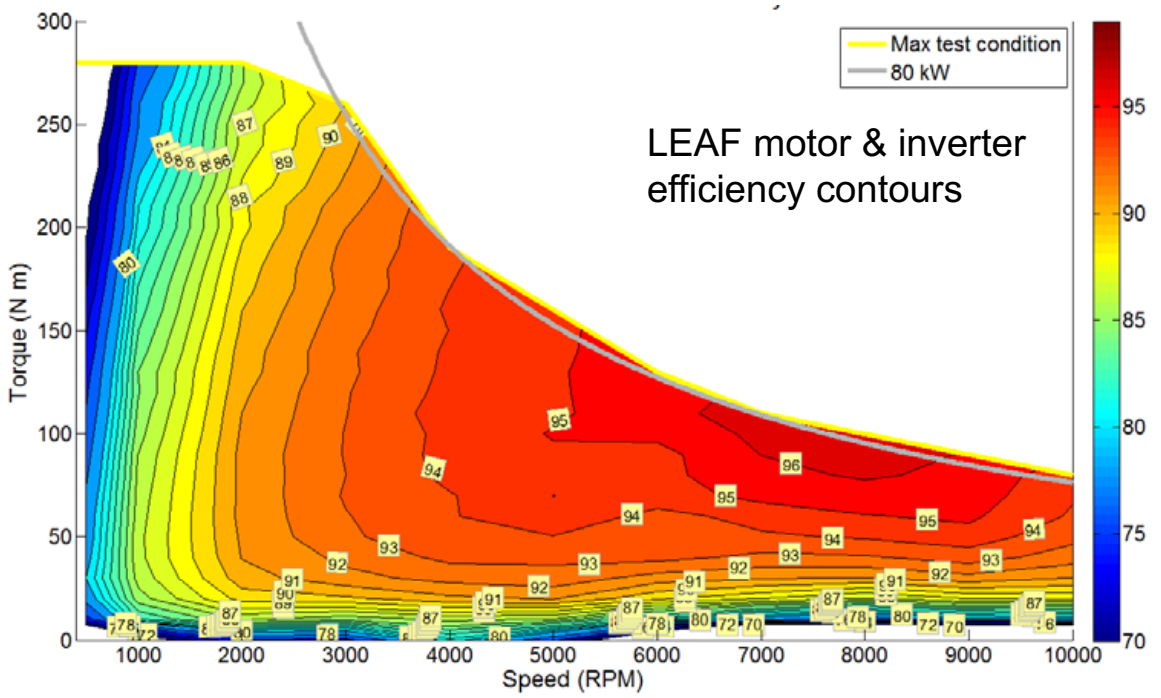

Figure 3-4 Combined LEAF Inverter & Motor Efficiency Map [58]

This map is imported to Simulink using a two-dimensional look-up table, where each pair of speed and torque are associated with an efficiency percentage. The rest of the map is interpolated from the inputted values using cubic spline. This means that the richer the data set provided to the 2D look-up table, the more accurate the reproduced efficiency map will be. Table 3-2 shows the look-up table data, while figure 3-5 presents the reconstructed efficiency map.

	0	5.25	15.75	26.25	36.75	47.25	57.75	68.25	77.7	88.2	98.7	109.2
0	0	0	0	0	0	0	0	0	0	0	0	
200	40	70	78	80	80	80	80	78	78	78	78	
400	40	70	81	83	83	83	83	83	82	82	81	
600	40	78	84	85	86	86	86	86	85	85	85	
800	40	78	85	86	87	87	87	87	87	87	86	
1000	70	80	85	87	88	88	88	88	88	88	87	
1200	70	81	86	88	89	89	89	89	89	89	88	
1400	70	81	87	89	89	90	90	90	90	90	89	
1600	70	81	87	89	90	90	91	91	91	91	90	
1800	70	81	88	90	91	91	91	91	91	91	91	
2000	70	82	88	90	91	91	91	91	91	91	91	
2220	70	82	88	90	91	91	92	92	92	92	92	
2420	70	82	88	90	91	92	92	92	92	92	92	
2620	70	82	88	90	91	92	92	92	92	92	92	
2820	70	82	88	90	92	92	93	93	93	93	93	
3030	70	82	88	91	92	92	93	93	93	93	93	
3230	71	82	88	91	92	93	93	93	93	93	93	
3430	71	82	88	91	92	93	93	93	93	93	93	
3640	71	82	88	91	92	93	93	93	93	94	94	
3840	72	82	88	91	92	93	93	94	94	94	94	
4040	72	82	88	91	92	93	93	94	94	94	94	
4250	74	82	88	91	92	93	93	94	94	94	94	
4450	74	83	90	92	92	93	94	94	94	94	94	
4650	74	83	90	92	93	93	94	94	94	94	94	
4850	72	82	88	92	93	93	94	94	94	94	94	

Table 3-2 2-D Look-up Table for input motor efficiency map

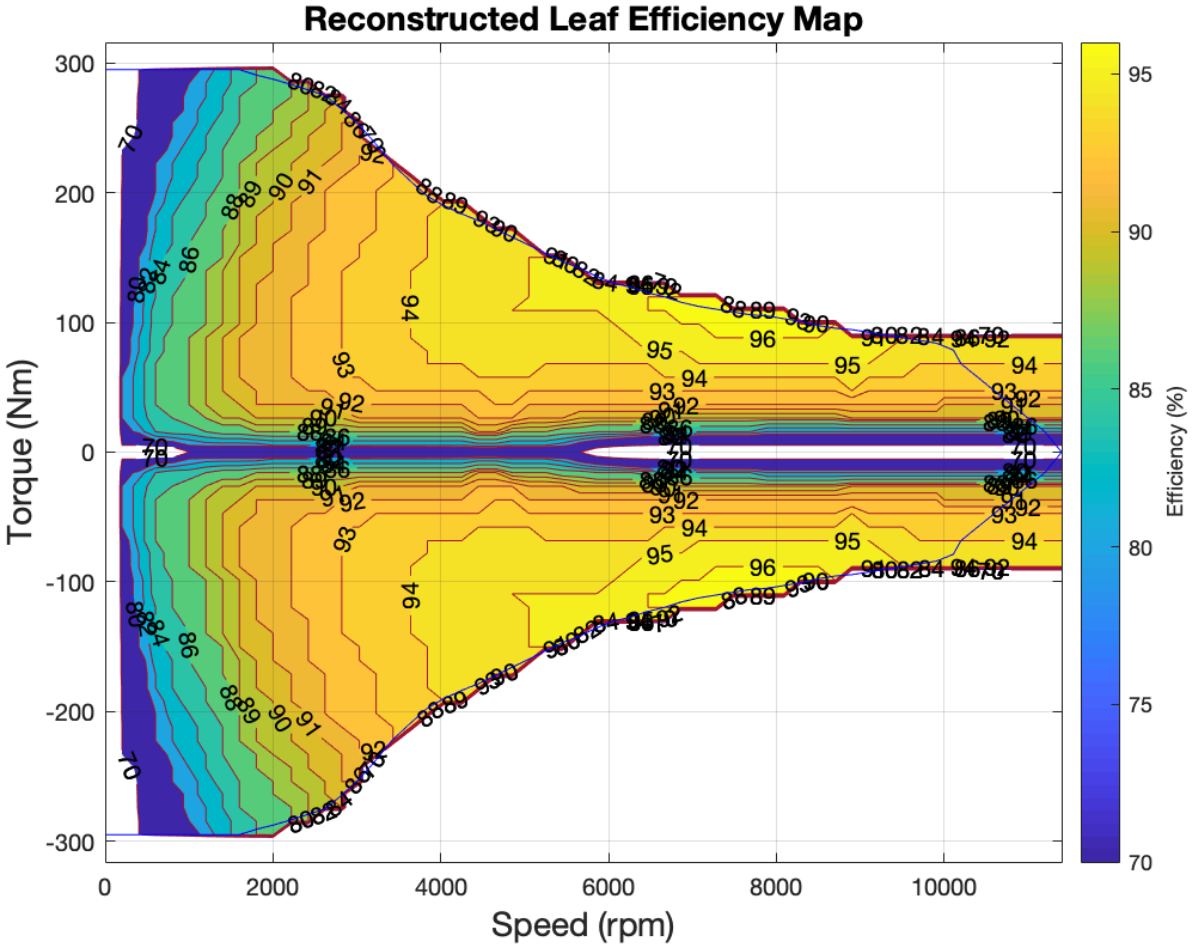

Figure 3-5 Reconstructed input motor efficiency map

3.1.3 Gear Reduction Unit

A gear reduction unit is placed between the electric motor and the transmission. This allows to reduce the angular velocity observed at the input of the CVT. The purpose of this speed reduction is to avoid unnecessarily large speeds within the two planetary gear sets, as it is postulated that within specific conditions, the sun gears would spin three times as fast as the input shaft of the transmission. A high speed at the sun would cause undesirable side effects, such as vibrations, noise, as well as requiring a faster motor connected to the sun gears.

$$\frac{\omega_{GR,in}}{\omega_{GR,out}} = 3 \quad (3\text{-}1)$$

3.2 Transmission

The continuously variable transmission is implemented using two planetary gear set blocks from the SimDriveLine library. The teeth ratios are set to be R1 = 2 and R2 = 4, respectively, following the design of the experimental test bed. The sun and ring gears of these two blocks are perpetually connected with each other.

The band brake used on the ring gear, and the plate brakes on the sun from the DBT design are maintained in the simulation. In addition, an ideal torque source is used to simulate an additional electric motor connected directly to the sun gear, henceforth, the Sun Motor. This motor is assumed to be smaller than the traction electric motor of the electric vehicle.

The set up for the DBT is the same, except the additional electric motor is removed. For single speed testing, the transmission block is removed entirely.

3.2.1 Final Drive

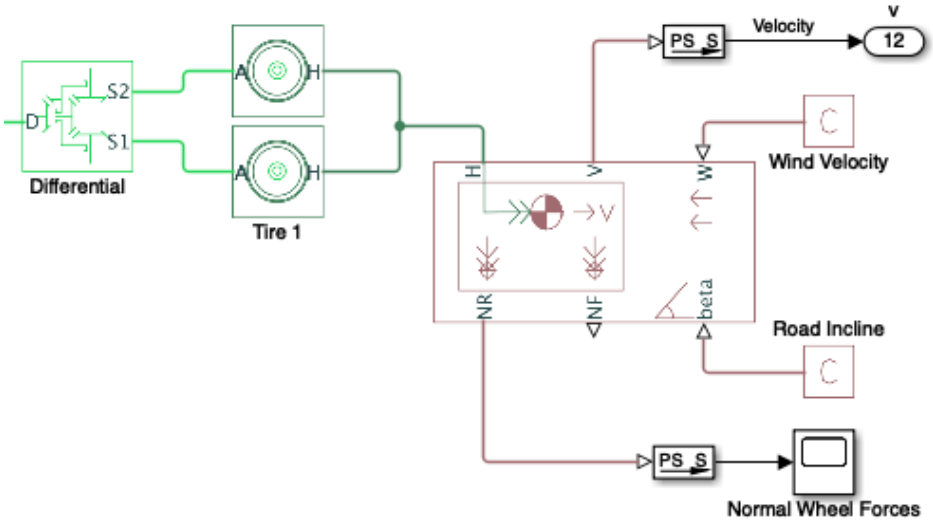

Figure 3-6 Final Drive

We simulate the effect of the differential and the wheel size on the overall gear ratio of the powertrain using a final drive block.

A typical vehicle differential permits, in addition to letting the outer drive wheel to rotate faster than the inner drive during vehicle turn, an additional gear reduction. The relationship of speed at the input to the output of the differential, chosen for the simulation when equipped with DBT and CVT, is:

$$\frac{\omega_{D,in}}{\omega_{D,out}} = 2.07 \quad (3\text{-}2)$$

3.3 Driver Simulation

3.3.1 Drive Cycle

We use the Simulink drive cycle source, which generates a reference speed based on a pre-specified drive cycle file. The Drive Cycle Data support package contains the most commonly used drive cycles, but this block also permits importing custom made drive cycle data files if needed. The block also allows for cyclic repetitions of drive cycles, which is useful when it comes to testing the vehicle over longer periods of time, as well as normalizing data across different drive cycles.

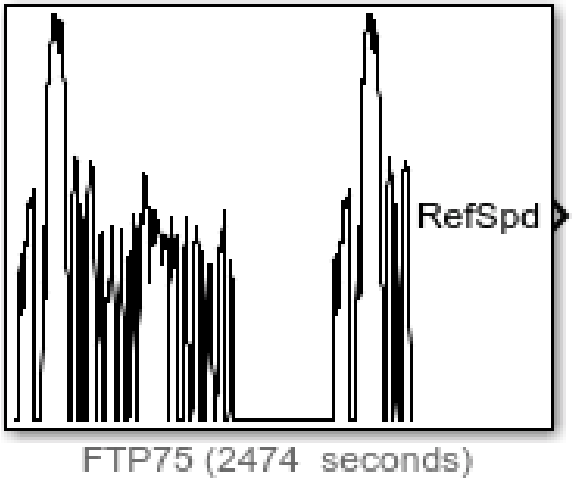

Figure 3-7 Drive Cycle Simulink Block

3.3.2 Longitudinal Driver

A Simulink longitudinal driver block is used in order to track the drive cycle reference velocity, compared to the feedback velocity of the vehicle, both of which are expressed in meters per second. This block generates normalized acceleration and deceleration commands, with values ranging from 0 to 1. The driver is set up as a Proportional-Integral (PI) controller, with tracking windup and feed-forward gains. Careful selection of the controller gains is performed to limit tracking error and overshoot.

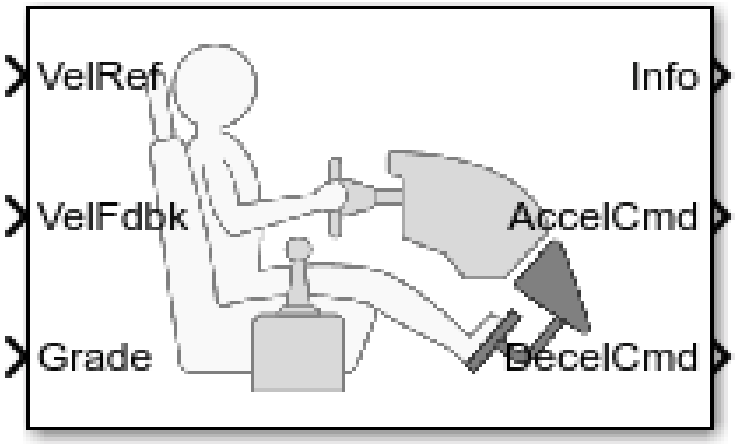

Figure 3-8 Longitudinal Driver Simulink Block

3.3.3 Input Motor Controller

Given a drive cycle test, and the acceleration and deceleration commands provided by the longitudinal driver, a controller is designed to output the corresponding torque demand on the input motor of the vehicle to appropriately track the reference velocity.
First, a real-life vehicle acceleration pedal is simulated, using a two-dimensional look table outputting a percentage of pedal "pressing" depending on the current vehicle speed and the acceleration command of the longitudinal driver. In other words, at low speeds, small acceleration command would output relatively higher pedal pressing than the same acceleration command at high speeds. At high speeds, only a very high acceleration command would equate to a large pressing of the pedal.
Following this, a 1-D look-up table is used to model the torque speed curve characteristics of the input motor. It maps the current speed of operation of the motor to maximum available torque it can provide. The pedal and available torque values are then multiplied to output the torque demand of the input motor.
On the other hand, this same torque available value at the current speed of the vehicle is multiplied by a ramped braking command, the negative of which corresponds to the torque demand when the vehicle is decelerating.
Only one of these positive or negative torque demands are sent to the motor, depending on the whether the acceleration is positive or null. This torque demand is sent to an ideal torque source Simulink block, and is used to drive the rest of the powertrain.

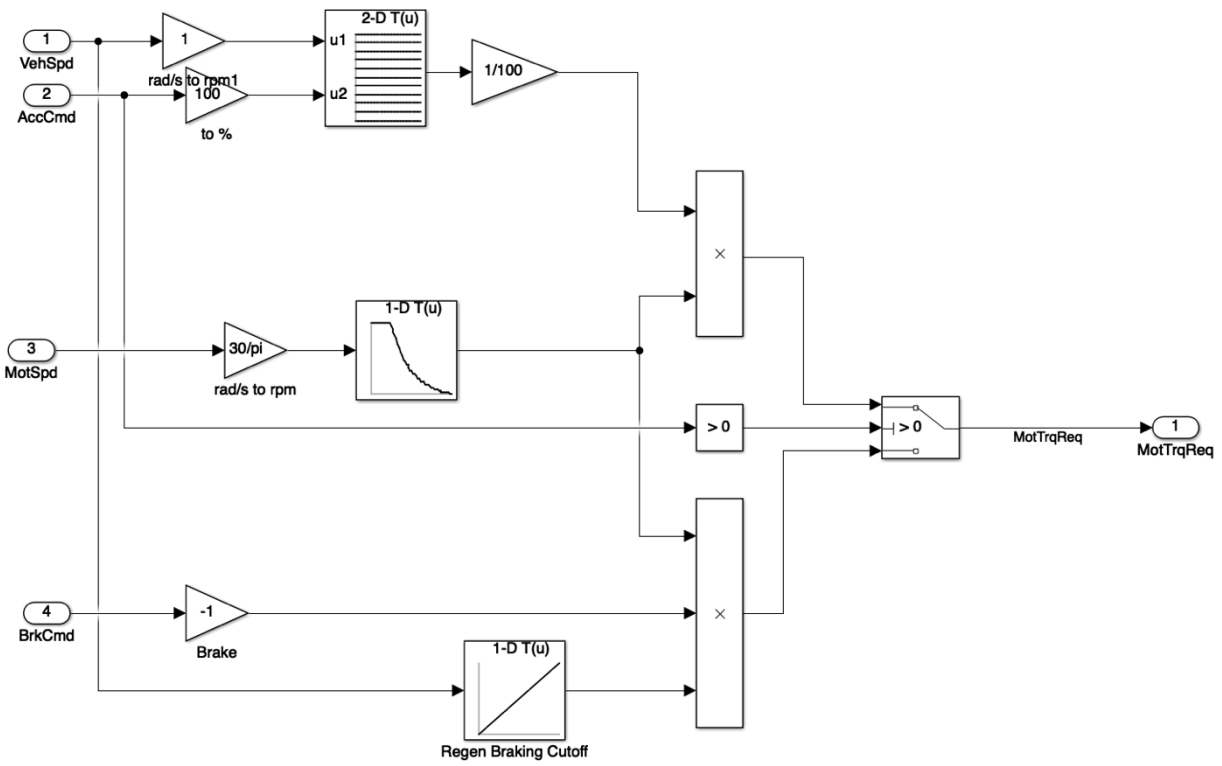

Figure 3-9 Input Motor Controller Simulink Block Diagram

3.4 Energy Management

In order to properly measure energy efficiency of the vehicle, an energy management platform is used. This platform contains an accumulator to simulate a battery, calculate the energy use of the different powertrain components, and account for losses when using electrical energy.

3.4.1 Battery Accumulator

As explained in the literature review, simulating an electric battery is no simple task, and has been the subject of multiple studies. Many factors can affect battery capacity and charge depletion, such as temperature, voltage and composition. This study aims at comparing energy efficiency savings through the usage of a transmission system, by comparing results of different transmissions on the same EV model. It is thus not necessary to create the most accurate battery model, and a preference is given for simplicity.

A simple accumulator is used to model the vehicle battery. It specifies a battery capacity of 24 kWh, and an initial state of charge (SoC) of 90%. This accumulator can be discharged when different components require electrical energy, namely the two electric motors. It can also be recharged if energy is generated through braking by either motor.

Constraints are imparted on this accumulator, as it cannot surpass a maximum SoC of 100%. It also stops the simulation, and thus defining maximum range, if the SoC falls below a specified threshold. This threshold is chosen to be 10% to closely resemble real life scenarios.

3.4.2 Electrical Efficiency

As explained in 3.1.2, the input motor efficiency is a major focal point of this analysis. As detailed in the literature review, while electric motors can achieve a wide range of torques and speeds, their efficiency can greatly vary across that spectrum. The simulated model of input electrical motor has efficiency $\alpha_{input\ motor}$ varying from 50 to 98%, depending on the region of operation. In this simulation, the instantaneous mechanical power of either motor at each iteration is calculated using the following:

$$P_{motor,inst} = \omega_{motor} \times T_{motor} \qquad (3\text{-}4)$$

Where ω_{motor} and T_{motor} are the current speed and torque of the motor, respectively. The corresponding mechanical energy is obtained, given a simulation step of Δt, by:

$$E_{mech} = P_{inst} \times \Delta t \quad (3\text{-}5)$$

Finally, the electrical energy drawn from the battery, depends on α, the efficiency of the motor at that specific operating point, following:

$$E_{elec} = \frac{E_{mech}}{\alpha_{motor}} \qquad (3\text{-}6)$$

If E_{elec} is positive, the motor is drawing energy from the battery, and that is reflected in a depletion of the battery accumulator SoC. However, if E_{elec} is negative, the electric motor is said to be acting as a generator and increases the battery SoC. This increase in charge must account for the energy lost in the process, and is reflected by an efficiency factor $\alpha_{recharge}$ in the battery recharge.

These calculations are made at each iteration of the simulation for both motors. Based on the assumption that the Sun Motor is much smaller than the Input Motor, its efficiency $\alpha_{sun\ motor}$ is presumed to have a small impact on the overall energy consumption. It is however varied, as it determines the efficiency of the CVT mechanism compared to the DBT.

Finally, as explained in the literature review, the main factor preventing mass adoption of CVTs is the assumption that their efficiency might offset the gains made in electric motor efficiency. For the sake of comparing the different transmissions tested in this study, different values are given to the efficiency of the CVT, the DBT and SST modes.

In particular, the CVT simulation is performed with the same efficiency as the DBT, since it is the same mechanism. The addition of the sun motor introduces a level of inefficiencies that is considered in the sun motor efficiency parameter. The following table presents the values chosen for the aforementioned parameters.

Parameter	**Value** (unitless)
$\alpha_{input\ motor}$	Varies between 0.5 and 0.96
$\alpha_{sun\ motor}$	Varies between 0.85 and 0.99
$\alpha_{recharge}$	Varies from 0.90 to 0.99
$\alpha_{ring\ brake}$	0.98
$\alpha_{sun\ brake}$	0.98
α_{CVT}	0.97
α_{DBT}	0.97
$\alpha_{single\ reduction}$	0.99

Table 3-3 Simulation Efficiency Parameters

3.5 CVT Optimal Control

3.5.1 Transmission Controller

The transmission controller designed for the CVT is a real-time controller that, given the current speed of the vehicle and operating point of the electric input motor, can utilize the sun and ring brakes, as well as vary the speed of the Sun Motor, to modify the gear ratio of the transmission in order to operate the input motor in its optimal region. This controller is presented in the MATLAB script presented in Appendix A.
When the tracked reference speed of the vehicle is null, the drive management unit outputs zero torque demand, and thus the whole system is inactive. It is unnecessary to activate either braking mechanisms as it would result in energy losses.
As the reference speed starts increasing, the CVT controller activates the ring brake, and lets the sun gear freely spin. This recreates the underdrive ratio of GR1 = 1.6667 found in the DBT, necessary during phases where high torque is needed for acceleration.
As the vehicle exceeds a predetermined threshold speed, the CVT controller releases the ring gear. The transmission now has a gear ratio GR_T detailed in equation (2-4). The controller varies the speed of the Sun Motor, ω_S to achieve a desired gear ratio, given the angular velocity of the ring gears. The selection of ω_S is made in real time following the optimization technique detailed in the following section. It is however constrained to a maximum value to prevent ω_R spinning negatively.
At high speeds, when overdrive is desired, the Sun Motor decelerates the sun gears. Once the latter reaches an appropriately low speed, the CVT controller activates the sun brake, achieving the overdrive gear ratio GR2 = 0.883 of the DBT.

3.5.2 Power Lines Optimization

The optimization of the gear ratio of the CVT is a line search performed in real-time by the controller. This search is performed along power lines of the input motor torque and speed curve. At each simulation iteration, multiple points corresponding to equivalent input motor power but different speeds; are selected, and the corresponding input motor efficiency (IME) is inferred from the two-dimensional look

up table presented in 3.3.3. The highest efficiency is selected and determines the direction the CVT should move towards. Increasing ω_S increases the observed gear ratio of the transmission, while decreasing the former subsequently decreases the latter. In turn, increasing the gear ratio displaces the operating point of the input motor in the right direction of increasing speed and lowering torque. This indirect relationship between ω_S and the input motor operating point is fundamental to this design.

The line search is facilitated using a pre-calculated normalized gradient mapping of the IME, also made using a two-dimensional look-up table. This gradient, noted ∇IME, varies from -1 to 1, and is a representation of the direction the gear ratio of the CVT should move the operating point of the input motor. Using this value, the line search can anticipate the direction of search, as well as reduce the step size of the search for lower absolute values of ∇IME, which demonstrate a proximity to the optimal operating point.

Figure 3-10 illustrates this line search. The red curve represents operating points of equivalent power, and the green section denotes the achievable points given the range of CVT gear ratios. The red cross is the current operating point of the motor, blue crosses are the different tested gear ratios.

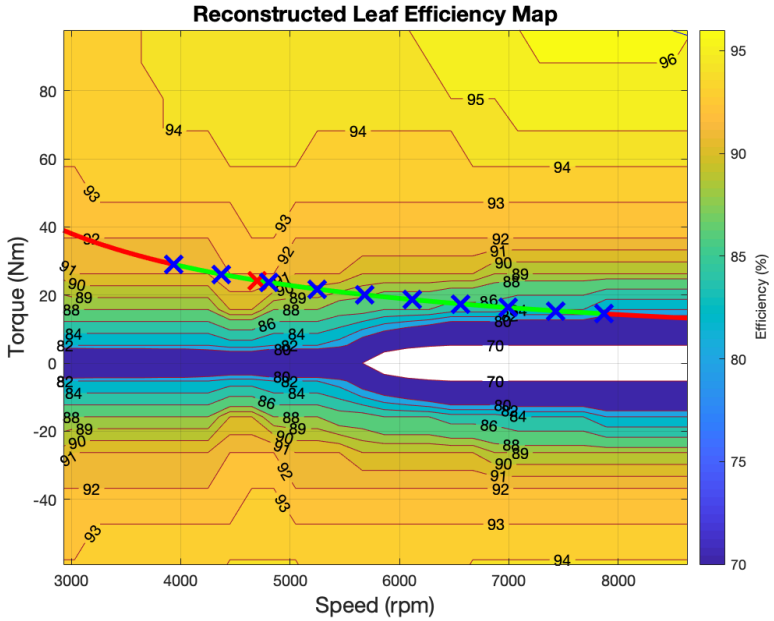

Figure 3-10 Power Line Search in the Efficiency Map

4 Simulation Results

4.1 Testing Protocol

Having presented the framework of the electric vehicle simulation, the obtained results are presented in this chapter. These simulations follow a strict protocol to allow for depiction of key differences between the designed CVT, the DBT and a SST mode. Simulations are also conducted with different driving cycles, given the major discrepancies in efficiency depending on the driving style of the EV.
To obtain a range of the vehicle equipped with a given transmission within a specific driving style, a different set of simulations is allowed to run indefinitely and stopped when the battery level falls below a desired threshold of 10% SoC. Battery capacity and initial state of charge are kept constant. This allows proper measurement of vehicle range given identical battery settings and varying transmission systems.

Another variable kept constant throughout testing is the gear switch breakpoint of the DBT, which is shown to have a great influence over performance and efficiency results. While optimizing this value is not the primary objective of this work, a sufficiently good value must be used to legitimize this comparative study. The transmission control unit (TCU) for the DBT switches gears when the vehicle speed exceeds 65 km/h. This speed is selected to maximize operations in the high efficiency regions of the motor. A tolerance band is used, while discriminating acceleration and deceleration of the vehicle, and thus preventing the phenomenon known as gear hunting. This phenomenon happens when the vehicle frequently accelerates and decelerates around the gear shift value, resulting in the TCU going back and forth between gear ratios.

In addition, efficiency values in the Sun Motor of the CVT, the braking mechanisms used in the DBT and the CVT, and the battery recharge are kept constant across all simulations. However, as explained in the previous section, no definite value is

measured for the CVT mechanism efficiency, and simulations are performed varying only that number across a realistic, an optimistic and a pessimistic value.

Finally, the parameters of the driver PID controller are kept constant. These values are selected to best track drive cycle, avoiding error accumulation or over actuation of the motor speeds, resulting in overshoot or oscillations.

Measurements include speed tracking accuracy, input motor average efficiency, overall energy efficiency, and vehicle range. First, speed tracking accuracy is measured by averaging the percentage of the error at each sample. At each sample, the percentage error ζ_{sample} is measured as:

$$\zeta_{sample} = \frac{|v_{ref} - v_{sample}|}{v_{ref}} \times 100 \qquad (4\text{-}1)$$

$$\varphi = 100 - \mu(\zeta) \qquad (4\text{-}2)$$

where φ is the tracking accuracy and $\mu(\zeta)$ the average of all errors.

The average Input Motor Efficiency (IME) is read from the 2-D table presented in the previous chapter, representing the efficiency map of the motor.

The overall energy efficiency is the ratio of mechanical energy at the output of the vehicle, $E_{mech,output}$, to the consumed electrical energy. Multiple elements are consuming electrical energy in the system, including the motors, the brakes, and the losses in the system. The motors, when acting as generators, can produce energy to refill the battery. The computation for overall energy efficiency $\alpha_{overall}$, is given by:

$$\alpha_{overall} = \frac{E_{mech,output}}{(batt_{SOC,initial} - batt_{SOC,final}) \times batt_{capacity}} \qquad (4\text{-}3)$$

Where $batt_{SOC,initial}$ and $batt_{SOC,final}$ are the initial and final SoC of the battery, and $batt_{capacity}$ the charge capacity of the battery in Wh.

Finally, the following table presents the characteristics of the different drive cycles used in the simulations.

Drive Cycle	EUDC	HWFET	WLTP1	UDDS
Full Name	Extra Urban Drive Cycle	Highway Fuel Economy	Worldwide Harmonized Light Vehicles Test Procedure - Class 1	Urban Dynamometer Driving Schedule
Characteristics	Aggressive high-speed driving modes	Highway driving conditions	Low Speed driving conditions	City driving for passenger vehicles
Duration (s)	400	769	1022	1369
Total Distance (km)	6.9549	16.5065	8.0909	11.9902
Average Velocity (km/h)	62.5164	77.627	28.4864	31.5186
Maximum Acceleration/Deceleration (km/h^2)	3/-5	5.1499/-5.3108	2.9/-4.1	5.3108/ -5.3108
Average Acceleration (km/h^2)	1.3592	0.699	0.7929	1.8164
Average Deceleration (km/h^2)	-3.3333	-0.5526	-0.5033	-1.197
Number of Starts/Stops	1	1	6	17

Table 4-1 Selected Drive Cycle Characteristics

4.2 Benchmark 1: Single Speed Transmission

To establish a benchmark performance, consistent with current EVs equipped with a single speed transmission, the simulated vehicle is first tested in SST configuration. This means that the overall speed ratio of the vehicle, between the input motor and output of the drivetrain, is constant. The single reduction gear ratio corresponds to that of the 2013 Nissan Leaf, namely 7.94:1.

Simulations of this set up are conducted for all four selected driving cycles, namely UDDS, WLTP, NYCC and EUDC.

The resulting power at the input and output are presented in figure 4-1. Given the simplicity of such a configuration, simulations are conducted with minimal losses in the system from input motor to vehicle output, which explains the marginal difference between input and output power.

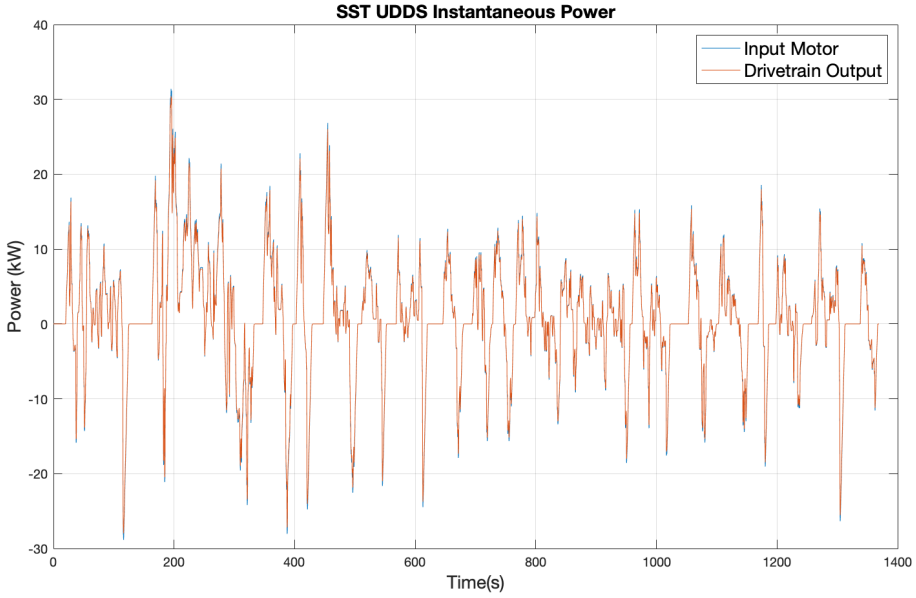

Figure 4-1 SST UDDS Instantaneous Input (blue) and Output (red) Power

Figure 4-2 depicts the torque speed curve of the input motor, with the different levels representing the efficiency of operating the motor at the given torque and speed. The green crosses represent the operating point of the input motor throughout the drive cycle. The corresponding readings are also presented in figure 4-2.

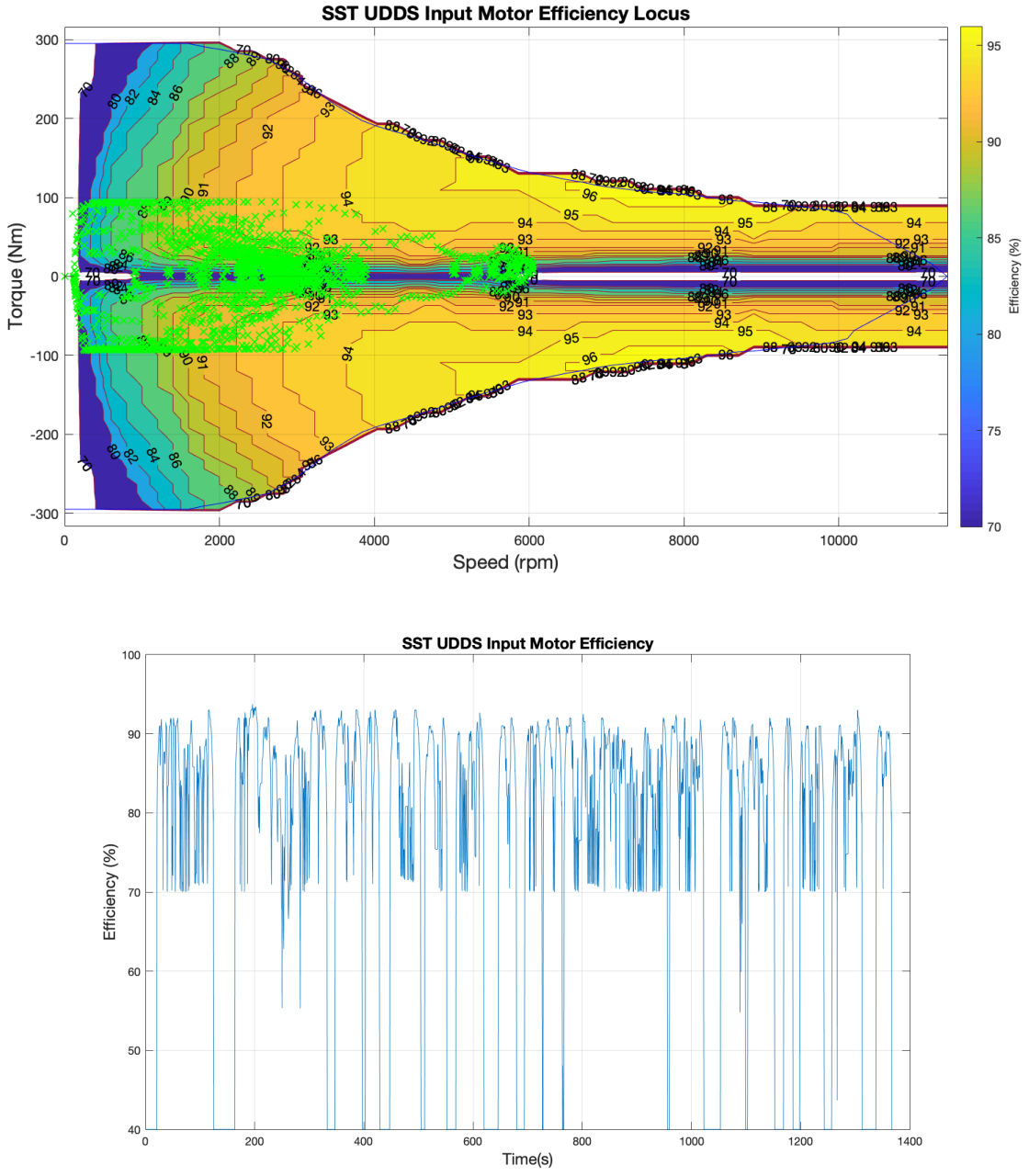

Figure 4-2 SST UDDS Input Motor Efficiency Map (top) and efficiency reading (bottom)

Because this configuration only allows for a single speed ratio, the input motor is operating at sub-optimal torque speed points. Given that the overall transmission ratio was selected to allow for a sufficient vehicle top speed, this limits the time spent by the motor at high efficiency regions for urban drive cycles such as UDDS.

The electrical energy consumed by the electric motor is calculated given the efficiency value and the instantaneous energy at any given time. It is displayed in figure 4-3. The mechanical energy at the output of the drivetrain, is depicted in figure 4-4.

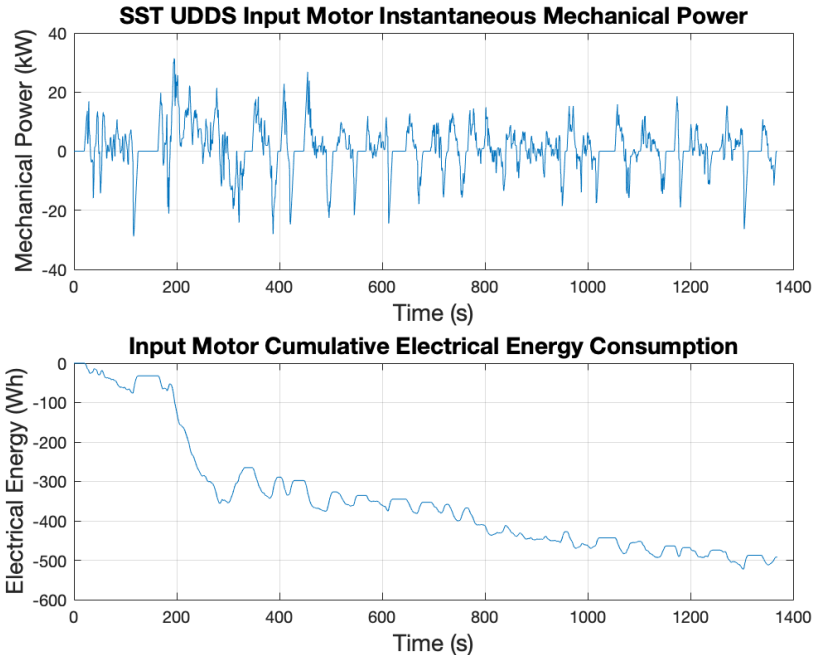

Figure 4-3 SST UDDS Instantaneous Power Input Motor (top, left) and Output of Drivetrain (top, right). Cumulative energy values (bottom figures)

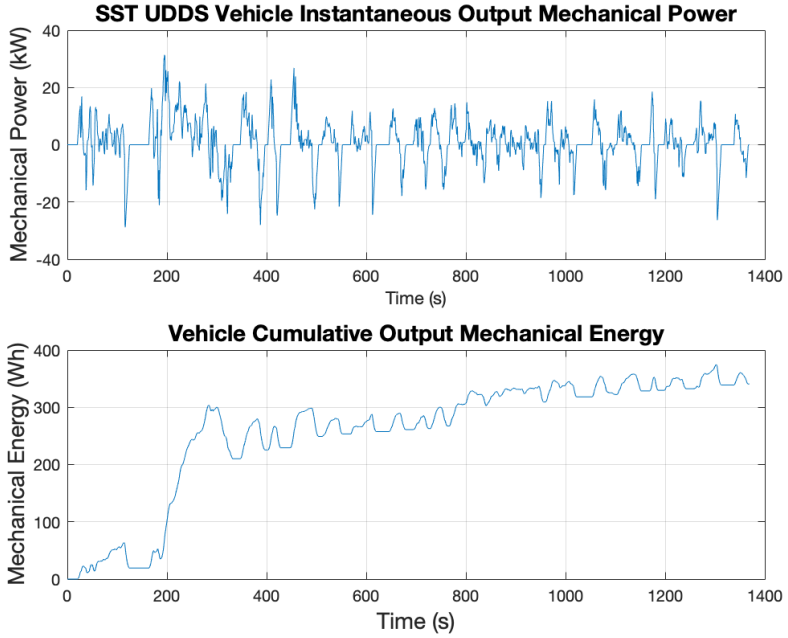

Figure 4-4 SST UDDS Instantaneous Power Input Motor (top, left) and Output of Drivetrain (top, right). Cumulative energy values (bottom figures)

According to these figures, for the UDDS drive cycle, the vehicle equipped with a single speed transmission (SST) consumes 492.2Wh to produce the required 340.6Wh to track the reference speed, which is equivalent to an overall efficiency of 69.21%. Simulations of the EV equipped with a SST output the following results for the different drive cycles considered:

Drive Cycle	Tracking Accuracy (%)	Average IME (%)	Electrical Energy Consumption (Wh)	Mechanical Energy Output (Wh)	Overall Efficiency (%)	Range on 24kWh Battery (km)
EUDC	99.4204	80.89	565.0246	469.2933	83.06	295.81
HWFET	99.7123	83.4649	1347.5	1120.1	83.12	294.03
WLTP	97.7017	73.3521	225.3572	162.5156	72.11	863.90
UDDS	97.5932	75.938	492.2011	340.6451	69.21	585.58

Table 4-2 SST Simulation Results for 4 drive cycles

4.3 Benchmark 2: Dual-Brake Transmission

A second benchmark of performance is obtained by simulating the EV equipped with the DBT design. In this situation, the gear reduction unit is selected to have a different value than in the SST simulation. This is made possible given the addition of a second gear ratio in the transmission, allowing to achieve equivalent output speeds while operating the motor more slowly during high speed operations, and equivalent output torques while producing lower motor torques during acceleration. Just like what was conducted for the first benchmark, simulations are performed following the four driving cycles.

Figure 4-5 displays the input motor, the ring and sun gear and output mechanical power during simulation of the UDDS drive cycle. A closer look is given to this figure for high speed operations, where the transmission operates an upshift, followed by a downshift.

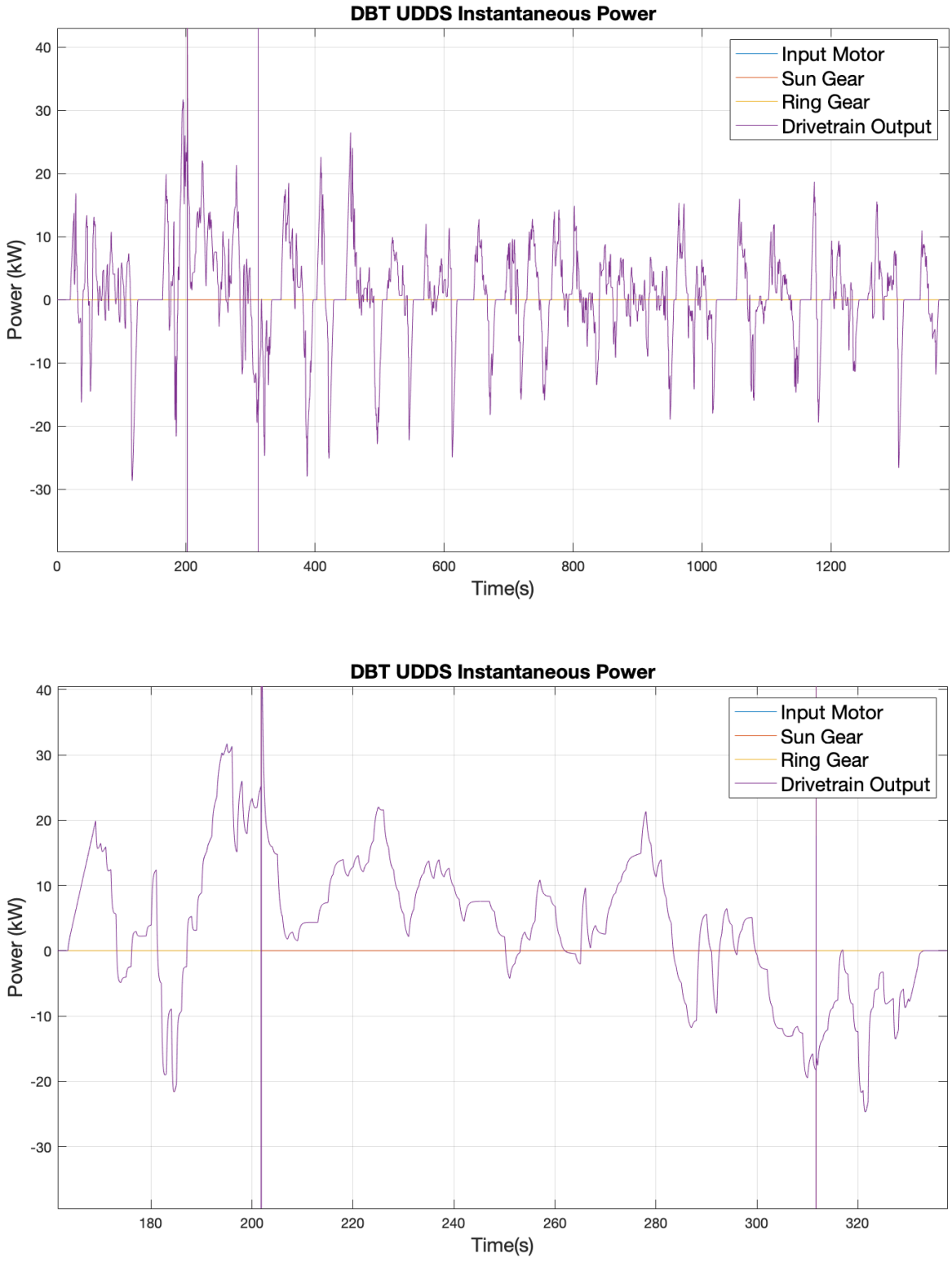

Figure 4-5 DBT UDDS Instantaneous Power at Input (blue), Sun (red) and ring (yellow) gears, and output (purple). Top is whole simulation, Bottom is from t=150s to t=350s.

At low vehicle speeds, before reaching the gear switch breakpoint, the ring gear is grounded, and the power is transmitted through the sun gear to the output of the powertrain. Once that breakpoint speed is passed, the transmission engages the up-shift sequence, which progressively activates the sun brakes and disengages the ring gear. During that transition, both the sun and ring gears transmit power. Once this process is complete, figure 4-5 shows that the ring gear now holds all the power within the transmission. The gear switching process is measured to last under 1 seconds, in this non-optimized simulation. This gear switch is visible on the figure 4-6, presenting the speed ratio observed in the DBT.

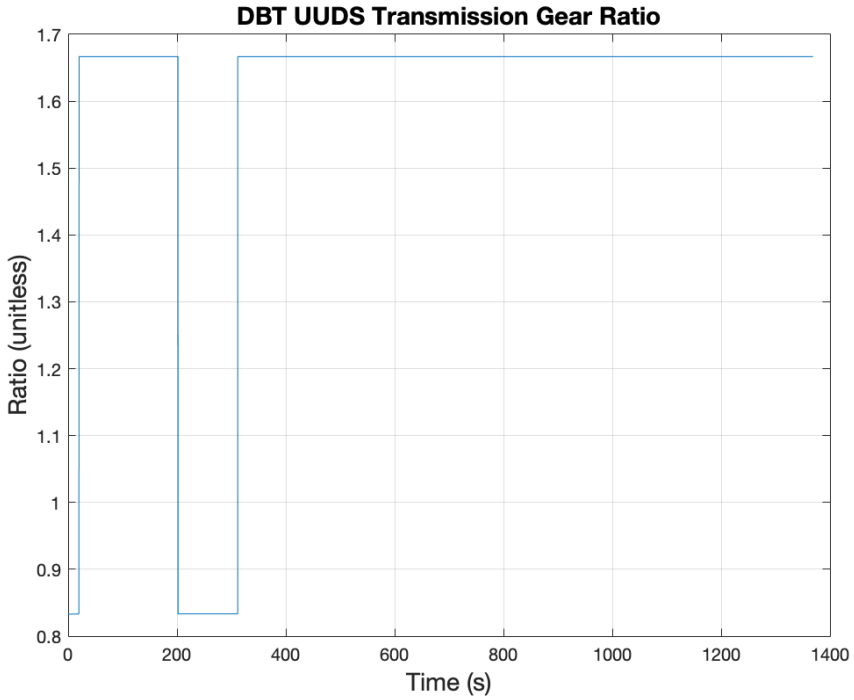

Figure 4-6 DBT UDDS Transmission Gear Ratio

Given the prevalence of low speeds observed during the UDDS drive cycle, the DBT operates for the most part in the underdrive mode. The DBT goes into overdrive mode only when the vehicle speeds exceed 65 km/h. This speed breakpoint was selected to optimize the time spent in the high efficiency regions of the input motor, as can be seen in figure 4-7. This breakpoint speed is subject to optimization and depends highly on the configuration of the efficiency map, the overall gear ratio of the powertrain, and the vehicle parameters.

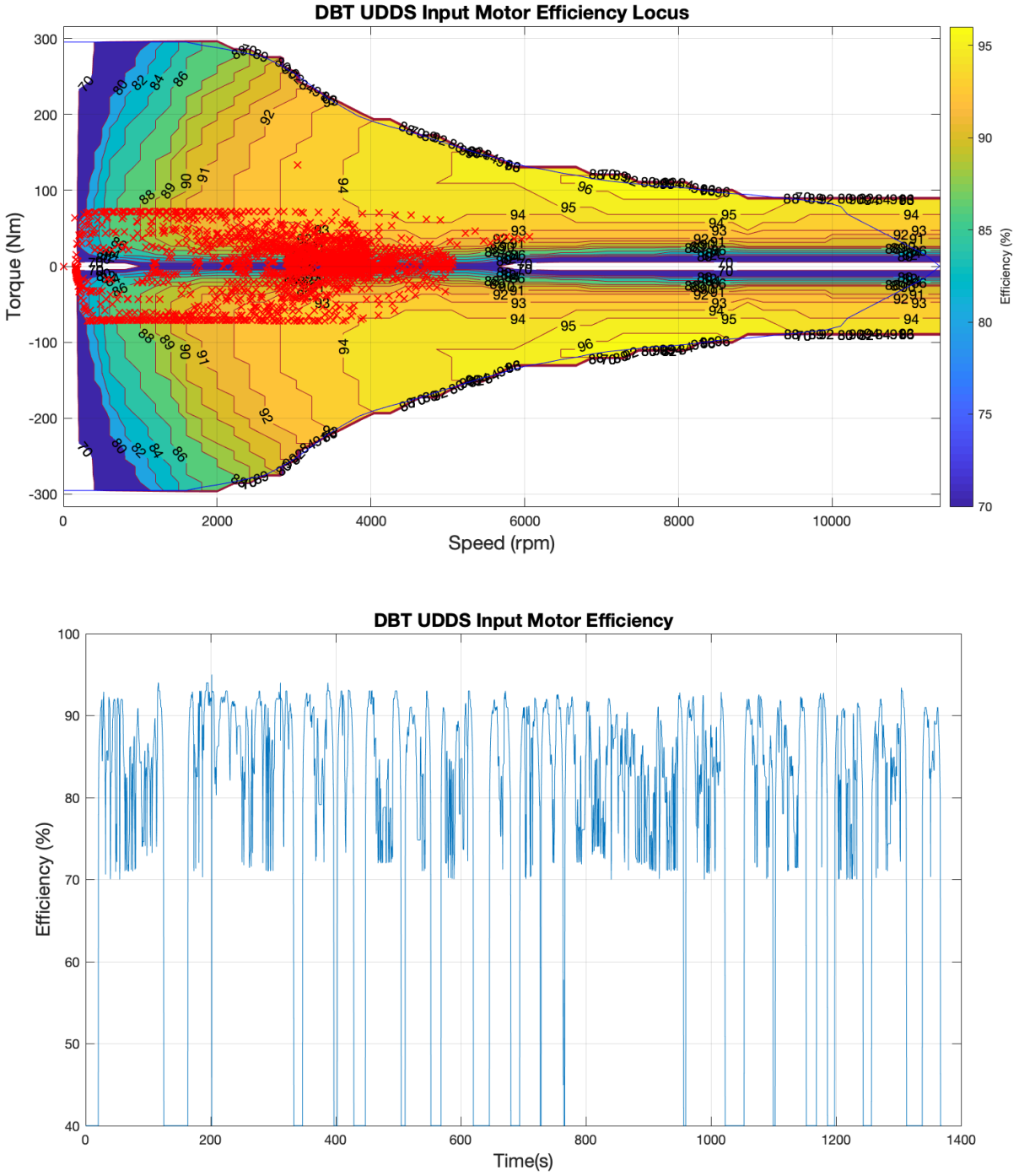

Figure 4-7 DBT UDDS Input Motor Efficiency Map (top) and efficiency reading (bottom)

At higher speeds, this flexibility allows the input motor to be operated in significantly better regions than in the first benchmark. Throughout the drive cycle, the input motor averages an efficiency of 76.26%.

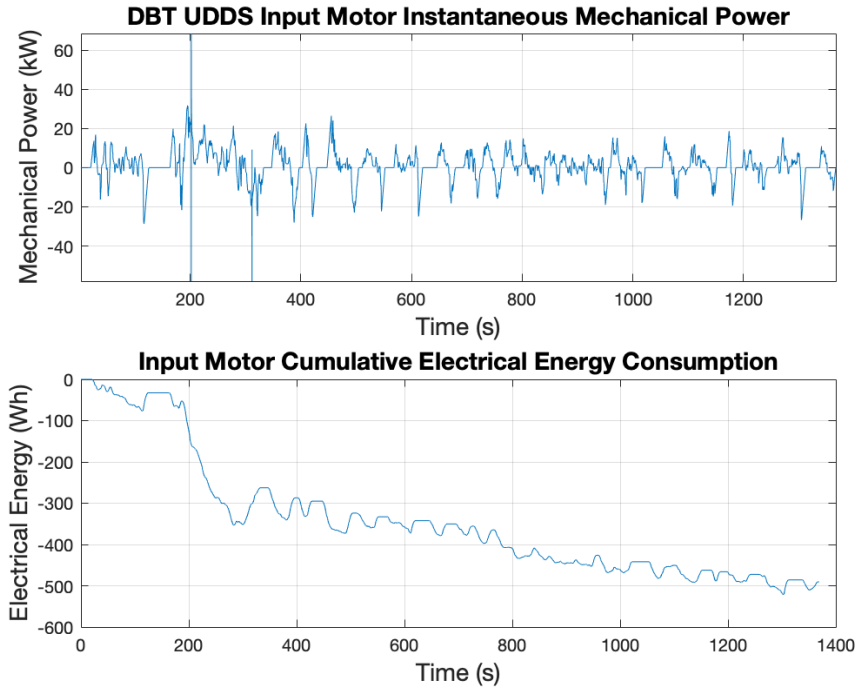

Figure 4-8 DBT UDDS Instantaneous power (top) and cumulative power (bottom) consumption input motor

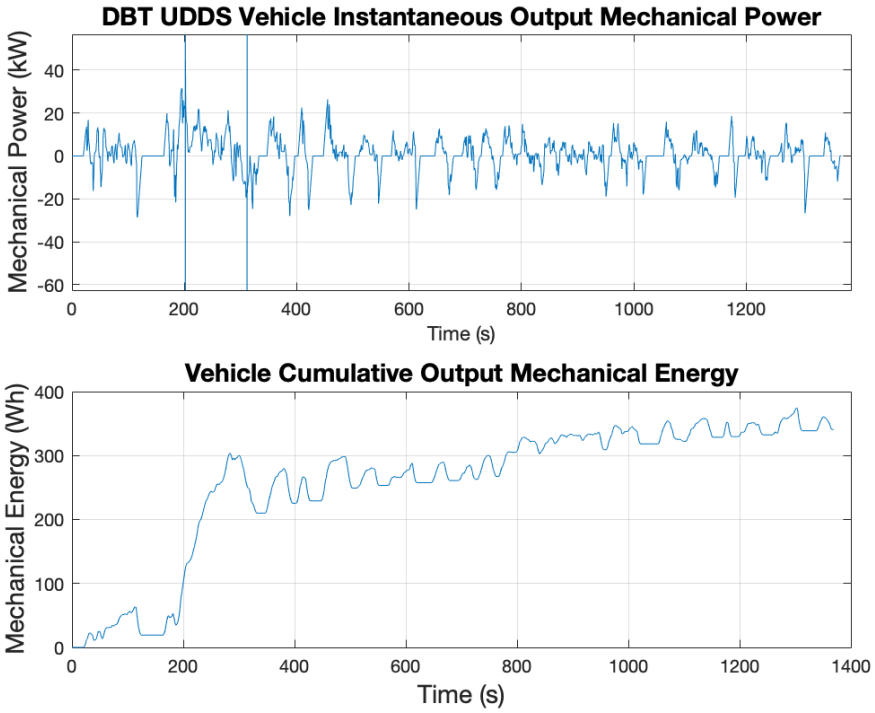

Figure 4-9 DBT UDDS Instantaneous power (top) and cumulative energy (bottom) output of vehicle

According to figure 4-8 and 4-9, the vehicle equipped with the DBT consumes 491.34Wh to produce the 340.59Wh required to track the UDDS drive cycle. While this mechanism allows for a slight increase in input motor efficiency, additional energy cost comes from operating the braking mechanisms of the ring and sun gears to perform the gear switch. In addition, the added complexity of a DBT transmission over a simple SST configuration is simulated at a 98% efficiency.

Drive Cycle	Tracking Accuracy (%)	Average IME (%)	Electrical Energy Consumption (Wh)	Mechanical Energy Output (Wh)	Overall Efficiency (%)	Range on 24kWh Battery (km)
EUDC	99.43	79.42	568.29	469.22	82.57	294.08
HWFET	99.71	86.61	1315.20	1120.10	85.17	301.23
WLTP	97.75	73.07	230.49	162.49	70.50	844.63
UDDS	97.72	76.26	491.34	340.59	69.32	586.59

Table 4-3 DBT simulations results for 4 drive cycles

4.4 Continuously Variable Transmission

The following section details the use of the novel CVT system on the simulated EV to track, successively, the UDDS, WLTP, HWFET and EUDC drive cycles.

To allow for accurate comparison, the CVT is tested with the exact same powertrain configuration as the DBT. In other words, since the CVT can achieve the same gear ratios at its extremum cases as the DBT, the vehicle retains the same overall gear ratio, with unchanged differential.

In addition, the overall efficiency of the CVT design is a key aspect of the simulation, as envisaged in the literature review. Given that the physical set-up of the CVT is the same as the DBT, except for the addition of the Sun Motor, the simulations are run with the same 98% efficiency on the planetary gear sets. However, an additional loss mechanism is considered in the operation of the Sun Motor. The simulations are performed with 5 settings of decreasing efficiency, presented in the following table:

Transmission	Sun Motor Efficiency (%)	Battery Recharge Efficiency (%)
CVT 1	99	99
CVT 2	96	98
CVT 3	92	95
CVT 4	90	92
CVT 5	85	90

Table 4-4 CVT Simulation Efficiency Parameters

Furthermore, as explained in the previous chapter, both the Input and Sun motors can act as generators when providing negative power to the system. In such a case, the generated power is used to recharge the battery. The process of recharging the battery is assumed to vary in degree of efficiency as well.

4.4.1 UDDS

The first set of results presented is the performance of the CVT on the UDDS drive cycle, similarly to the results shown for the two benchmark transmissions. Figure 4-10 displays the drive cycle reference speed and the vehicle actual speed.

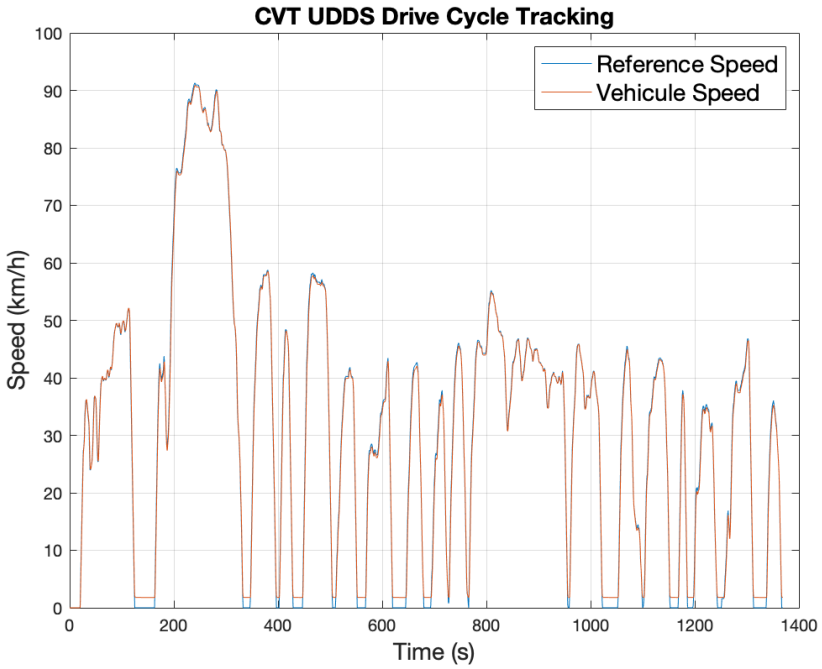

Figure 4-10 CVT UDDS Speed Tracking

Detailed breakdown of the dynamics of the different parts of the CVT going through the drive cycle, is detailed in the following 4-11 and 4-12, presenting the speed and torques of the input motor, the sun motor, the ring gear and the output of the drivetrain.

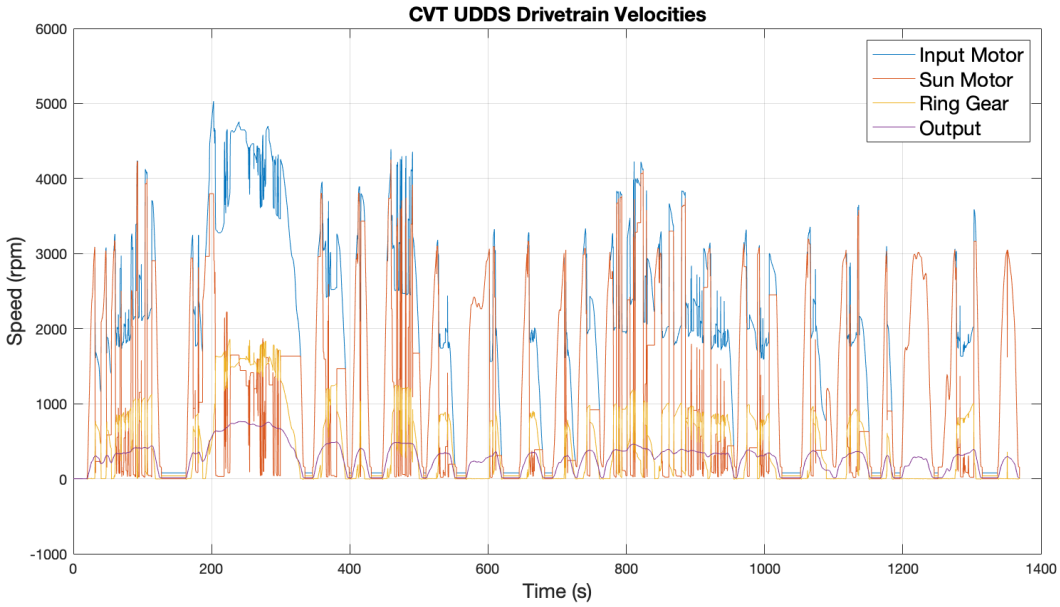

Figure 4-11 CVT UDDS Drivetrain Velocities. Input Motor (blue), Sun Motor (red), Ring Gear (yellow) and output (purple).

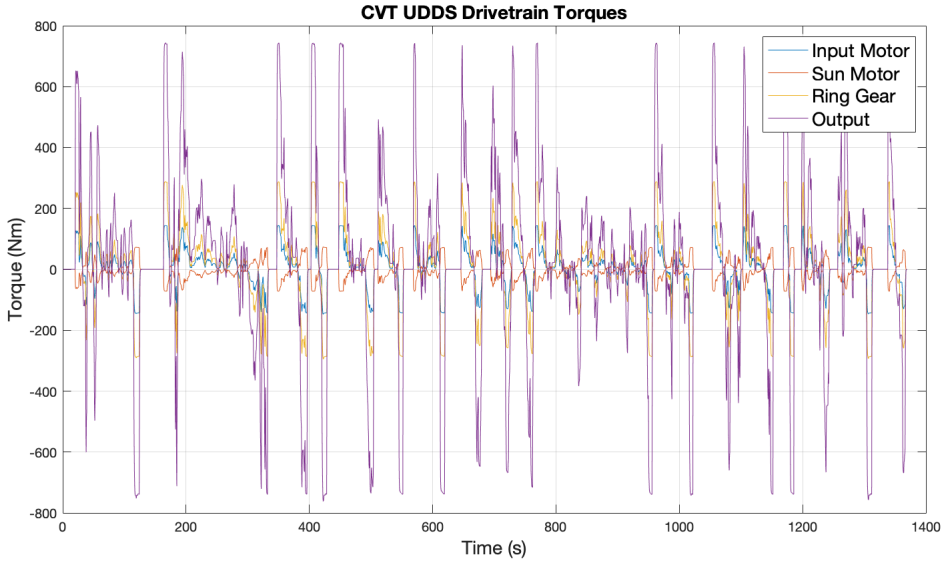

Figure 4-12 CVT UDDS Drivetrain Torques. Input Motor (blue), Sun Motor (red), Ring Gear (yellow) and output (purple).

The instantaneous power present in the different components is presented next, at different points in time:

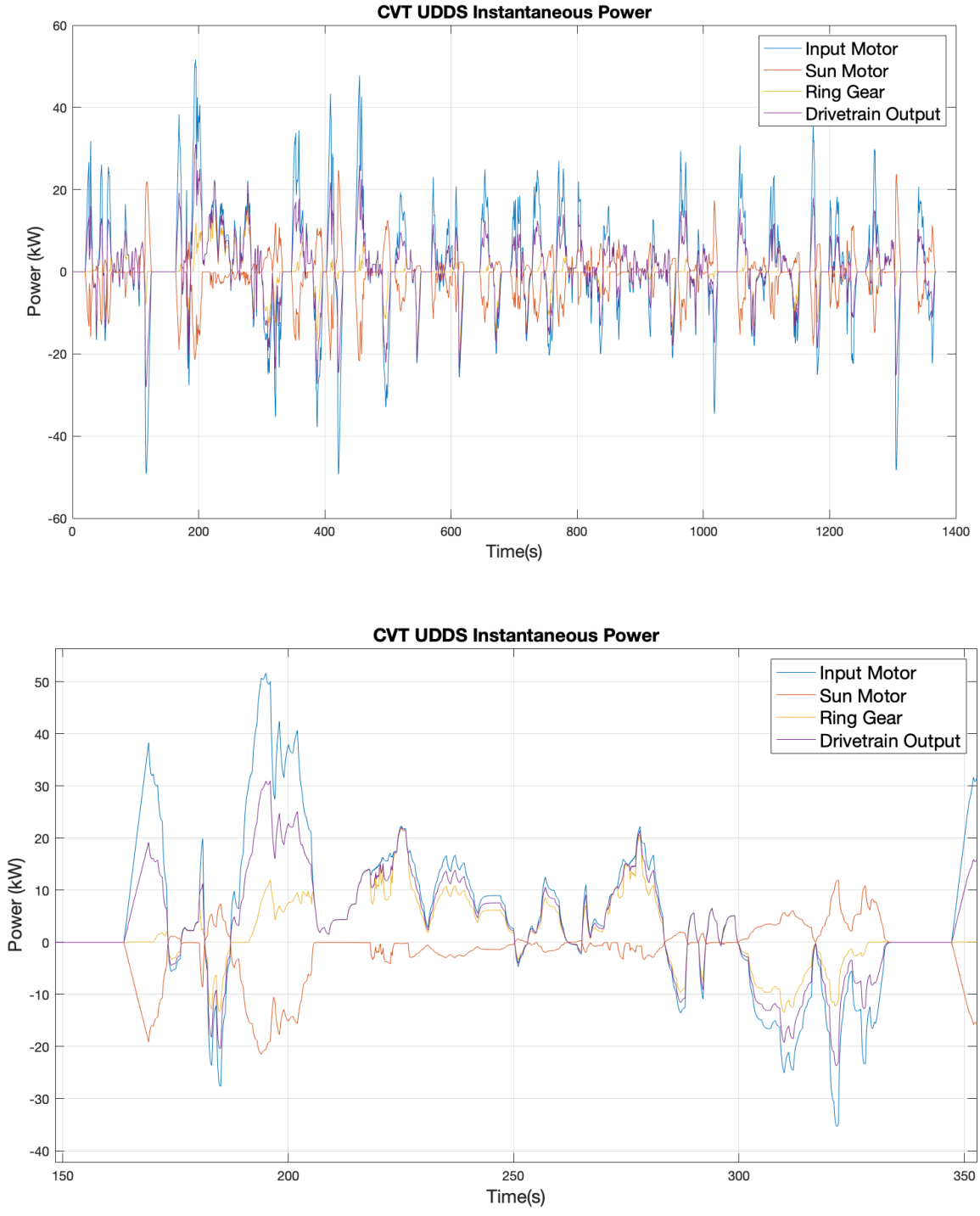

Figure 4-13 Top: CVT UDDS Instantaneous Power at Input (blue), Sun (red) and ring (yellow) gears, and output (purple). Bottom: CVT UDDS Instantaneous Power between t=150s and t= 350s.

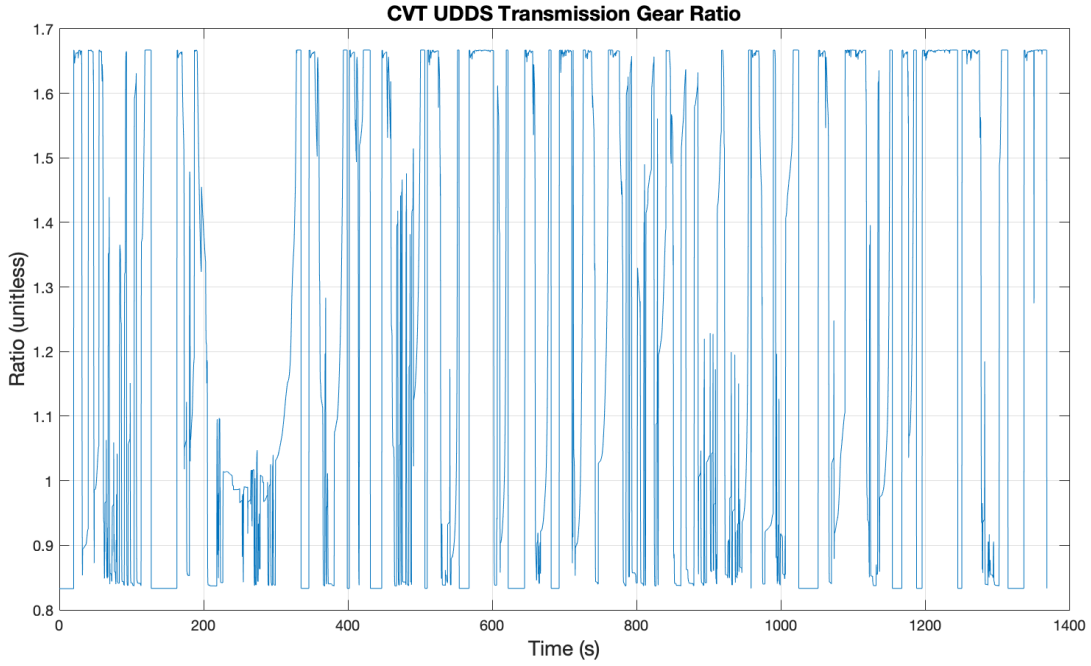

Figure 4-14 CVT UDDS Gear Ratio

The next figures present the location of operation of the input motor on its speed-torque curve, along with the efficiency readings.

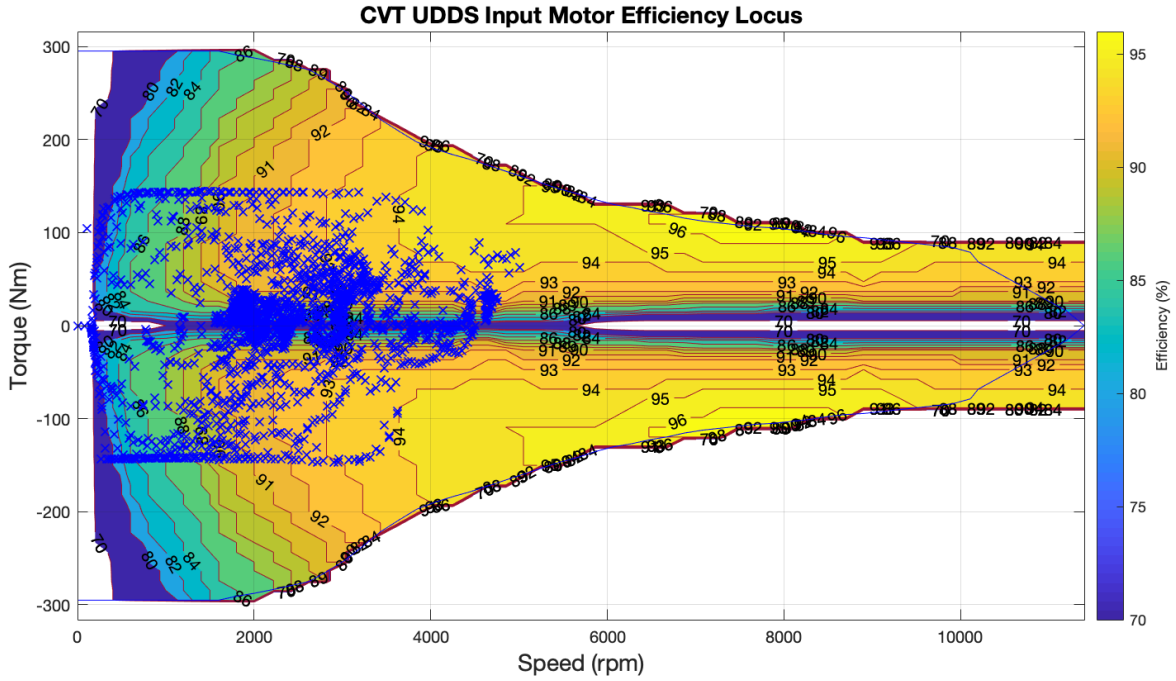

Figure 4-15 CVT UDDS Input Motor Efficiency Map with speed/torque operation (blue path)

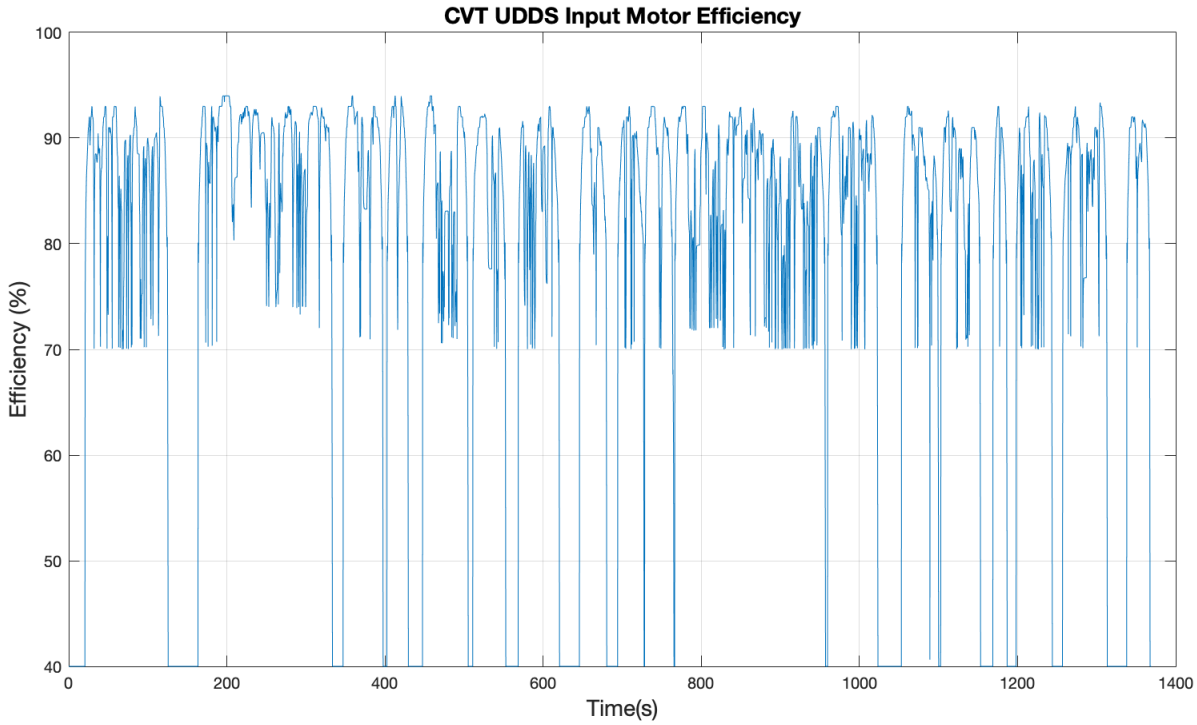

Figure 4-16 CVT UDDS Input motor efficiency readings

As the speed of the vehicle increases, the CVT is able to bring the input motor to higher efficiency regions. This is particularly marked when the speed of the vehicle is above 50km/h, where the motor operates at its highest efficiency points. However, this situation is only observed for a limited time in UDDS. A significant portion of the time is spent at much lower speeds, where the input motor is less efficient.

The next figures 4-17 through 4-19 present the instantaneous and cumulative energy consumption of the input and sun motors, as well as the output of the drivetrain.

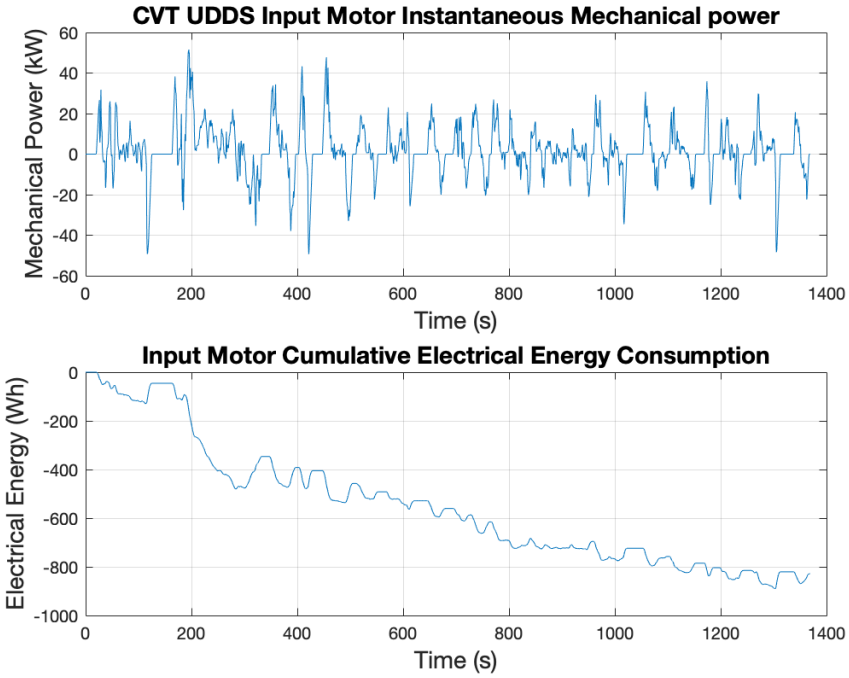

Figure 4-17 CVT UDDS Input motor instantaneous power (top) and cumulative energy consumption (bottom)

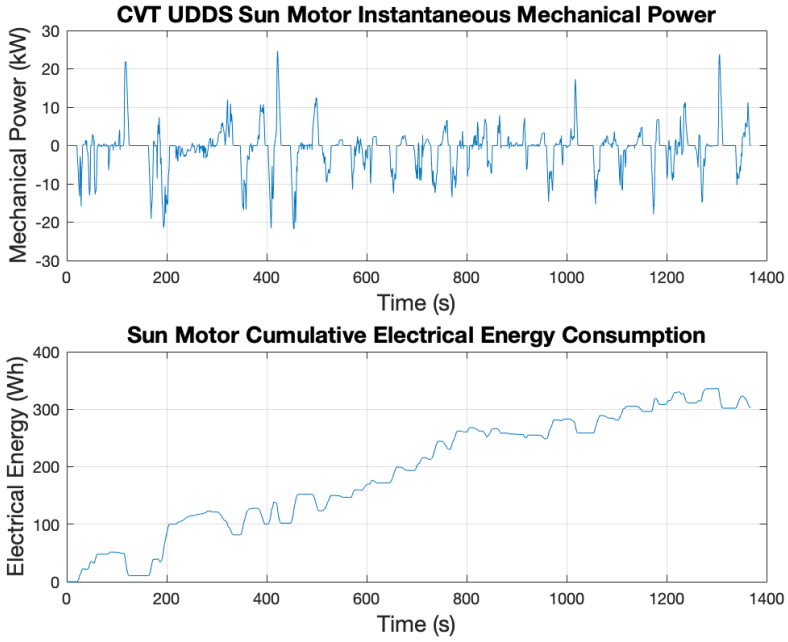

Figure 4-18CVT UDDS Sun motor instantaneous power (top) and cumulative energy consumption (bottom)

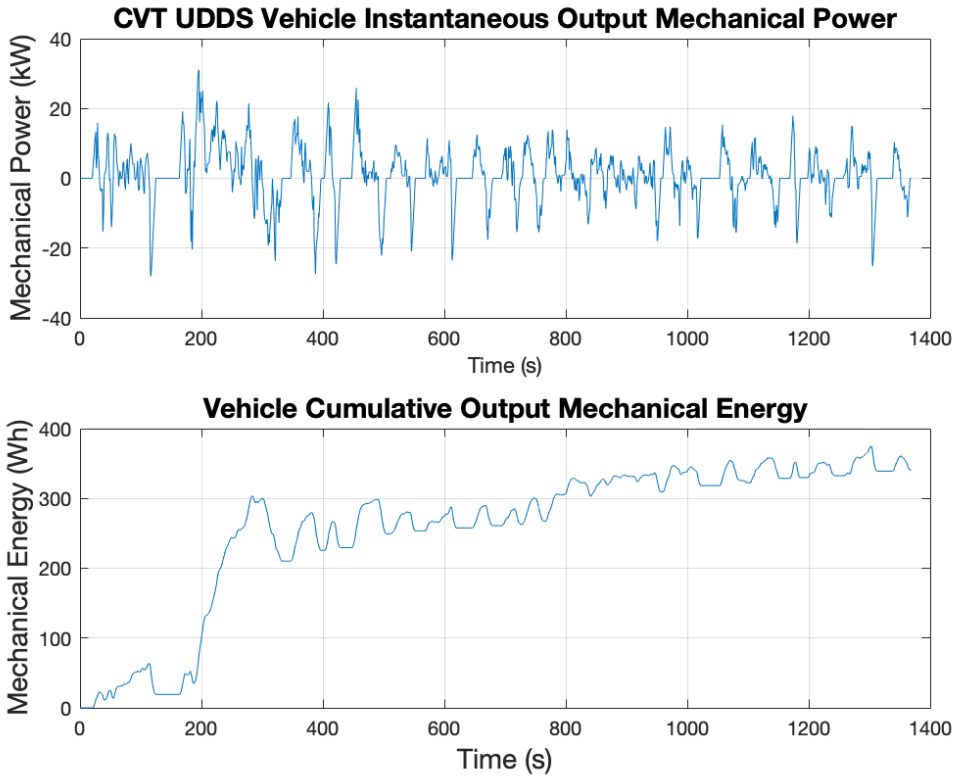

Figure 4-19 CVT UDDS Vehicle output instantaneous power (top) and cumulative energy (bottom)

Negative energy in the sun motor equates to operating as a generator, which recharges the battery. This process is simulated with decreasing levels of efficiency, as can be seen in the table below:

Drive Cycle	Tracking Accuracy (%)	Average IME (%)	Total Electrical Energy Consumption (Wh)	Total Mechanical Energy Output (Wh)	Overall Efficiency (%)	Range on 24kWh Battery (km)
CVT 1	97.12	77.78	525.35	340.80	64.87	548.61
CVT 2	97.12	77.78	555.76	340.80	61.32	518.59
CVT 3	97.12	77.78	594.59	340.80	57.32	484.73
CVT 4	97.12	77.78	625.07	340.80	54.52	461.09
CVT 5	97.12	77.78	664.84	340.80	51.26	433.51

Table 4-5 CVT UDDS Simulation Results, with varying efficiency levels

4.4.2 WLTP

Results of simulating the vehicle with CVT on the WLTP drive cycle are presented in Appendix B-1. The table below is a summary of the results obtained from the simulations.

Drive Cycle	Tracking Accuracy (%)	Average IME (%)	Electrical Energy Consumption (Wh)	Mechanical Energy Output (Wh)	Overall Efficiency (%)	Range on 24kWh Battery(km)
CVT 1	97.54	75.52	230.93	162.64	70.43	843.17
CVT 2	97.54	75.52	241.14	162.64	67.44	805.34
CVT 3	97.54	75.52	253.51	162.64	64.15	766.04
CVT 4	97.54	75.52	262.27	162.64	62.01	740.48
CVT 5	97.54	75.52	276.53	162.64	58.81	702.28

Table 4-6 CVT WLTP Simulation Results, with varying efficiency levels

It is noted that this drive cycle presents a very low average speed, which translates in the input motor operating mostly in sub-optimal torque speed regions.

4.4.3 HWFET

Similarly, the results of the HWFET tracking with a CVT equipped vehicle are presented in Appendix B-2. The results are summarized below:

Drive Cycle	Tracking Accuracy (%)	Average IME (%)	Electrical Energy Consumption (Wh)	Mechanical Energy Output (Wh)	Overall Efficiency (%)	Range on 24kWh Battery (km)
CVT 1	99.65	88.07	1284.49	1120.30	87.22	308.47
CVT 2	99.65	88.07	1291.89	1120.30	86.72	306.66
CVT 3	99.65	88.07	1301.69	1120.30	86.07	304.35
CVT 4	99.65	88.07	1309.91	1120.30	85.52	302.44
CVT 5	99.65	88.07	1319.08	1120.30	84.93	300.34

Table 4-7 CVT HWFET Simulation Results, with varying efficiency levels

HWFET presents the highest average velocity of the drive cycle in this study. This allows the input motor to reach the highest efficiency operating regions more frequently and translates into a high average IME.

4.4.4 EUDC

Finally, EUDC testing is presented in Appendix B-3, and the results summarized below:

Drive Cycle	Tracking Accuracy (%)	Average IME (%)	Electrical Energy Consumption (Wh)	Mechanical Energy Output (Wh)	Overall Efficiency (%)	Range on 24kWh Battery (km)
CVT 1	99.32	83.08	546.71	469.49	85.88	305.75
CVT 2	99.32	83.08	562.29	469.49	83.50	297.28
CVT 3	99.32	83.08	572.73	469.49	81.97	291.86
CVT 4	99.32	83.08	598.59	469.49	78.43	279.25
CVT 5	99.32	83.08	619.40	469.49	75.80	269.87

Table 4-8 CVT EUDC Simulation Results, with varying efficiency levels

Just like HWFET, EUDC presents high speed aggressive driving characteristics, which allows the motor to operate in high efficiency operating points regularly.

4.5 Summary of Results

This section aims at summarizing the results presented in this chapter, for all transmission configuration and drive cycle tested. Figure 4-20 presents a juxtaposition of the trace of the input motor operation, going through the UDDS drive cycle, with a vehicle equipped with a SST (green path), the DBT (red path) and the CVT (blue path). The efficiency readings are presented in the subsequent figure 4-21.

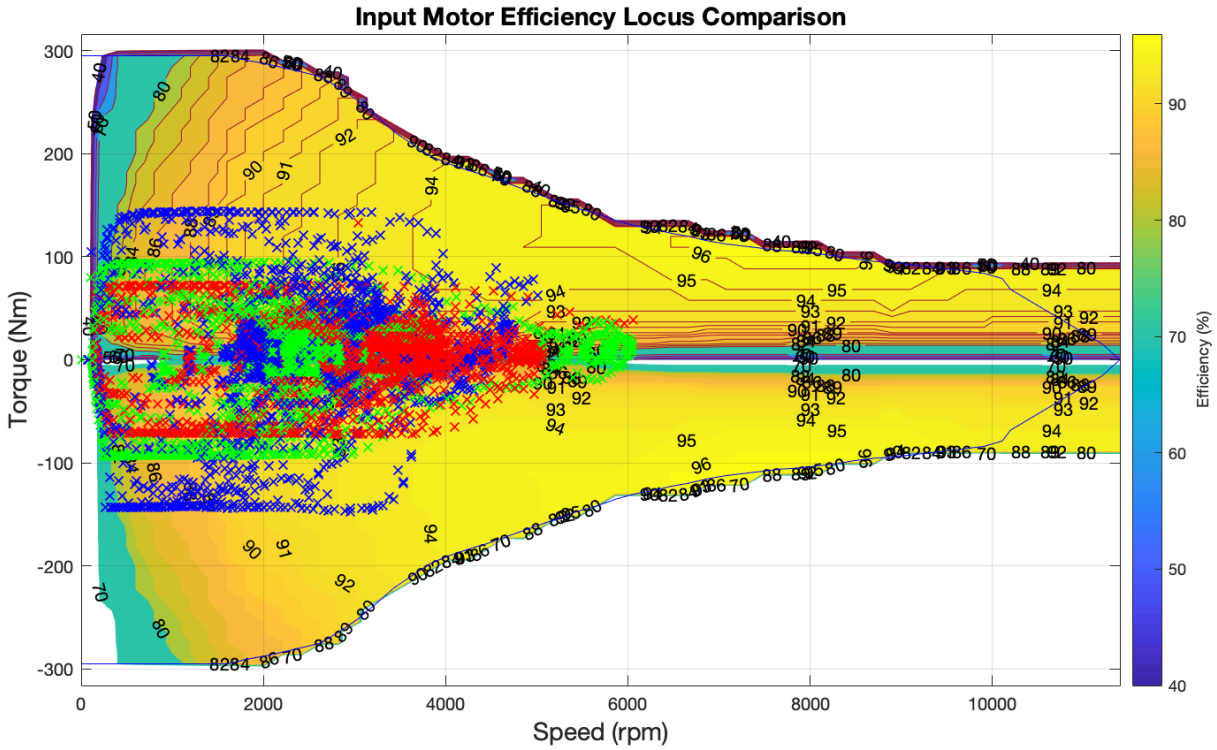

Figure 4-20 Input Motor Efficiency with UDDS motor operation path for SST (green), DBT (red) and CVT (blue) configurations

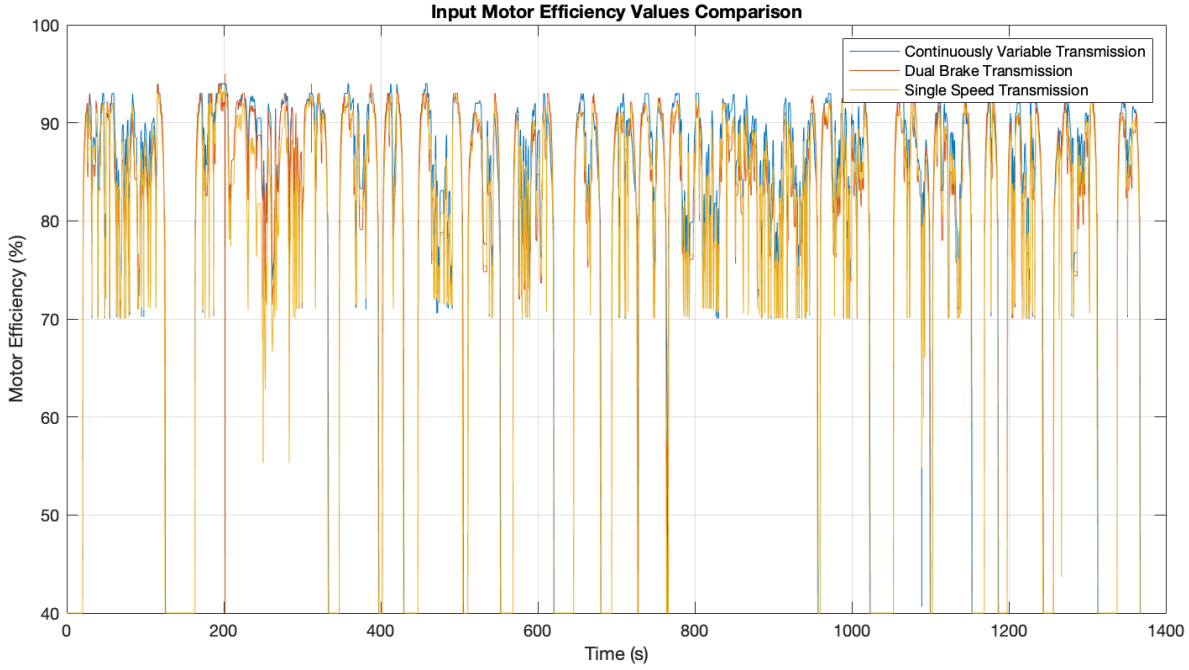

Figure 4-21 UDDS Input motor efficiency reading for SST (green), DBT (red) and CVT (blue)

Transmission	Tracking Accuracy (%)	Average IME (%)	Input Motor Electrical Energy Consumption (Wh)	Sun Motor Efficiency (%)	Sun Motor Electrical Energy Consumption (Wh)	Battery Recharge Efficiency (%)	Total Electrical Energy Consumption (Wh)	Total Mechanical Energy Output (Wh)	Overall Efficiency (%)
CVT 1	99.32	83.08	647.12	99.00	-100.41	99.00	546.71	469.49	85.88
CVT 2	99.32	83.08	647.12	96.00	-84.83	98.00	562.29	469.49	83.50
CVT 3	99.32	83.08	647.12	92.00	-74.39	95.00	572.73	469.49	81.97
CVT 4	99.32	83.08	647.12	90.00	-48.53	92.00	598.59	469.49	78.43
CVT 5	99.32	83.08	647.12	85.00	-27.72	90.00	619.40	469.49	75.80
DBT	99.43	79.42	568.29	N/A	0.00	95.00	568.29	469.22	82.57
SST	99.42	80.89	565.02	N/A	0.00	95.00	565.02	469.29	83.06

Table 4-9 EUDC Drive Cycle overall efficiency simulations results summary

Transmission	Tracking Accuracy (%)	Average IME (%)	Input Motor Electrical Energy Consumption (Wh)	Sun Motor Efficiency (%)	Sun Motor Electrical Energy Consumption (Wh)	Battery Recharge Efficiency (%)	Total Electrical Energy Consumption (Wh)	Total Mechanical Energy Output (Wh)	Overall Efficiency (%)
CVT 1	99.65	88.07	1423.60	99.00	-139.11	95.00	1284.49	1120.30	87.22
CVT 2	99.65	88.07	1423.60	96.00	-131.71	98.00	1291.89	1120.30	86.72
CVT 3	99.65	88.07	1423.60	92.00	-121.91	95.00	1301.69	1120.30	86.07
CVT 4	99.65	88.07	1423.60	90.00	-113.69	92.00	1309.91	1120.30	85.52
CVT 5	99.65	88.07	1423.60	85.00	-104.52	90.00	1319.08	1120.30	84.93
DBT	99.71	86.61	1315.20	N/A	0.00	95.00	1315.20	1120.10	85.17
Direct Drive	99.71	83.46	1347.50	N/A	0.00	95.00	1347.50	1120.10	83.12

Table 4-10 HWFET Drive Cycle overall efficiency simulations results summary

Transmission	Tracking Accuracy (%)	Average IME (%)	Input Motor Electrical Energy Consumption (Wh)	Sun Motor Efficiency (%)	Sun Motor Electrical Energy Consumption (Wh)	Battery Recharge Efficiency (%)	Total Electrical Energy Consumption (Wh)	Total Mechanical Energy Output (Wh)	Overall Efficiency (%)
CVT 1	97.54	75.52	213.70	99.00	17.23	99.00	230.93	162.64	70.43
CVT 2	97.54	75.52	213.70	96.00	27.44	98.00	241.14	162.64	67.44
CVT 3	97.54	75.52	213.70	92.00	39.81	95.00	253.51	162.64	64.15
CVT 4	97.54	75.52	213.70	90.00	48.56	92.00	262.27	162.64	62.01
CVT 5	97.54	75.52	213.70	85.00	62.83	90.00	276.53	162.64	58.81
DBT	97.75	73.07	230.49	N/A	0.00	95.00	230.49	162.49	70.50
Direct Drive	97.70	73.35	225.36	N/A	0.00	95.00	225.36	162.52	72.11

Table 4-11WLTP Drive Cycle overall efficiency simulations results summary

Transmission	Tracking Accuracy (%)	Average IME (%)	Input Motor Electrical Energy Consumption (Wh)	Sun Motor Efficiency (%)	Sun Motor Electrical Energy Consumption (Wh)	Battery Recharge Efficiency (%)	Total Electrical Energy Consumption (Wh)	Total Mechanical Energy Output (Wh)	Overall Efficiency (%)
CVT 1	97.12	77.78	828.65	99.00	-303.31	99.00	525.35	340.80	64.87
CVT 2	97.12	77.78	828.65	96.00	-272.89	98.00	555.76	340.80	61.32
CVT 3	97.12	77.78	828.65	92.00	-234.07	95.00	594.59	340.80	57.32
CVT 4	97.12	77.78	828.65	90.00	-203.59	92.00	625.07	340.80	54.52
CVT 5	97.12	77.78	828.65	85.00	-163.82	90.00	664.84	340.80	51.26
DBT	97.72	76.26	491.34	N/A	0.00	95.00	491.34	340.59	69.32
Direct Drive	97.59	75.94	492.20	N/A	0.00	95.00	492.20	340.65	69.21

Table 4-12 UDDS Drive Cycle overall efficiency simulations results summary

Transmission	Average IME (%)	Overall Efficiency (%)	Energy Economy (km/kWh)	Range on 24kWh Battery (km)
CVT 1	83.08	85.88	12.74	305.75
CVT 2	83.08	83.50	12.39	297.28
CVT 3	83.08	81.97	12.16	291.86
CVT 4	83.08	78.43	11.64	279.25
CVT 5	83.08	75.80	11.24	269.87
DBT	79.42	82.57	12.25	294.08
Direct Drive	80.89	83.06	12.33	295.81

Table 4-13 EUDC Range Simulation Result Summary

Transmission	Average IME (%)	Overall Efficiency (%)	Energy Economy (km/kWh)	Range on 24kWh Battery (km)
CVT 1	88.07	87.22	12.85	308.47
CVT 2	88.07	86.72	12.78	306.66
CVT 3	88.07	86.07	12.68	304.35
CVT 4	88.07	85.52	12.60	302.44
CVT 5	88.07	84.93	12.51	300.34
DBT	86.61	85.17	12.55	301.23
Direct Drive	83.46	83.12	12.25	294.03

Table 4-14 HWFET Range Simulation Result Summary

Transmission	Average IME (%)	Overall Efficiency (%)	Energy Economy (km/kWh)	Range on 24kWh Battery (km)
CVT 1	75.52	70.43	35.13	843.17
CVT 2	75.52	67.44	33.56	805.34
CVT 3	75.52	64.15	31.92	766.04
CVT 4	75.52	62.01	30.85	740.48
CVT 5	75.52	58.81	29.26	702.28
DBT	73.07	70.50	35.19	844.63
Direct Drive	73.35	72.11	36.00	863.90

Table 4-15 WLTP Range Simulation Result Summary

Transmission	Average IME (%)	Overall Efficiency (%)	Energy Economy (km/kWh)	Range on 24kWh Battery (km)
CVT 1	77.78	64.87	22.86	548.61
CVT 2	77.78	61.32	21.61	518.59
CVT 3	77.78	57.32	20.20	484.73
CVT 4	77.78	54.52	19.21	461.09
CVT 5	77.78	51.26	18.06	433.51
DBT	76.26	69.32	24.44	586.59
Direct Drive	75.94	69.21	24.40	585.58

Table 4-16 UDDS Range Simulation Result Summary

5 Discussion

5.1 Electric Vehicle Simulation Conformity

Considering the results presented in the previous chapter, some conclusions can be drawn about the simulated EV. First of all, the Simulink block diagram configuration was successful in representing the full operation of an electric vehicle, from motor, to drivetrain to controllers to battery. The input motor introduces a given torque demand, calculated by the input motor controller, to drive the powertrain. After a series of speed reduction from the gear reduction unit, the transmission, the differential and the wheel, the power of the input motor is translated into movement of the vehicle. Road load is calculated based on the vehicle characteristics, the current speed and acceleration levels, and fed back as resistive torque onto the drivetrain. The consumed energy of the motor (input and sun motor for the CVT) is calculated in real-time and deducted from the battery accumulator.

Second, the motor used to model the synchronous motor of the Nissan Leaf, is able to drive the vehicle in the simulation to a maximum speed of at least 150 km/h for all powertrain configurations. Irrespective of the transmission the vehicle is equipped with, it is consistently able to track the reference speed of the different drive cycles. Across all transmission systems and drive cycles, the tracking accuracy is above 97%. It is worth noting that the tracking is slightly improved with the SST and CVT operations, as opposed to the DBT mode. This slight difference can be justified by the gear switching events, where the error is large over a small period of time. Such an error can be greatly reduced by implementing the control algorithm developed in [10], where the ring and sun brakes are released or triggered in a more progressive manner. The error reduction being so small, it was deemed insignificant for the purpose of this study and was thus not pursued. On the other hand, the SST has a constant gear ratio and thus no interruption of power flow. The CVT, while it exhibits a wide range of gear ratios, can smoothly change within that range and thus no abrupt switching is observed.

5.2 CVT Operation Analysis

Careful analysis of the continuously variable transmission operation is necessary to understand the gains observed in the previous chapter. To do so, the operation of the CVT for the HWFET drive cycle is examined. As explained in Chapter III, at low vehicle speeds the CVT is forced to operate in the first gear ratio of the DBT, GR1 = 1.667. That is, when the ring brake is active, the sun is transmitting all the power through the transmission.

Once this breakpoint has been crossed, the CVT controller examines the current state of input motor operation efficiency. It also performs a line search along the equivalent power line of the input motor torque speed curve. This search is however limited by the achievable operating points by varying the transmission gear ratio.

Given a higher efficiency point, the controller determines the direction of increasing or decreasing the sun gear velocity that would allow achieving such operating point. The Sun Motor is used to adjust the sun gear velocity, changing the gear ratio of the transmission in the process.

An important observation is to note that the Sun Motor is sometimes injecting negative torques into the drivetrain, and since it is constrained to move at positive speeds, acts as a generator. The instantaneous power reading presented in the following figure 5-1 illustrates that point. The Sun Motor is actually absorbing power away from the drivetrain and explains the difference between input power and drivetrain output power in the figure 5-1 for all drive cycles. The closer the Sun Motor power is to zero, the more power is maintained from input to output in the powertrain.

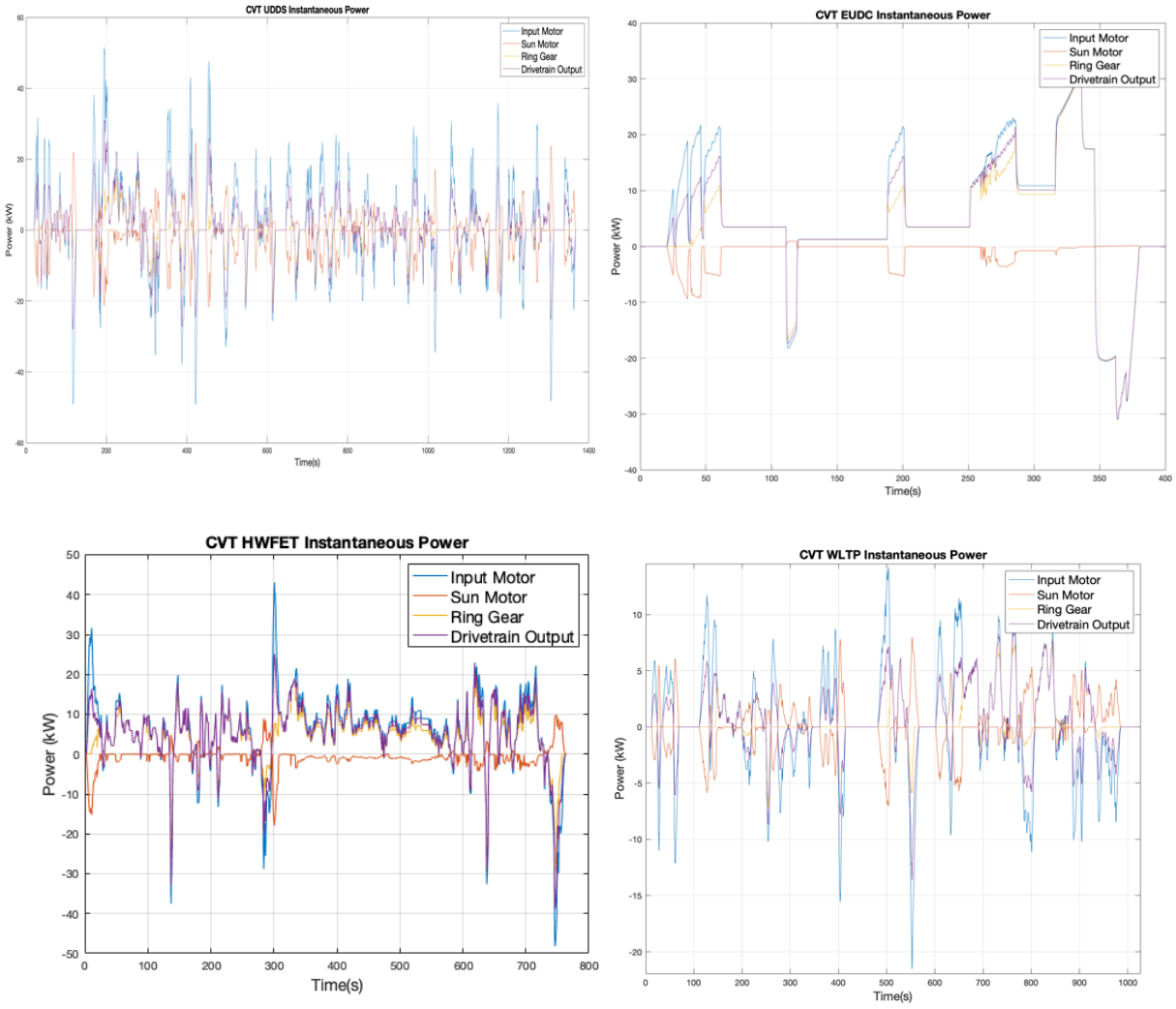

Figure 5-1 Instantaneous Power of input motor (blue), sun motor (red), ring gear (yellow) and drivetrain output (purple). Top, left: UUDS. Top, right: EUDC. Bottom, left: HWFET. Bottom, right: WLTP.

When acting as a generator, the Sun Motor is recharging the battery accumulator. During simulations, this process is assumed to be incrementally more lossy. As presented in table 4-4, recharging the battery is assumed to be between 90-99% efficient. This large difference between optimistic and pessimistic values is justified by the central role this process has in CVT operations. In other terms, the pessimistic value is used to determine a lower end to the benefits of this transmission set up.

5.3 Performance

5.3.1 Input Motor Efficiency

Figure 5-2 is a bar chart summarizing the average input motor efficiency presented in tables 4-9 to 4-12. It compares the average input motor efficiency with the vehicle equipped with SST, DBT and CVT across four different drive cycles.

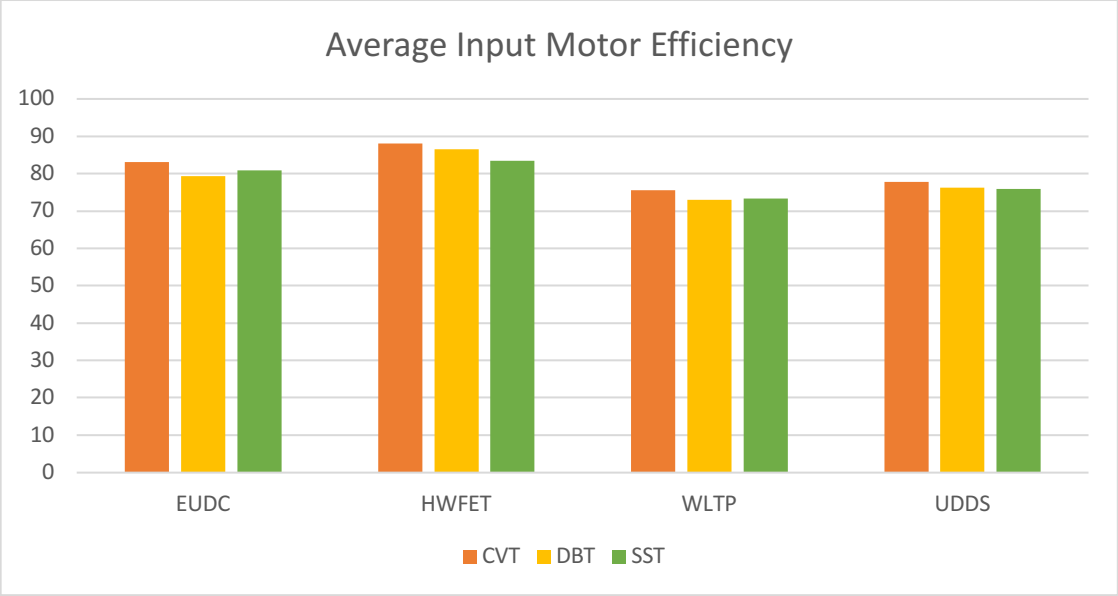

Figure 5-2 Average Input Motor Efficiency Comparison

On the one hand, when simulating for drive cycle with high average velocity, namely EUDC (62.5 km/h) and HWFET (77.6 km/h), supplying the vehicle with a CVT clearly improves the time spent in high efficiency regions of the input motor, compared to when the vehicle is equipped with the DBT or no transmission. In terms of average input motor efficiency, gains of 2.2 and 4.6% are observed using CVT compared to using SST, in EUDC and HWFET respectively. Comparing CVT to DBT, gains of 3.7 and 1.5% are observed over the same drive cycles.

On the contrary, for drive cycles averaging lower speeds, such as WLTP (28.5 km/h) and UDDS (31.5 km/h), more typical of urban driving, less significant improvements are observed, with both CVT, DBT and SST averaging 75.5, 73.1 and 73.4% for WLTP respectively, and 77.8, 76.3 and 76.0% for UDDS respectively.

Figure 5-3 serves to illustrate the reasons limiting the multi-speed transmissions ability to improve on the IME. The red cross is the operating point of the input motor 30 seconds into the UDDS simulation. The red curve represents the power line at the given input motor speed and torque. All points on the power line have equivalent power. The green portion of the latter line is the range of achievable points by altering the gear ratio of the CVT, within the limits of GR1 = 1.667, the rightmost part of the power line, and GR2=0.833, the leftmost portion.

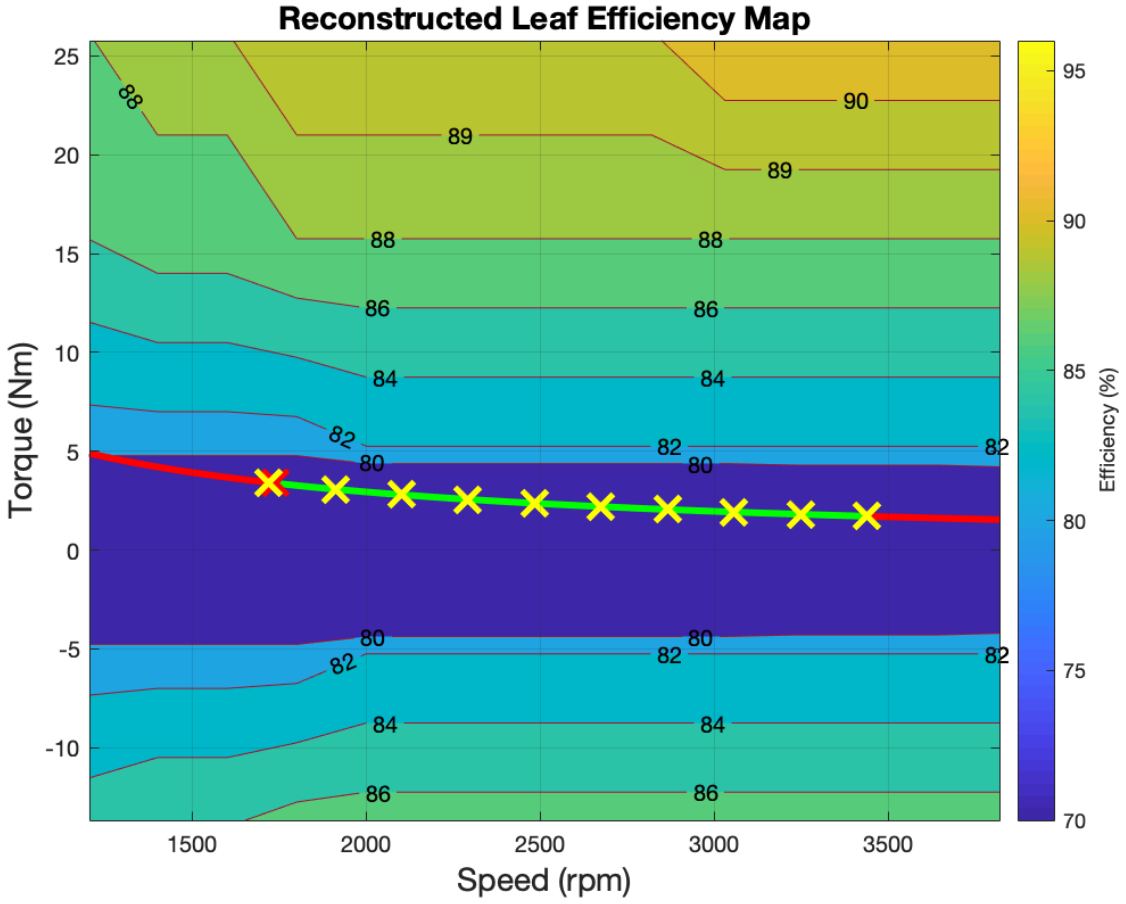

Figure 5-3 CVT UDDS Input Motor operating point on efficiency map at t=70s.

As can be seen in this figure 5-3, which corresponds to a vehicle speed of 38.8km/h, while the range of achievable operating points of the input motor is broad, none present a significant improvement of motor efficiency. This results in the transmission operating around unity gear ratio, which doesn't justify the added complexity of the system.

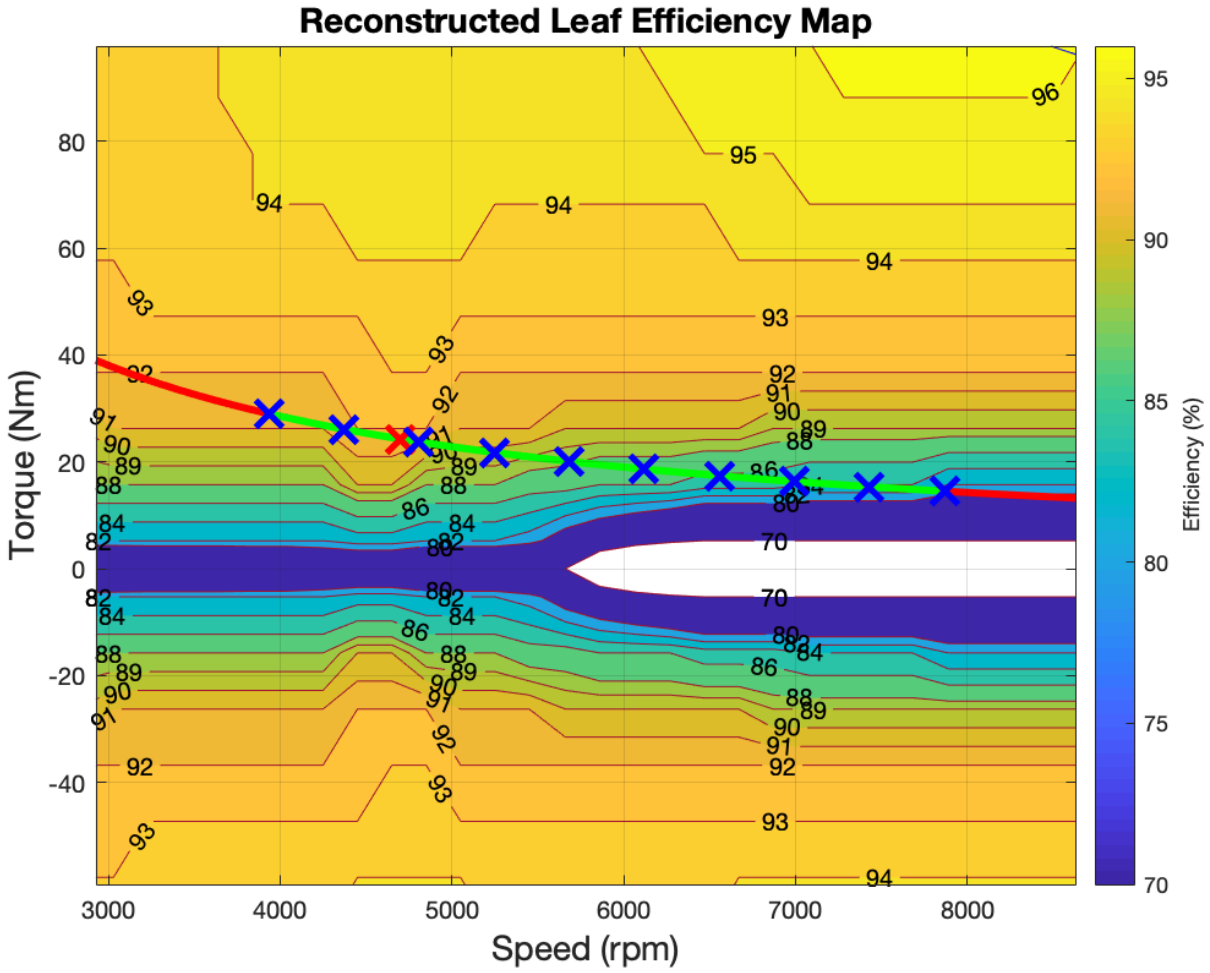

Figure 5-4 CVT UDDS Input Motor operating point on efficiency map at t=240s

On the contrary, operating the vehicle at higher speeds, as can be seen in figure 5-4, where the vehicle now has a velocity of 91.1km/h, shows the CVT can significantly improve IME. The green portion of the equivalent power line now encompasses areas ranging from 91 to 93% efficiency. The CVT adopting a gear ratio of 1.2 maximizes the efficiency of the input motor at that point in time.

5.3.2 Motors Energy Consumption

Having discussed the average efficiency of the input motor, which was concluded to be improved by the CVT at higher speeds of operations, the energy consumption of the same motor is studied for the different drive cycles and transmission configuration.

Input Motor Consumption

Despite the significant improvement in motor efficiency noted in the previous sections, the input motors are quoted to consume more energy when the vehicle is equipped with a CVT than with the DBT or SST.

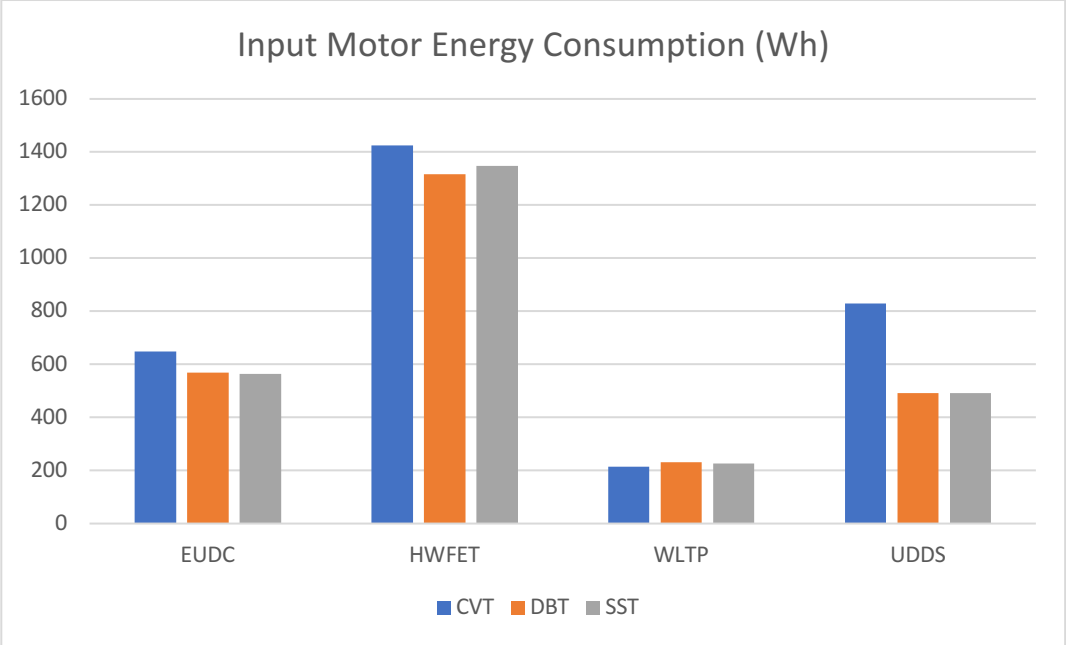

Figure 5-5 Input Motor Energy Consumption Comparison

This increase is particularly marked in the UDDS drive cycle, as can be observed in the figure 5-5 above. Compared to SST consuming 492Wh, a vehicle equipped with the CVT uses 829Wh in this drive cycle, which represents an 68% augmentation. EUDC, WLTP and HWFET drive cycles respectively sees an 15%, 5% and 6% increase.

This rise in consumption is explained by the sun motor acting as a generator during certain parts of the CVT operation, as explained in section 5.2. During those times, the sun motor is absorbing power away from the output of the transmission. This means that the input motor must offset that consumption to deliver the necessary output power for drive cycle tracking.

Sun Motor Consumption

Figure 5-6 below details the energy utilisation of the sun motor, for the different drive cycles as well as the different assumed efficiencies of the CVT.

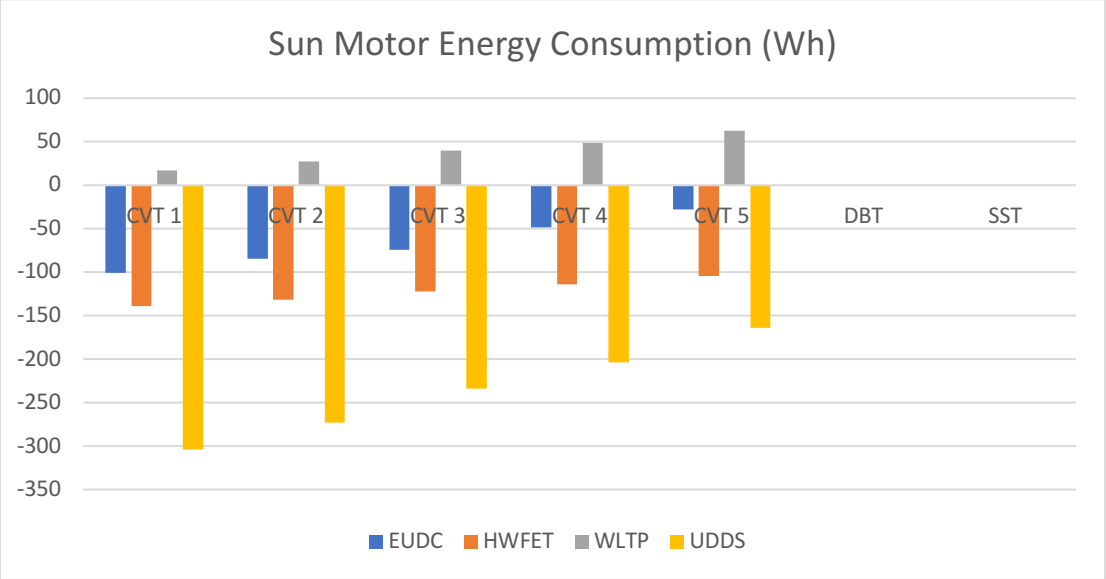

Figure 5-6 Sun Motor Energy Consumption Comparison (negative values imply energy regeneration)

It is noted that the consumption is particularly high for the UDDS drive cycle, as could be expected given the input motor consumption data. Comparing for the optimistic cases of the CVT, noted CVT1, where the sun motor is assumed to have an efficiency of 99% at all times, and the battery is recharged at 95% efficiency. In such a scenario, the sun motor actually recharges the battery by 303Wh, as opposed to 164Wh in the pessimistic scenario.

On the other hand, in the WLTP drive cycle, the sun is motor is inputting more power into the drivetrain, and thus consumes 17Wh in an optimistic scenario versus 63Wh in the pessimistic one.

Of course, no sun motor is present in the DBT and SST modes, which explains the zero-energy consumption observed.

5.3.3 Overall Efficiency

Given the data presented thus far, the overall efficiency of the different transmission systems, for the four test drive cycles, is presented in the following figure 5-7.

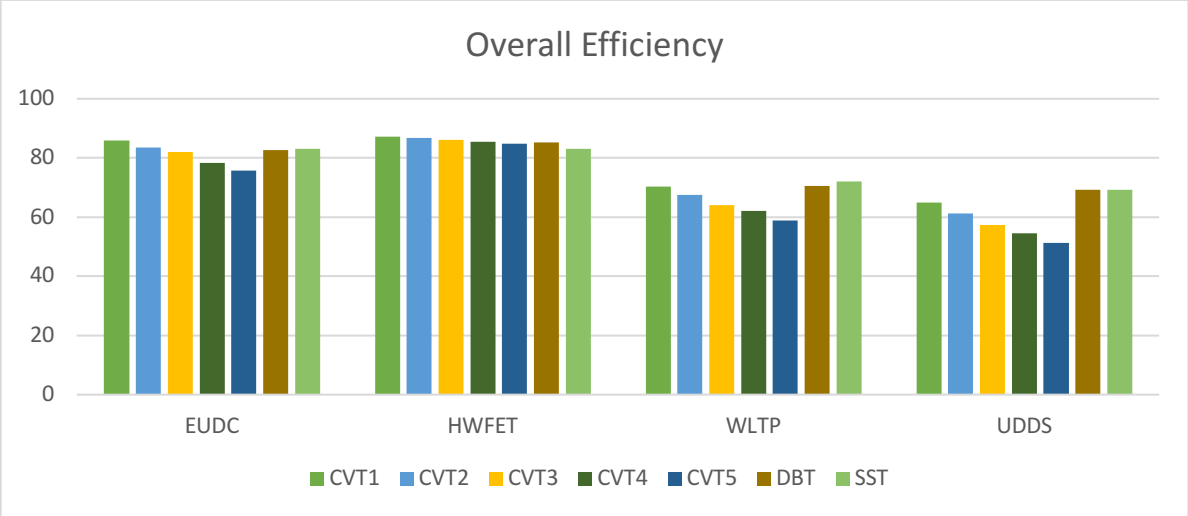

Figure 5-7 Vehicle Overall Efficiency Comparison

For EUDC drive cycle, the benchmark overall efficiencies are 83.1 and 82.6% for the SST and the DBT, respectively. Depending on the loss levels assumed in the CVT, the CVT displays an overall efficiency ranging from 75.8 to 85.9%.

Likewise, for the HWFET simulations, benchmarks report 83.1% and 85.2%, compared to a range of 84.9 to 87.2%.

For the WLTP tests, benchmarks overall efficiencies are 72.1 and 70.5%, whereas the CVT operations operate at 58.8 to 70.4% overall efficiency.

Finally, UDDS drive cycle simulations, the obtained benchmark overall efficiencies are 69.2 and 69.3%, associated with a range of 51.3 to 64.5% in the CVT operations.

Again, a marked difference is observed in the high-speed drive cycles, EUDC and HWFET, where the best-case scenarios predict a much more efficient operation of the vehicle overall when equipped with a CVT system, as opposed to the same vehicle with a DBT or an SST. This difference is calculated to be 2.8 and 2 percentage points respectively. On the contrary, for the low averaging velocities drive cycle WLTP and UDDS, even best-case projections suppose a decrease in overall efficiency.

These results are again expected from the motor consumption data presented previously. At higher speed, the input motor is controlled to operate in a higher

efficiency region, which results in improved average IME. However, this control is performed by using the sun motor to vary the speed of the sun gear. This results in the sun motor, acting as a generator, drawing power away from the output of the transmission. In turn, it increases the power consumption of the input motor. However, the generated power is used to recharge the battery of the vehicle. This process, and the losses imparted from executing it, determine the overall efficiency of the entire vehicle. It explains the large swing in overall efficiency values obtained with varying degrees of efficiency in the sun motor and the battery recharge.

Comparatively, at lower speeds, the gains to be made from varying the gear ratio, in terms of input motor operation efficiency, are reduced. The CVT design thus introduces complexity and losses in the system and fails to justify the added complexity.

5.3.4 Range

Range is measured for the vehicle on a 24kWh battery. Equipped with the same battery, the EV is tested, following all four drive cycles, successively operated with a SST, the DBT and the CVT. Simulations are allowed to run indefinitely, until the battery SoC of the vehicle falls below 10%. The results are shown in the figure 5-8 below:

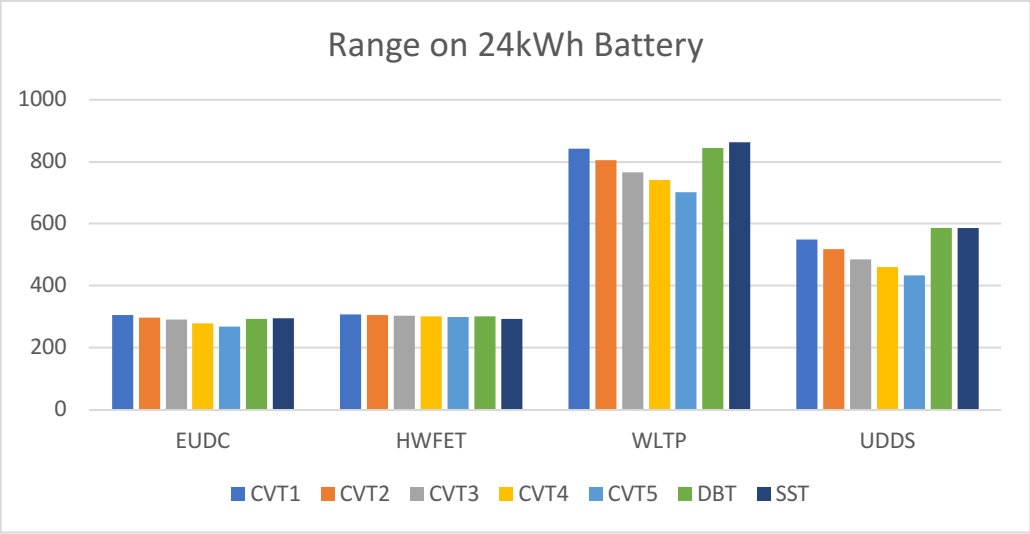

Figure 5-8 Vehicle range comparison on 24kWh battery

Nissan advertises a 200km range on the NEDC drive cycle [32], which wasn't tested in these simulations. Higher values are observed in these simulations, for all drive cycles and transmission types. This is explained by inefficiencies in the powertrain, the regenerative braking, the road and weather conditions, climbs and other conditions affecting power consumption not considered in the simulations. However, since the point of the simulations is to compare the performance of each transmission type, it was deemed an acceptable simplification.

It is worth noting that, for the high average velocity drive cycles, the measured range are much lower than for the low speed drive cycles. This fact is irrespective of the transmission system the vehicle is simulated with. Despite the high overall efficiencies calculated for both EUDC and HWFET, the energy economy, or ratio of distance traveled to energy spent is smaller compared to the low speed drive cycles. This observation is explained by the load torque imparted on the vehicle. The aerodynamic drag, identified as the dominant resisting load on the vehicle at high speeds. It is by definition quadratically scaling with the speed of the vehicle. Thus, at high speeds, much higher resistive torque is imparted on the vehicle, making the vehicle energy economy decrease.

When comparing between the CVT and the benchmark transmission systems, an increase in range of 3.4 and 2.4%, corresponding to 10 and 7.2km is noticed, on the 24kWh battery for EUDC and HWFET. However, for WLTP and UDDS, the range is actually decreased by 2.4 and 6%. This improvement is however limited to the higher values of battery recharge efficiencies, with worsening ranges observed in more pessimistic simulations. The observed range results are in line with the overall energy efficiency results previously obtained.

6 Conclusion

6.1 Summary

To test for the viability of a novel Continuously Variable Transmission design, a full electric vehicle simulation was implemented. This vehicle consists of an input motor, a gear reduction unit, a transmission system, a differential, wheels and a battery. The parameters of these components were chosen to best simulate the existing testbed of the Dual-Brake Transmission. Different controllers were designed to allow the vehicle to track chosen driving cycles. The vehicle was simulated in a direct drive configuration, i.e. without transmission, then with the DBT and finally with the CVT. Adding the transmission required the addition of a transmission controller, and a sun motor for the CVT. This controller was used to optimize the operations of the input motor, by modifying the gear ratio of the transmission.

In all configurations, the vehicle was successful in accurately tracking the four tested drive cycles. Significant improvements in average input motor efficiency were observed testing for all four drive cycles, when the vehicle was equipped with the CVT over the other two benchmarks. The addition of the sun motor however resulted in some of the power being absorbed away from the drivetrain by the sun motor. Overall vehicle efficiency was improved despite that fact, given the ability of the sun motor to recharge the battery of the vehicle, in high average velocity drive cycles. Simulations were conducted with varying degrees of battery recharge efficiency, to establish the breakpoint where the addition of the CVT no longer improved driving efficiency. Results show an improvement in high speed driving cycles given a battery recharge efficiency greater than 95%, and for lower speed driving cycles the addition of the CVT resulted in decrease in performance.

6.2 Limitations & Future Work

Battery Recharge Efficiency

As alluded to in section 6.1, battery recharge plays a key role in operating the designed CVT. While simulations have determined benchmark values above which the system improves overall vehicle efficiency, an accurate measurement of these

losses would improve confidence in the design. The rate of losses is highly dependent on the battery type of the vehicle, the type of motor chosen to operate the CVT, and the mechanical layout of the CVT.

Vehicle Type

Improvements in overall efficiency were achieved with this Nissan Leaf simulation for high speed drive cycles. At lower speeds, the addition of a more complex, lossy mechanism wasn't justified. For heavier vehicles, where higher torques are observed throughout the drive cycle, the benefit of a CVT would be substantial. Better results are predicted for a truck equipped with such a transmission.

Performance Metrics

The key performance metric in this analysis has been efficiency and vehicle range. However, the addition of a transmission system could allow improvements in vehicle acceleration, top speed, hill climbing and comfort (with no gear shifting).

Sun Motor Sizing

Another key aspect affecting the overall performance of the CVT is the size of the sun motor. Restricting this size would limit the amount of power the sun would draw from the transmission. However, a non-negligible amount of power was necessary to operate the CVT within the band of gear ratios defined by the underdrive and overdrive modes of the DBT. These ratios correspond to both the common sun and common ring gears of the planetary sets to rotate in the same positive directions. Other bands of operations, where the common ring or common sun operate in negative directions with respect to the carrier gears, result in higher or lower gear ratios. More importantly, operating the sun gear closer to its zero value, in both positive and negative direction, would allow to maintain a large range of achievable gear ratios while limiting the size of the sun motor.

Cost-Benefit of CVT

Significant improvements were observed when equipping the vehicle with the CVT. These improvements would come at a financial and complexity cost. The initial cost of each component of the CVT can calculated, and their lifetime maintenance fees estimated. This cost should then be compared to the energy savings of a higher overall

energy efficiency over the lifetime of the vehicle. The initial cost could be directly offset by downsizing the traction motor and diminishing its price, since the added transmission extends the maximum torque and speed achieved by the same motor without transmission.

Prototyping the Continuously Variable Transmission

If this exhaustive list of limitations is explored and the design validated through simulations, the next step would be the fabrication of a prototype. This would be the opportunity to validate the simulations with a real-life assessment, given the added uncertainties and complexities.

References

[1] L. Canals Casals, E. Martinez-Laserna, B. Amante García and N. Nieto (2016) "Sustainability analysis of the electric vehicle use in Europe for CO2 emissions reduction", Journal of Cleaner Production, vol.127, pp.425-437.

[2] W. J. Sweeting, A. R. Hutchinson and S. D. Savage (2011) "Factors affecting electric vehicle energy consumption", International Journal of Sustainable Engineering,4(3), 192-201, DOI: 10.1080/19397038.2011.592956.

[3] R. Alvarez Fernandez (2018) "A more realistic approach to electric vehicle contribution to greenhouse gas emissions in the city", Journal of Cleaner Production, vol.172, pp.949-959.

[4] International Energy Agency (2018) Global EV Outlook 2018: Towards cross-modal electrification.

[5] M. Ehsani, Y. Gao, S. Gay and A. Emadi (2009) Modern Electric, Hybrid Electric, and Fuel Cell Vehicles: fundamentals, theory, and design. CRC Press.

[6] J. Larminie, J. Lowry (2012) Electric Vehicle Technology Explained. John Wiley & Sons.

[7] A. Khajepour, M. Saber Fallah and A. Goodarzi (2014) Electric and Hybrid Vehicles: Technologies, Modeling and Control - A Mechatronic Approach, John Wiley & Sons.

[8] Y. Zhang, C. Mi (2018) Automotive Power Transmission System, John Wiley & Sons.

[9] R. Fischer et al. (2015) The Automotive Transmission Book, Springer.

[10] M. S. Rahimi Mousavi (2017) "Seamless Dual-Brake Transmission for Electric Vehicles: Design, Modeling, Estimation, and Control", Ph.D dissertation, Department Electrical Engineering, McGill University, Montreal, Canada.

[11] S. Manzetti, F. Mariasiu (2015) "Electric vehicle battery technologies: from present state to future systems", Renewable and Sustainable Energy Reviews, vol.51, 1004-1012.

[12] S. J. Gerssen-Gondelach, A. P. C.Faaij (2012) “Performance of batteries for electric vehicles on short and longer term”, Journal of Power Sources, vol.212, pp. 111-129.
[13] B. Canis (2013) “Battery Manufacturing for Hybrid and Electric Vehicles: Policy Issues”, United States Congressional Research Service.
[14] B. Scosati, J. Hassoun, Y.K. Sun (2011) “Lithium-ion batteries. A look into the future”, Energy & Environmental Science, vol.4, pp.3287-3295.
[15] L. Ahmadi et al. (2017) “A cascaded life cycle: reuse of electric vehicle lithium-ion battery packs in energy storage systems”, Int J Life Cycle Assess, vol.22, pp.111-124.
[16] Q. Qiao, F. Zhao, Z. Liu and H. Hao (2019) “Electric Vehicle Recycling in China: Economic and Environmental Benefits”, Resources, Conservation & Recycling, vol.140, pp.45-53.
[17] L. Ahmadi et al. (2014) “Energy efficiency of Li-ion battery packs re-used in stationary applications”, Sustainable Energy Technologies and Assesments, vol.8, pp.9-17.
[18] S. Shokrzadeh, E. Bibeau (2016) “Sustainable integration of intermittent renewable energy and electrified light-duty transportation through repurposing batteries of plug-in electric vehicles”, Energy, vol.106, pp.701-711.
[19] B. Swain (2018) “Cost effective recovery of lithium from lithium ion battery by reverse osmosis and precipitation: a perspective”, Chemical Technology & Biotechnology, vol.93, pp.311-319.
[20] H. Gu, Z. Liu, Q. Qing (2017) “Optimal Electric Vehicle Production Strategy Under Subsidy and Battery Recycling”, Energy Policy, vol.109, pp.579-589.
[21] X. Gu, P. Ieromonachou and L. Zhou (2018) “Optimizing quantity of manufacturing and remanufacturing in an electric vehicle battery closed-loop supply chain”, Industrial Management & Data Systems, vol. 118, no.1, pp.283-302.
[22] K. C. Bayindir, M. A. Gözüküçük, A. Teke (2011) “A comprehensive overview of hybrid electric vehicle: Powertrain configurations, powertrain control techniques and electronic control units”, Energy Conversion and Management, vol.52, pp.1305–1313.

[23] T. Hutchinson, S. Burgess, G. Hermann (2014) "Current hybrid-electric powertrain architectures: Applying empirical design data to life cycle assessment and whole-life cost analysis", Applied Energy, vol.119, pp.314-329.
[24] N. Kim, A. Rousseau (2013) "Assessment by Simulation of Benefits of New HEV Powertrain Configurations", Oil & Gas Science and Technology, vol.68, no.1, pp.3-178.
[25] C.-T. Chung, Y.-H. Hung (2015) "Performance and energy management of a novel full hybrid electric powertrain system", Energy, vol.89, pp.626-636.
[26] B.W. Lane et al. (2018) "All plug-in electric vehicles are not the same: Predictors of preference for a plug-in hybrid versus a battery-electric vehicle", Transportation Research Part D, vol.65, pp.1-13.
[27] G. Napoli et al. (2017) "Development of a fuel cell hybrid electric powertrain: A real case study on a Minibus application", Intl. J. of Hydrogen Energy, vol.42, pp.28024-28047.
[28] E. Yoo, M. Kim, H.H. Song (2018), "Well-to-wheel analysis of hydrogen fuel-cell electric vehicle in Korea", Intl. J. of Hydrogen Energy, vol.43, pp.19267-19278.
[29] J. Ribau, C. Silva and J.M.C. Sousa (2019) "Efficiency, cost and life cycle CO2 optimization of fuel cell hybrid and plug-in hybrid urban buses", Applied Science, vol.129, pp.320-335.
[30] G.J. Offer et al. (2010) "Comparative analysis of battery electric, hydrogen fuel cell and hybrid vehicles in a future sustainable road transport system", Energy Policy, vol.38, pp.24-29.
[31] Tesla Inc. Website "Tesla Model S" Tesla.com
https://www.tesla.com/models (accessed Feb 1, 2019).
[32] Nissan Inc Website "Nissan Leaf" Nissan.co.uk
https://www.nissan.co.uk/vehicles/new-vehicles/leaf/prices-specifications.html#grade-LEAFZE1A-0 (accessed Feb 1,2019).
[33] J. Ruan P. Walker, N. Zhang (2016) "A comparative study energy consumption and costs of battery electric vehicle transmissions", Applied Energy, vol.165, pp.119-134.

[34] Q. Ren, D.A. Crolla, A. Morris (2009) "Effect of transmission design on Electric Vehicle (EV) performance" presented at the Vehicle Power and Propulsion Conference, October 2009.

[35] L. Jian, K.T. Chau (2009) "A novel electronic-continuously variable transmission propulsion system using coaxial magnetic gearing for hybrid electric vehicles", *J. of Asian Electric Vehicles*, vol.7, n.2, pp.1291-1296.

[36] Y. Wang, M. Cheng and K.T. Chau (2009) "Review of Electronic-continuously Variable Transmission Propulsion System for Full Hybrid Electric Vehicles", *J. of Asian Electric Vehicles*, vol7, n.2, pp.1297-1302.

[37] L. Zhang *et. Al.* (2011) "Research on Control Strategy and Experiment of Electronic Mechanical Continuously Variable Transmission", *Appl. Mechanics & Materials,* vols.88-89, pp.191-196.

[38] A. Pakniyat, P. Caines (2014) "The Gear Selection Problem for Electric Vehicles: an Optimal Control Formulation", presented at the Intl. Conference on Control, Automation, Robotics & Vision, in Marina Bay Sands, Singapore, 10-12th Dec. 2014.

[39] S. Rinderknecht, T Meier (2010) "Electric Power Train Configurations and Their Transmission Systems" at Intl. Symposium on Power Electronics Electric Drives, Automation and Motion.

[40] J.W. Shin et al. (2014) "Design of 2-speed transmission for electric commercial vehicle", *Intl. J. of Automotive Technology,* vol.15, no.1, pp.145-150.

[41] A. Sorniotti *et. Al.* (2010) "Optimization of a Multi-Speed Electric Axle as a Function of the Electric Motor Properties" presented at IEEE Vehicle Power and Propulsion Conference, in Lille France, 1-3 Sept. 2010.

[42] B. Zhu *et. Al.* (2013) "Two-Speed DCT Electric Powertrain Shifting Control and Rig Testing", *Advances in Mechanical Engineering,* vol. 5, pp.1-10.

[43] N. Srivastava, I. Haque (2009) "A review on belt and chain continuously variable transmissions (CVT): Dynamics and control", *Mechanism & Machine Theory,* vol.44, pp.19-41.

[44] F. Bottiglione *et al.* (2014) "Energy Consumption of a Battery Electric Vehicle with Infinitely Variable Transmission", *Energies*, vol.7, pp.8317-8337.

[45] M. Delkhosh, M.S. Foumani (2013) "Optimisation of full-toroidal continuously variable transmission in conjunction with fixed ratio mechanism using particle swarm optimisation", *Vehicle System Dynamics*, vol.51:5, pp.671-683.
[46] M. Delkhosh *et. Al.* (2011) "Geometrical optimization of half toroidal continuously variable transmission using particle swarm optimization", *Scientia Iranica,* vol.18:5, pp.1126-1132.
[47] M. Pesgens et.al (2006) "Control of a hydraulically actuated continuously variable transmission", *Vehicle System Dynamics*, vol.44:5, pp.387-406.
[48] G. Mantriota (2002) "Performances of a parallel infinitely variable transmissions with a type II power flow", *Mechanism & Machine Theory*, vol.37, pp.555-578.
[49] G. Mantriota (2002) "Performances of a series infinitely variable transmissions with a type I power flow", *Mechanism & Machine Theory*, vol.37, pp.579-597.
[50] A. Rousseau *et.al.* (2014) "Electric Drive Vehicle Development and Evaluation Using System Simulation", in IFAC World congress, Cape Town, South Africa, Aug. 24-29, 2014, pp.7886-7891.
[51] N. Janiaud, F.-X. Vallet, M Petit and G. Sandou (2009) "Electric Vehicle Powertrain Architecture and Control Global Optimization", in EVS24, Stavanger, Norway, May 13-16, 2009.
[52] J. Wijkniet, T. Hofman (2018) "Modified computational design synthesis using simulation-based evaluation and constraint consistency for vehicle powertrain systems", *IEEE Transactions on Vehicle Technology,* vol.67, no.9, pp.8065-8076.
[53] A. Abdelrahman, K.S. Algarny, M.Z. Youssef (2018) "A Novel Platform for Powertrain Modeling of Electric Cars With Experimental Validation Using Real-Time Hardware in the Loop (HIL): A Case Study of GM Second Generation Chevrolet Volt", *IEEE Transactions on Power Electronics,* vol.33, no.11, pp.9762-9771.
[54] L. Boulon et.al. (2010) "Simulation Model of a Military HEV With a Highly Redundant Architecture", *IEEE Transactions on Vehicle Technology,* vol.59, no.6, pp.2654-2663.

[55] F. Syed *et.al.* (2006) "Derivation and Experimental Validation of a Power-Split Hybrid Electric Vehicle Model", *IEEE Transactions on Vehicle Technology,* vol.55, no.6, pp.1731-1747.

[56] M. S. Rahimi Mousavi, A. Pakniyat, T. Wang and B. Boulet (2015) "Seamless Dual-Brake Transmission for electric vehicles: Design, control and experiment", *Mechanism and Machine Theory,* vol.94, pp.96-118.

[57] B. Boulet, M.S. Rahimi Mousavi, H. V. Alizadeh (2017) "Seamless transmission systems and methods for electric vehicles", U.S. Patent 9702438, Jul. 11, 2017.

[58] T. Burress (2013) "Benchmarking State-of-the-Art Technologies", *U.S. DOE Hydrogen and Fuel Cells Program and Vehicle Technologies Program Annual Merit Review and Peer Evaluation Meeting,* ID APE006, May 14, 2013.

Appendix A

```
function [WS,GRT,NBR,NBS,WS_free,maxed,WShold] =
fcn(CVT,VehSpeed,WM,WMnext,WR,WSprev,WShold)

R1 = 2;
R2 = 4;
GRT = ((R1+1)*(WSprev + R2*WR))/((R2+1)*(WSprev + R1*WR));

CVT_Speed_BP_1 = 2;
CVT_Speed_BP_2 = 40;
WS_free = 0;
breaking_force = 100;
maxed = 0;
damping = 0.2;

GRmax = ((R1+1)*(WS_max + R2*WR))/((R2+1)*(WS_max + R1*WR));

% Vehicle is stopped
% No movement in the transmission
if abs(VehSpeed) < 0.1
   NBR = 0;
   NBS = 0;
   WS = 0;
else
   % Vehicle Speed is below first breakpoint
   % Activate Brakes on Ring Gear, Disengage Sun Brake
   % Allow Sun to freely spin
   % This represents the underdrive mode of the DBT
   if VehSpeed < CVT_Speed_BP_1
      NBR = breaking_force;
      NBS = 0;
      WS = WSprev;
      WS_free = 1;
```

```
else
    % Vehicle Speed is above second breakpoint
    % Activate Brakes on Sun Gear, Disengage Ring Brake
    % Sun should be grounded
    % This condition is a failsafe in case the optimizer doesn't
    % already use the overdrive mode at very high speed
    if VehSpeed > CVT_Speed_BP_2
        NBR = 0;
        NBS = breaking_force;
        WS = 0;
    else
        % CVT operations, both ring and sun gear are allowed to freely
        % spin
        NBR = 0;
        NBS = 0;
        % WM is already at max efficiency
        % Optimizer is directing the transmission to remain at current
        % velocity
        if abs(WMnext-WM) < 1
            if ~WShold
                WShold = WSprev;
                WS = WSprev;
            else
                WS = WShold;
            end
        % WMnext is different from current WM
        else
            WShold = 0;
            % Optimizer indicates that the input motor speed should
            % increase to increase motor efficiency
            if WMnext > WM
                % Increasing the sun speed increases the gear ratio,
                % which in turn increases the speed of operation of the
                % input motor, given same output speed of the vehicle
                WS = WSprev + damping*(WMnext - WM);
            % Optimizer indicates that the input motor speed should
```

```
            % decreaase to increase motor efficiency
            else
               % Decreasing the sun speed decreases the gear ratio,
               % which in turn decreases the speed of operation of the
               % input motor, given same output speed of the vehicle
               WS = WSprev + damping*(WMnext - WM);
            end
         end
      end


   end
end

if WR < 0 && abs(WR) > 0.0001
   maxed = 1;
   WS = WSprev-1;

end
if WS < 0 && abs(WS) > 0.0001
   maxed = -1;
   WS = 0;
end



GRT = ((R1+1)*(WS + R2*WR))/((R2+1)*(WS + R1*WR));
```

Appendix B-1

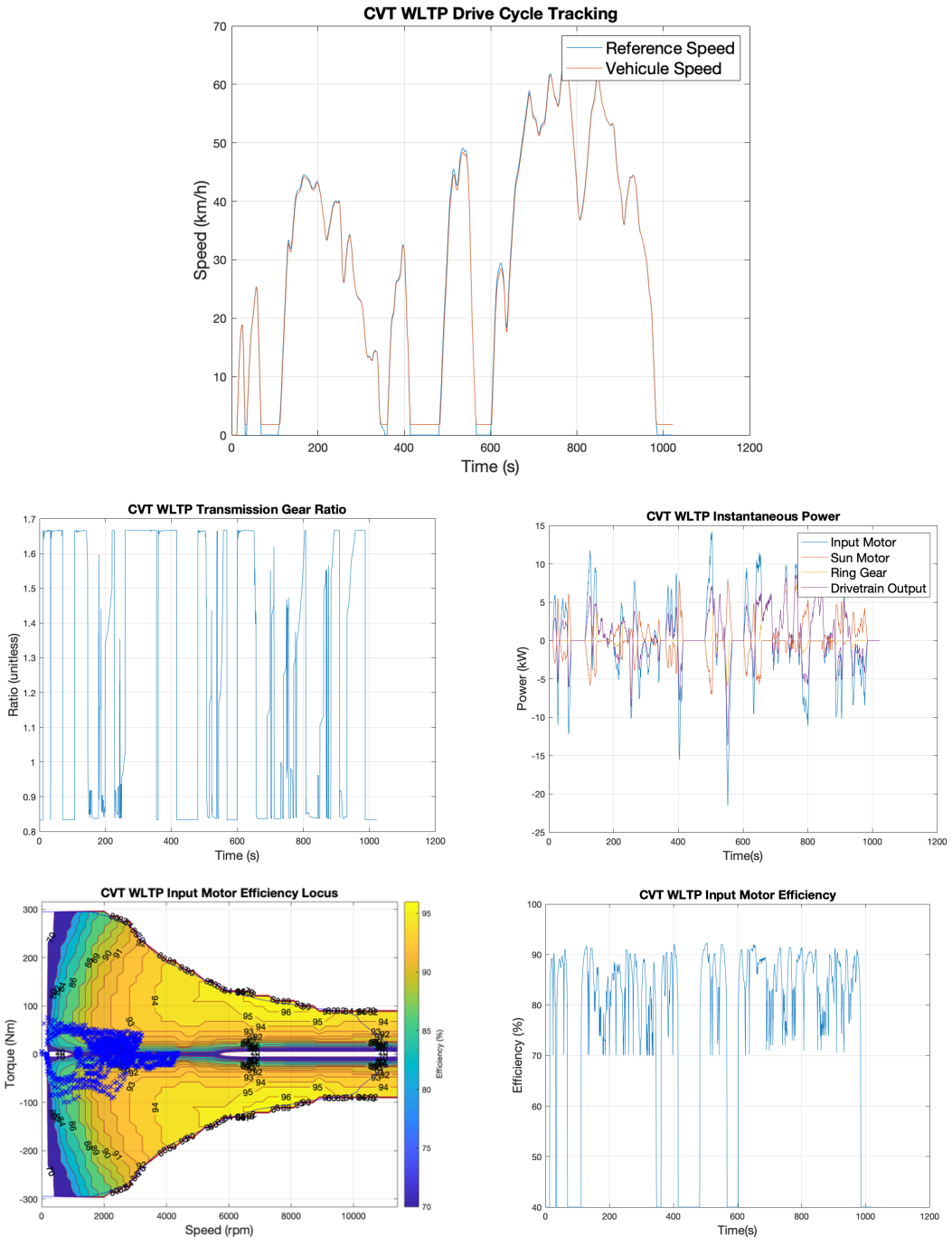

Figure 6-1 CVT WLTP Simulation Results. Speed Tracking (top), CVT gear ratio (middle, left), instantaneous powers (middle, right), efficiency map with operation path (bottom, left) and efficiency reading (bottom, right)

Appendix B-2

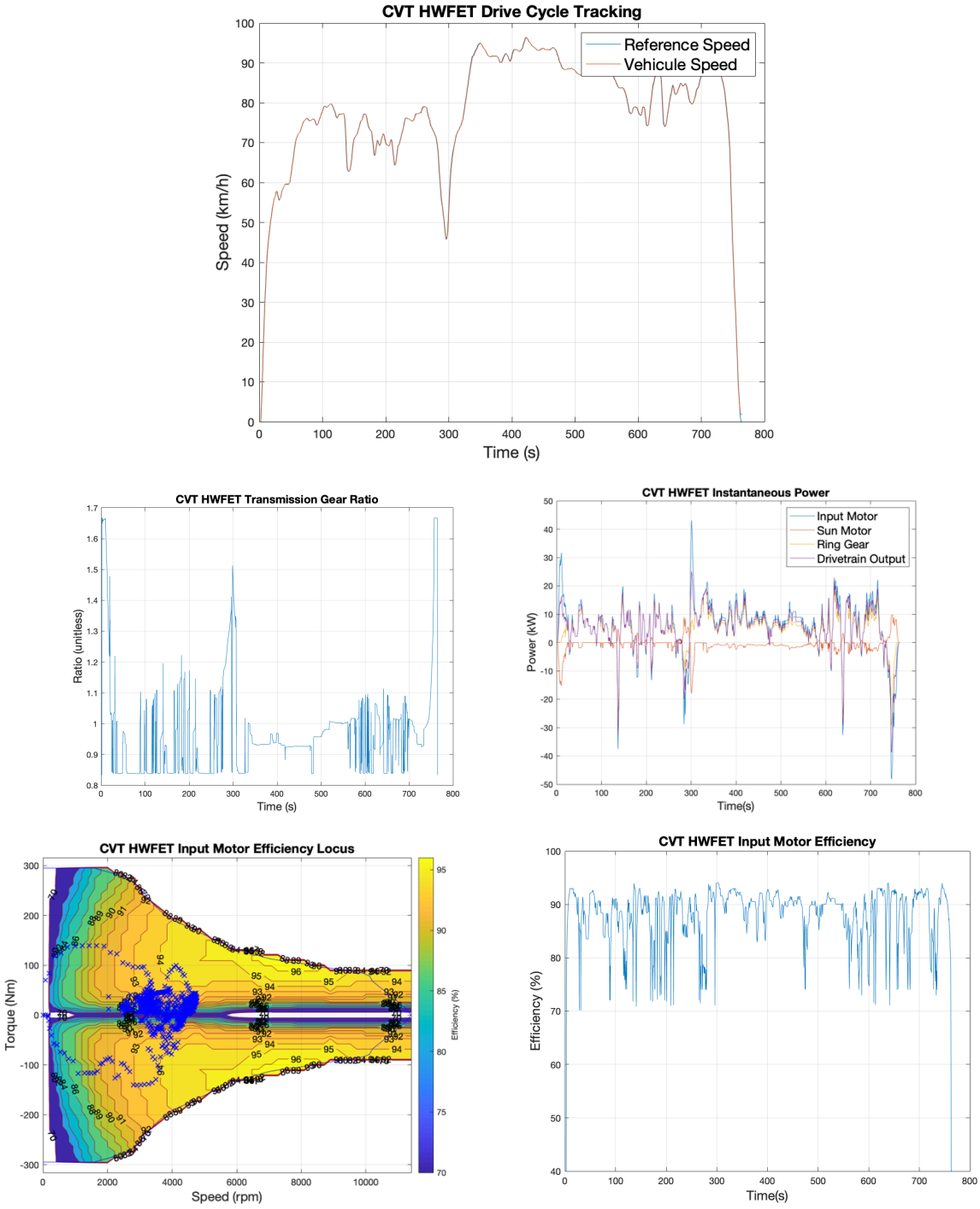

Figure 6-2 CVT HWFET Simulation Results. Speed Tracking (top), CVT gear ratio (middle, left), instantaneous powers (middle, right), efficiency map with operation path (bottom, left) and efficiency reading (bottom, right)

Appendix B-3

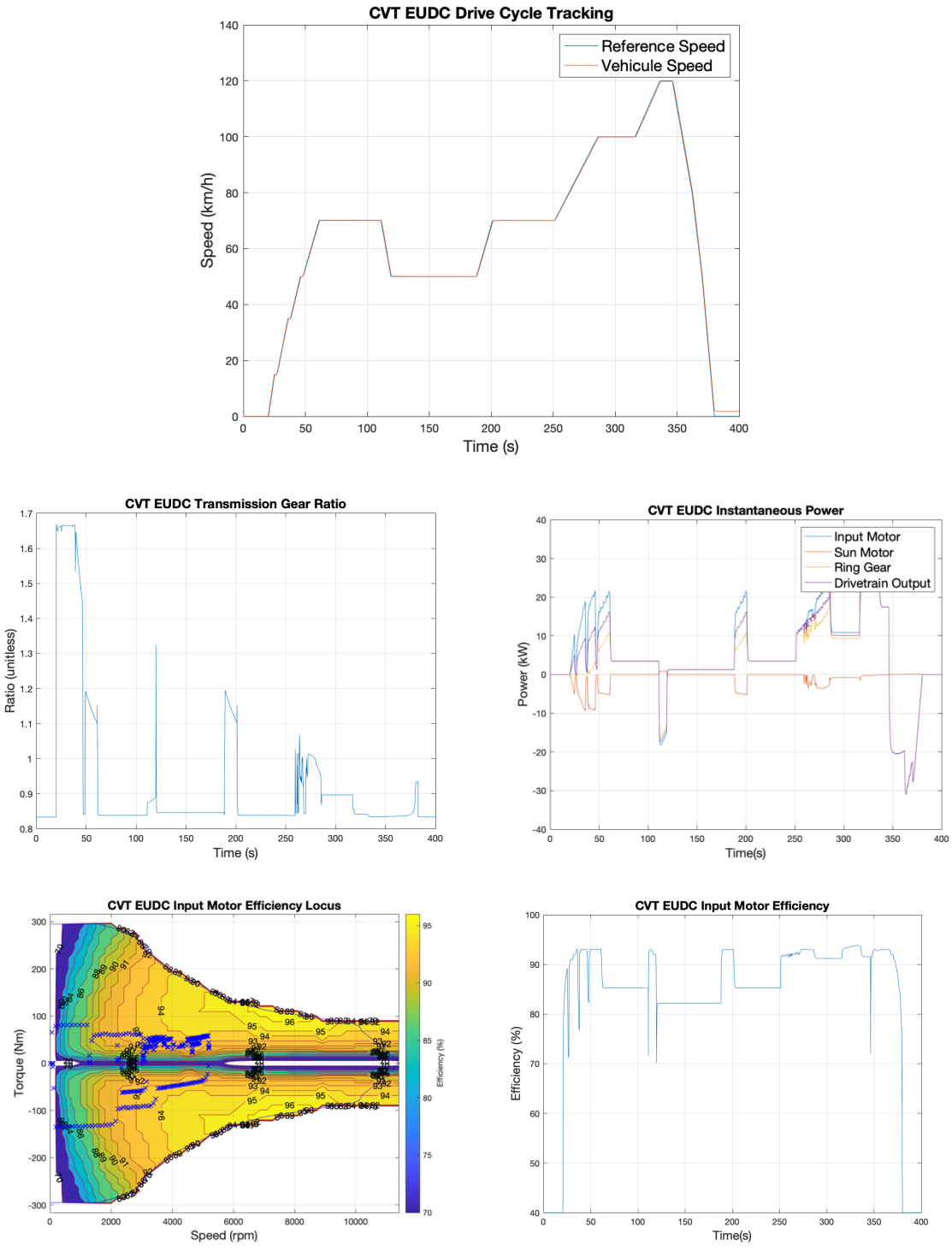

Figure 6-3 CVT EUDC Simulation Results. Speed Tracking (top), CVT gear ratio (middle, left), instantaneous powers (middle, right), efficiency map with operation path (bottom, left) and efficiency reading (bottom, right)